

DISSERTATION

Traffic Efficiency Optimization Through V2X Communication

submitted in partial fulfillment of the requirements for the degree of
Doktor der technischen Wissenschaften

under supervision of

Univ.-Prof. DI Dr.-Ing. Christoph F. Mecklenbräuer
Institute of Telecommunications

to the

TU Wien

Faculty of Electrical Engineering and Information Technology

by

Christian Backfrieder

Wien, Feb. 2018

This thesis was supervised by:

Univ.-Prof. DI Dr.-Ing. Christoph F. Mecklenbräuer
Institute of Telecommunications
TU Wien

The reviewers were:

1. Univ.-Prof. DI Dr. Andreas Springer
Institute for Communications Engineering and RF-Systems
JKU Linz
2. Ao. Univ.-Prof. Mag. Dr. Günter EMBERGER
Institute of Transportation
TU Wien

————— to Birgit —————

Abstract

Transport delays due to traffic jams are manifest in many urban areas worldwide. For the purpose of making road traffic networks more efficient, Intelligent Transport Systems (ITSs) are currently being developed and deployed. In order to mitigate (or even avoid) congestion, Vehicle-to-Vehicle (V2V) and Vehicle-to-Infrastructure (V2I) communication provide a means for cooperation and intelligent route management in transportation networks. In this thesis, the novel Predictive Congestion Minimization in combination with an A*-based Router (PCMA*) algorithm is introduced, which provides a comprehensive framework for detection, prediction and avoidance of traffic congestion. It assumes utilization of Vehicle-to-Everything (V2X) communication for transmission of contemporary vehicle data such as route source and destination or current position, as well as for provision of routing advice for vehicles. By processing the vehicle data, an early congestion detection and subsequently the calculation of alternative routes becomes possible. As a consequence of the early detection, detours over a wide area can be a solution in appropriate situations to bypass traffic jams and avoid critical areas completely, whereas the degree of improvement of course also depends on the structure of the road network. The routing component takes the current road conditions and predicted future congestion into consideration. PCMA* further contains a component for intelligent and target-oriented selection of vehicles to be rerouted in case of a congestion.

In the first part of this thesis, the performance is proven by dynamic, microscopic traffic simulations in an artificial and real-world road network scenario. Due to the well performing prediction, the results reveal substantial advantages in terms of time and fuel consumption and hence also CO₂ emissions, compared to situations with no active rerouting system. PCMA* is further contrasted with simple rerouting algorithms without any functionality for congestion prediction but with different approaches of how the current situation on the road is assessed and quantified. Additionally, a more sophisticated predictive approach from literature is evaluated and the results are compared to those which can be achieved by applying PCMA*. Within the very same configuration for environment and traffic emergence, all the reference algorithms are outperformed by PCMA*.

With the objective of optimizing traffic flow and in the best case avoiding congestion, it was assumed that 100% of all vehicles participate actively in the system in the initial

simulation configurations so far. Notwithstanding, the transition from very low penetration rates of vehicles that are equipped with communication functionality to a situation where basically all vehicles have the capability to send and receive information will not be completed overnight. To a greater degree, the penetration of connected vehicles will increase more and more, which further will result in a very long period of mixed composition. The second part of this thesis focuses on the analysis of a variable ratio of vehicles having routing and communication functionality to those who do not have these capabilities. It analyzes the performance of the rerouting algorithm when a varying percentage of vehicles is unable to communicate for distinct traffic densities, and proves by simulations that even penetration rates far below hundred percent lead to improvements of the average time and fuel consumption as well as CO₂ emissions per vehicle.

Finally, the router requires a functional communication infrastructure to contribute route guidance to vehicles which are affected by traffic jams. However, variable message delays or a complete loss of messages can influence the rerouting performance significantly, even if the penetration rate is 100 %, since either route advice could fail to reach their recipient, or the supposed knowledge of the road conditions could be outdated at the side of the router. The delay requirements of various routers may be divergent, and therefore two delay models which are independent of the underlying communication standard and the applied routing algorithm are proposed in the third part of the thesis. PCMA* is evaluated concerning its performance with varying delays and message loss probabilities by applying the introduced delay models in the traffic simulations. Furthermore, constraints are defined for both the delay and message loss probability, which define boundary conditions that are required to achieve certain improvements ensuing from intelligent rerouting. The results reveal a high robustness of PCMA* with regard to delays and message loss probabilities, which expresses itself by similarly low achieved average vehicle travel times for a large amount of the investigated communication setups, compared to a parametrization without message delays.

Kurzfassung

Verzögerungen durch Verkehrsstaus sind in vielen städtischen Gebieten weltweit an der Tagesordnung. Um bestehende Straßenverkehrsnetze effizienter nutzen zu können, werden intelligente Transportdienste (Intelligent Transport Systems (ITSs)) entwickelt und eingesetzt. Zur Reduktion oder sogar Vermeidung von Verkehrsüberlastungen bietet die Kommunikation zwischen Fahrzeugen (Vehicle-to-Vehicle (V2V)) bzw. auch zwischen Fahrzeugen und Infrastruktur (Vehicle-to-Infrastructure (V2I)) ein probates Mittel zur Koordination sowie zur intelligenten Routenwahl in Verkehrsnetzen. In dieser Arbeit wird der neuartige Algorithmus Predictive Congestion Minimization in combination with an A*-based Router (PCMA*) vorgestellt, welcher ein umfassendes System zur Erkennung, Vorhersage und Vermeidung von Verkehrsstaus bietet. Vehicle-to-Everything (V2X) Fahrzeugkommunikationstechnologien werden zur Übertragung von relevanten Informationen wie Start- und Zielort, aktuellen Positionsdaten sowie zum Senden von Routing-Anweisungen an das Zielfahrzeug genutzt. Nach der Verarbeitung der Fahrzeugdaten wird eine frühzeitige Stauerkennung möglich, was in weiterer Folge eine Berechnung von großräumigen Alternativrouten erlaubt. Damit können Staus umgangen und kritische Straßenabschnitte vollständig vermieden werden, wobei der Grad der Verbesserung natürlich auch von der Struktur des Straßennetzes abhängt. Die Routing-Komponente berücksichtigt dabei sowohl die aktuellen Straßenbedingungen als auch die vorhergesagte zukünftige Überlastung. PCMA* enthält ferner eine Komponente zur intelligenten und zielgerichteten Auswahl von Fahrzeugen, die im Falle einer Überlastung umzuleiten sind.

Im ersten Teil dieser Arbeit wird die Leistungsfähigkeit durch dynamische, mikroskopische Verkehrssimulationen in einem künstlich generierten und einem realen Straßennetz dargestellt. Aufgrund der exakten Vorhersage weisen die Ergebnisse erhebliche Vorteile in Bezug auf durchschnittliche Fahrzeit und Kraftstoffverbrauch im Vergleich zu Situationen ohne aktivem Routing auf. PCMA* wird einfachen Routing-Algorithmen ohne jegliche Funktionalität zur Stauvorhersage gegenübergestellt, wobei unterschiedliche Ansätze zur Bewertung der aktuellen Situation auf der Straße zur Anwendung kommen. Zudem wird ein prädiktiver Ansatz aus der Literatur evaluiert und die Ergebnisse mit denjenigen verglichen, die durch die Anwendung von PCMA* innerhalb der gleichen Szenarien und mit gleicher Verkehrsdichte erzielt werden können.

Mit dem Ziel, den Verkehrsfluss zu optimieren und im besten Fall Staus zu vermeiden, wurde vorerst angenommen, dass 100 % aller Fahrzeuge am System teilnehmen. Ungeachtet dessen wird es einen längeren Zeitraum geben, in dem unterschiedliche Fahrzeugtypen auf den Straßen unterwegs sind. Zum einen sind das Fahrzeuge, die nicht mit Kommunikationsfunktionalität ausgestattet sind sowie andere, die Informationen senden und empfangen und sich damit aktiv am System beteiligen können. Dieser Übergang von sehr niedrigen Durchdringungsraten von intelligenten Fahrzeugen zu einer Situation mit ausschließlich kommunikationsfähigen Fahrzeugen wird nicht über Nacht abgeschlossen sein. Vielmehr wird die Durchdringung von vernetzten Fahrzeugen immer mehr zunehmen, was folglich auch zu einem längeren Zeitraum gemischter Fahrzeugzusammensetzung führt. Der zweite Teil dieser Arbeit konzentriert sich auf die Analyse der beschriebenen Situation, nämlich eines variablen Verhältnisses von Fahrzeugen mit Routing- und Kommunikationsfähigkeiten zu welchen, die dazu technisch nicht imstande sind. Es wird die Leistung von PCMA* analysiert, wenn ein variabler Prozentsatz von Fahrzeugen nicht in der Lage ist zu kommunizieren. Die durchgeführten Simulationen zeigen, dass sogar Durchdringungsraten von weit unter 100 % zu einer deutlichen Verbesserung der durchschnittlichen Fahrzeit, des Kraftstoffverbrauchs und damit niedrigeren CO₂-Emissionen führen.

Um eine Routenführung für Fahrzeuge, die von Staus betroffen sind, bereitstellen zu können, benötigt PCMA* eine funktionierende Kommunikationsinfrastruktur. Eine Verzögerung der übertragenen Information oder ein vollständiger Nachrichtenverlust kann jedoch die Leistungsfähigkeit zur Optimierung signifikant beeinflussen, selbst wenn die Durchdringungsrate 100 % beträgt. Gründe dafür können entweder fehlgeschlagene übertragene Routenempfehlungen sein, die ihren Empfänger nicht erreichen, oder dass die vermeintliche Information über die aktuellen Straßenbedingungen aufseiten des Routers veraltet ist. Die Anforderungen von verschiedenen Optimierungsalgorithmen an das Kommunikationsnetz können natürlich variieren, weshalb im dritten Teil der Arbeit zwei generische Verzögerungsmodelle für übertragene Nachrichten vorgestellt werden. Diese Modelle sind grundsätzlich unabhängig vom zugrundeliegenden Kommunikationsstandard und auch vom Routing-Algorithmus. PCMA* wird hinsichtlich seiner Leistung mit unterschiedlichen Zeitverzögerungen und Wahrscheinlichkeiten von Nachrichtenverlusten evaluiert, indem die eingeführten Verzögerungsmodelle in den Verkehrssimulationen angewendet werden. Darüber hinaus werden Rahmenbedingungen sowohl der Verzögerungs- als auch der Nachrichtenverlustwahrscheinlichkeit definiert, die erforderlich sind, um bestimmte Verbesserungen erzielen zu können. Die Ergebnisse in diesem Teil zeigen eine hohe Robustheit von PCMA* gegenüber unterschiedlichen zeitlichen Verzögerungen und Verlustwahrscheinlichkeiten der Nachrichten. Diese drückt sich im Vergleich mit einer Parametrierung ohne Verzögerung durch ähnlich niedrige erreichte durchschnittliche Fahrzeiten für den Großteil der untersuchten Simulationskonfigurationen aus.

Acknowledgments

Working on my PhD has been a great experience I do not want to miss any more. It has been a continuous process of learning which improved myself in many directions, gaining both subject-specific and personal skills. It often challenged me to attack new problems, stay focused and not to give up, what strengthened my stamina a lot. However, it would not have been possible without the support and assistance of many individuals, to whom I would like to express my deep gratitude.

First, I would like to thank my supervisor Christoph Mecklenbräuer for cautiously guiding me towards graduation. It was a charming and instructive experience to work together during the past years. Thank you for showing confidence in my work and giving me enough time to comprehend the diverse aspects of your field of science - while also being open-minded for new ideas. Further, I would like to thank my reviewers Andreas Springer and Günter Emberger for their valuable input and also for opening up new perspectives of this interesting research area.

This work would not have been possible without the support of Gerald Ostermayer from the FH OÖ in Hagenberg. Not only did he develop the initial project idea as the basis of this research, he significantly contributed to my decision to start scientific working. Thank you for lots of interesting discussions, lunches we had together and also the motivation originating from our meetings, from which I profited immensely. I still can't explain how you managed to motivate me in a way that I had a better feeling and attitude after each of our talks than before, without exception. These countless hours are definitely one of the main reasons that enabled a successful completion of my PhD, for what I owe a debt of great gratitude towards you.

Special thanks also go to my current and former colleagues of the research group *Networks and Mobility (nemo)* in Hagenberg, especially Manuel Lindorfer, who is a great enrichment not only for our team, but also personally. In addition, I had the great pleasure to attend many conferences over the last several years, and the privilege to get to know a lot of great people there. Thanks to all colleagues I met, for interesting discussions, enjoyable evenings and mind-opening talks.

A very important part of my life and certainly also during the work on my PhD plays my family, who always gives me sufficient backing and support to achieve my goals. Thanks to my parents, who significantly supported me at all times, especially at the beginning of my studies in Hagenberg. Furthermore, I am very proud of my dearly loved daughters Julia and Lena, who often provide welcome variety in thinking and remind me of the really important things in life.

More than to anybody else, a really special thank you is due to my beloved wife Birgit for being extremely patient with me and helping me to keep my feet firmly on the ground. I am indebted to you for always giving me what I needed most, ranging from personal advice to a delicious meal or a cup of coffee together. Although it was sometimes definitely not easy, you stood and stand by me uncompromisingly, and with that encouraged me to complete this work.

Contents

Abstract	vi
Kurzfassung	viii
1 Introduction	1
1.1 Motivation	2
1.2 Overview	3
1.3 Aspects Related to Transportation Engineering	5
1.4 Thesis Organization	10
2 Elements of Vehicular Simulation	13
2.1 Simulation Theory and Background	14
2.1.1 Macroscopic Simulation	14
2.1.2 Microscopic Simulation	15
2.2 Models for Microscopic Traffic Simulation	15
2.2.1 Longitudinal Models	15
2.2.2 Lane Change Modeling	17
2.2.3 Cooperative Longitudinal and Lane Change Behaviour	18
2.2.4 Fuel Consumption Model	21
2.2.5 Model Validation	24
2.3 Overview of TraffSim and Capabilities	24
2.3.1 Simulation Mode	25
2.3.2 Data Recording	25
2.3.3 Intersection Regulation	26
2.3.4 Road Infrastructure	29
2.3.5 Routing	31
2.4 Vehicular Routing Basics	31
2.4.1 Dijkstra Algorithm	32
2.4.2 A* Algorithm	32

2.5	Categories of Traffic Optimization Systems	32
2.5.1	Dynamic Traffic Assignment (DTA)	32
2.5.2	Reactive Algorithms	33
2.5.3	Predictive Algorithms	33
3	The PCMA* Routing Algorithm	35
3.1	Introduction	36
3.1.1	Basic Routing	36
3.1.2	KSP Routing	37
3.2	Conception of PCMA*	39
3.2.1	Routing Graph Weighting	39
3.2.2	Congestion Detection	40
3.2.3	Footprint Calculation	41
3.2.4	Prediction Methodology	45
3.2.5	Vehicle Selection	46
3.2.6	Simplified PCMA* Example	48
3.3	Validation	49
4	V2X Communication Modeling	51
4.1	Communication Technology Overview	52
4.1.1	Applications	52
4.1.2	Important Technologies	53
4.1.3	Comparison	56
4.2	Abstract Modeling of Communication	58
4.2.1	Background Overview	58
4.2.2	Basic Radio Propagation	59
4.2.3	Abstraction	60
4.3	Message Exchange	61
4.3.1	Types of Messages	61
4.3.2	Sequence of Communication	62
4.3.3	Exceptional Cases	62
4.4	Delay Modeling	65
4.4.1	Geometric Delay Model	65
4.4.2	Uniform-loss Model	66
4.5	Validation	67
5	Evaluation Insights	69
5.1	Simulation Environment	70
5.2	Prediction Efficiency	72
5.3	Assessment of Routing Algorithms	73
5.3.1	Procedure of Analysis	73
5.3.2	Parameter Survey	74

5.3.3	Preconditions	77
5.3.4	Time and Fuel Consumption	78
5.3.5	Travel Distance	80
5.3.6	Vehicle Density Variation	81
5.3.7	Computational Cost and Complexity Analysis	89
5.4	Variation of PCMA* Penetration Rate	91
5.4.1	Procedure of Analysis	91
5.4.2	Penetration vs. Travel Time	91
5.4.3	Fuel Consumption, Carbon Emissions and Travel Distance	95
5.5	Investigation on Unideal Conditions	96
5.5.1	Success Rate of Periodic Messages (PMsgs)	96
5.5.2	Parametrization of On-Demand Messages (ODMsgs)	98
5.5.3	Fuel Consumption and Travel Distance	101
5.5.4	Volume of Transmitted Data	102
5.5.5	Perceptions	103
6	Conclusions and Outlook	105
6.1	Performance	106
6.2	Robustness in Suboptimal Conditions	107
6.3	Critical Evaluation of Transport Planning Issues	108
6.4	Future Directions	111
	List of Acronyms	113
	List of Symbols	117
	Bibliography	119

1

Introduction

THE volume of road traffic increases steadily, especially in conurbations and areas of high population density. Traffic jams cause, in addition to issues for the drivers stuck in congestion, huge public cost for cities or countries, and should therefore be reduced. For that reasons it is important to learn and understand how to deal with this problem, and to achieve an improvement by intelligent control and management of traffic, if not even trying to reduce traffic emergence.

1.1 Motivation

Congestion on the road is a major problem throughout the world, especially in urban and metropolitan areas. Increasing emergence of individual transport leads to big challenges in traffic management. Beyond doubt, traffic jams are manifest in many urban areas worldwide, and are disadvantageous for both travel costs and safety. A growing number of vehicles makes these problems more serious. Urbanization of people living in the surrounding areas of bigger cities and commuting to their work places is also a problem for road capacities [1]. By 2050, there will be 9.7 billion people in the world [2], 70 percent of whom will live in cities [3]. Global studies such as the Mobility Scorecard of the Texas Transportation Institute [4] or the INRIX Global Traffic Scorecard [5], which is one of the largest and a very detailed study of congestion to date, brings these facts to numbers. Accordingly, Americans spent over 42 hours per year in traffic jams on average, led by commuters in Los Angeles with an astronomic number of 104 hours of sitting in traffic jams per year. In the UK, this number was figured out to be 32 hours, in Germany 30 hours on average per driver. It was shown that this time corresponds to about 9 percent of the total travel time, averaged across 1064 cities in the world. Using Germany as example to analyze the cost of congestion, the INRIX study reveals €1.531 financial burden for each German driver and a total national congestion cost of over €69 billion in 2016 [5]. Beyond doubt, there exist more than the above-quoted consequences of an increasing individual traffic emergence, especially when focusing the environmental aspects. Negative effects are observable in the form of pollution, greenhouse emissions and noise.

The necessity of working against this formidable challenge seems obvious. Although traffic jams and congestion may seem to be inevitable in heavily overloaded situations, a great deal of effort takes place to improve the situation. In order to address these issues, road operators invest huge amounts of money to extend and improve existing infrastructure in order to provide the needed capacities. In the last decades, the paramount reaction on an increasing amount of vehicles was the expansion of road infrastructure, also due to lack of knowledge and alternative solutions. More roads with higher capacities were built, with both enormous planning and financial effort. In addition to broadening highways, nowadays coordination and regulation of this vehicular traffic is indispensable and can significantly improve traffic flow, reduce waiting time and cost for both the individual drivers and road operators. These days, variable speed limits, dynamic warning signs and important information can be displayed on demand on overhead traffic signs. Traffic jams, hazardous situations or upcoming environmental influences can be announced by the electronic traffic guidance system timely, so that the negative consequences are minimized [6] and traffic flow is improved. However, the possibilities of information dissemination are limited at the present time. In order to fight traffic jams target-oriented, changing the routes of some vehicles could be one solution that leads to advantages not only for the

rerouted drivers. Also, other drivers that are affected by a congested area may benefit from detours, which to some extent relieve the situation.

1.2 Overview

Basically, vehicular routing is indeed not a new topic in literature, but has been attracted the attention of research community for more than 50 years [7]. The density of traffic surveillance infrastructure on the road increases steadily, which allows traffic control operators to collect large amounts of data continuously. The traffic conditions can be monitored by flow detectors or cameras [8,9], which provide information for the authorities to inform drivers of current traffic conditions, accidents or road works. Other approaches of information gathering make use of mobile navigation devices or smartphones owned by the drivers to collect data and provide traffic information for their directly or indirectly paying customers. Examples are companies as Google [10,11], TomTom [12] or Microsoft [13,14]. Although also owned by Google since 2013 [15], 'waze' is a community-based and free online portal. Users are encouraged to provide current traffic data passively by a smartphone app. Additionally, one can actively report accidents or other important information and share this information - and of course also benefit from other users' reports [16, p. 44]. Certainly, the quality and topicality of information in all aforesaid user-dependent mechanisms are strongly reliant upon the user activity within a certain area. Few and sparsely distributed active participants cause bad coverage of information sources, and impede the determination of current and future conditions.

However, recent development in communication technology, infrastructure and standards enables application of cooperative and dynamic algorithms for automatic vehicular routing in practice. Obviously, there are more than the mentioned arguments for thinking of solutions to traffic problems, summarized as ITSs. Modern vehicular communication systems allow fast and accurate information propagation, and are the basis and prerequisite for the proposed approach. Within the scope of this thesis, a novel approach which tries to minimize or in the best case avoid traffic jams and standstill of vehicles is introduced. It is called PCMA* (**P**redictive **C**ongestion **M**inimization in combination with an **A***-based router) [17]. Most drivers may have experienced the situation where the information of an upcoming traffic jam arrives too late, what prevents from taking a spacious detour that allows to pass by the jam completely. Depending on the road network, a new route which is both far away from the original one and still not much longer in estimated travel time could be available, but the decision whether to use the original route must be made at a time where both routes seem to be free from congestion. Especially, but not only in such cases, a well-functioning and reliable prediction of future conditions can support the decision-making entity, whether this is a human or a machine. The PCMA*

algorithm predicts congestion spots prior to incidence in order to facilitate actions to be taken as early as possible. Naturally, not all future congestion can be solved this way. Therefore, PCMA* is also able to detect already existing traffic jams and react to those appropriately by calculation of alternative routes for the affected vehicles.

In order to carry out the mentioned tasks, information about the current road conditions are required. In the first stage, a fully functioning, latency and error free communication system is assumed, meaning that the router has complete knowledge of all necessary data. Although the technical features of current factory-fresh vehicles are often more than sufficient for making use of vehicular communication, it will still take decades until the penetration of vehicles that are able to both utilize the services and also provide valuable information reaches 100 percent. Of course, this claim assumes the question of how different companies and stakeholders could work together to be answered. According to [18], 50 percent of factory-new cars are connected somehow already by 2015, either by smartphone or embedded solutions. Approximately in 2025, every new car will be equipped with some kind of communication device. Obviously, it will still take multiple years from then until unequipped vehicles disappear more and more from the streets and their percentage will become negligible. Therefore, this thesis addresses also the difficulties related to this topic in the second stage. It analyzes how PCMA* behaves with penetration rates of vehicles that are able to communicate below 100 percent. Depending on the methodology of information gathering, this means incomplete knowledge of the current situation on the road. Moreover, it does also imply the impossibility to provide routing information for some of the vehicles on the road. In other words, the routing intelligence does not know anything of unequipped vehicles nor can it provide routing advice for them - they simply appear invisible. I analyze the performance by the help of microscopic simulations and application of the predictive rerouting algorithm PCMA* [17] with varying penetration rates and traffic densities.

The performance of intelligent cooperative vehicle routing algorithms such as PCMA* also depends on the quality of the information exchange by V2X communication. Ideal information exchange with no delays and perfect communication conditions does not exist in reality. In fact, the conditions can vary substantially depending on the infrastructure and environment [19] and therefore can significantly reduce the functioning ability of an intelligent traffic routing. The robustness of PCMA* against unideal communication conditions including delays and data loss is analyzed as a third major contribution. The border between achieved improvements that satisfy the operator of such an intelligent traffic optimization system to a bad performance is not hard, but to a greater degree follows a smooth behavior - depending on the communication quality, as the investigation shows. Instead of assuming defined properties of the network and determining how well a routing algorithm can perform by applying them, the problem is redefined by using

abstractions of channel models with few characteristic parameters, which can be used to characterize the necessary properties of the underlying communication standard.

1.3 Aspects Related to Transportation Engineering

Traffic on the road is often described to be comparable to liquids from the perspective of transportation engineers [20]. Basically, the liquid must pass through the road network and chooses the line of easiest resistance. In urban areas, the situation may to a greater extent be related to a gas, which tends to fill the available space [21]. Analogous to fluids, improvements in connection to road traffic of diverse kinds, be it capacity-increasing improvements of infrastructure or application of ITS also attract drivers which usually intend to use other routes, drive at different times or use an alternative transportation type. This circumstances eat up a certain part of the accumulated benefits again. The effect is comparable to the economic balance of supply and demand, which indicates the increase of a good's consumption as its price decreases. Put in other words, any change in available capacity can mean a shift in time or route of individual drivers, for example that commuters may less tend to avoid peak periods if the shortest route is at a lower congestion level during these periods.

Additionally, an increased total motor vehicle travel is a consequence. Practical reasons could be for example that the motivation to car pool is not at a sufficiently high level, and individual transport becomes more attractive since the experienced cost regarding travel time is lower due to lower congestion. Furthermore, migration to urban areas and also moving away from the city centers to suburbs is more attractive in case of a satisfying traffic connection. This further increases traffic volume [22]. Not least, population growth is a major contributor [23]. Research in travel time budget also shows that people tend to accept spending a defined time per day for mobility - regardless of the current traffic conditions [24]. Consequential, the travel distance varies, and the willingness of drivers to accept trips in congested situations is lower. Figure 1.1 illustrates a theory of supply and demand, stating that traffic volume grows until congestion occurs, and then flattens due to higher cost for drivers as a result, represented by the blue curve. The shown projected traffic growth seems to indicate the necessity of intervention for operators. As soon as the capacity is increased e.g. by additional lanes, this process repeats and again levels off as soon as equilibrium is achieved again (red curve) [25].

The future consequences of new traffic attraction by increasing road capacity can be distinguished into short-term, i.e. vehicles switch from other routes or mode shifts, and long-term effects [26]. The latter describe the accumulation of short-term effects over years, such as land use changes or overall increase in automobile dependency. The impacts are present in literature since the early 1960s [27] and referred to as *Generated Traffic* for

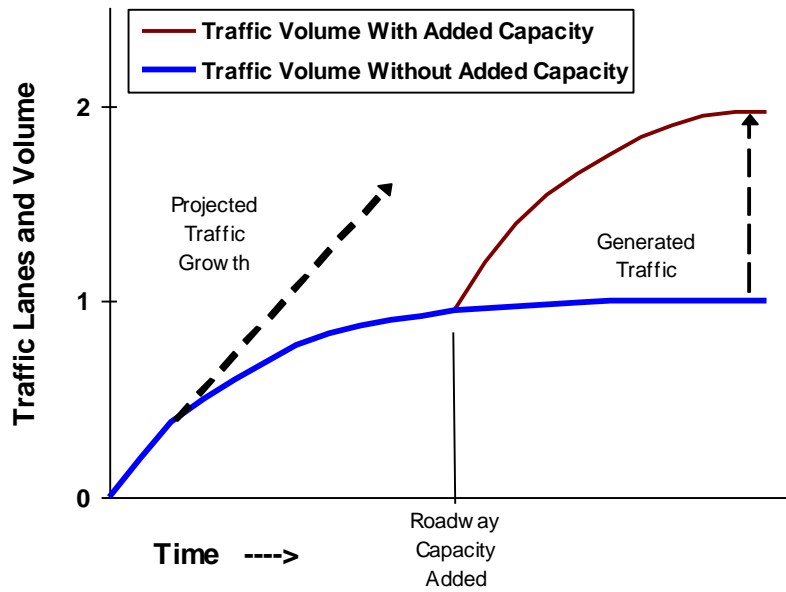


Figure 1.1: Generated Traffic by Road Capacity Expansion [25]

the short term [25] and *Induced Demand* or *Induced Traffic* for the long-term [25, 28–30]. These ratios define which percentage of the provided, increased road capacity is filled up again with newly generated traffic. The lower bound is obviously zero (no new traffic occurs), whereas the majority of references refer to an upper bound below one. But still, there exist documents which present results of an induced demand of 1.0 [31], or even greater than that [32].

The following list contains a brief summary of relevant projects from literature.

- The study of Hansen et al. in [23] analyzes the relationship between the available lane-miles supplied by highways, and the traffic, which is measured in Vehicle Miles Traveled (VMT). They consider data from the state of California, US from the years 1973 to 1990 and come to the conclusion that the induced demand (called lane-mile elasticity in this paper) is between 0.6 and 0.7 for urban areas, and 0.9 at a metropolitan level. According to the results therein, the impacts materialize within five years. The findings further include no evidence that the increase in state highway-miles has affected other traffic, but however, the authors append that the used data was limited for off-state highways.
- A very popular work regarding this topic is authored by Noland et al., who performed empirical measurements in the United States which quantify the amount of added traffic. Their results comprise an induced demand of half of the increased road capacity within 5 years. The authors further claim that "eventually 80 per cent" (induced traffic of 0.8) will be filled up in the long run [30].

- A distinction between two types of induced demand is made by a more recent work by Hymel et al. [28]. Those are on the one hand the accessibility increase of new locations and underdeveloped areas, and attraction of new traffic due to reduced congestion on the other hand. In summary, the estimated values for induced demand are based on VMT and income. The investigation yields values for induced demand of 0.05 in the short run and 0.16 in the long run. The presented results are at the low end with regard to the available literature, but the authors compare their results to other results (to the work from Noland [30], among others). They further argue that they considered total traffic on a wide area in contrast to other investigations, and most of the capacity expansion effects would occur only in highly congested urban areas. Additionally, the differences in results could be explained by different measurement time spans, capacity measures or other deviations in control variables.
- Cervero et al. [33] introduce a model which also accounts congestion for both interested time intervals by examining a freeway project in California, US. Over a 15-year period, the induced travel elasticities result in 0.10 and 0.39 for the short and long run, respectively.

Transportation elasticities can be calculated by several formulas based on different performance measures, which could be travel distance (VMT), vehicle emissions or travel time (Vehicle Hours Traveled (VHT)), among others [34]. "Elasticity" basically is described by the following general definition:

"An elasticity gives the impact of a change in an independent (or stimulus) variable on a dependent (or response) variable, both measured in percentage changes." [35]

In principle, the additionally materializing values which are determined after the capacity improvement are divided by a quantification of added capacity, such as equation (1.1) indicates.

$$\text{Elasticity} = \frac{\Delta \text{VMT}}{\Delta \text{LaneMiles}} \quad (1.1)$$

With respect to the existing investigations, it is certainly not easy to make a globally valid statement related to this issue [26, 28, 36, 37]. A comprehensive meta-analysis of different approaches and studies in literature can be found in [34]. The authors analyzed numerous studies and summarized the results for induced demand values separated into short and long-term (i.e. up to about 5 years and beyond that time, respectively), what is reproduced in figure 1.2. It reveals the significantly differing result values manifesting from numerous studies [23, 29, 31–33, 38–44]. The short and long time horizon separation

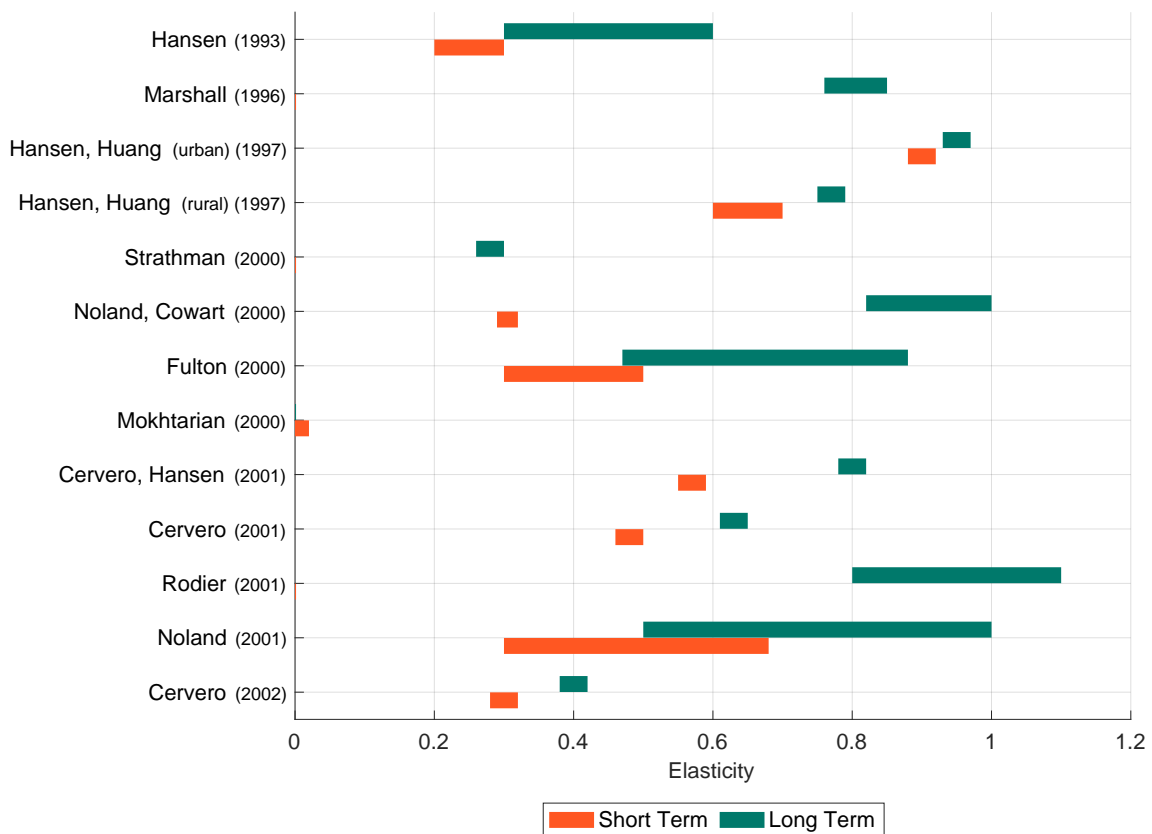


Figure 1.2: Comparison of Different Approaches for Determination of Induced Traffic (Elasticity) (reproduced from [34, p. 21] by permission of the authors)

is represented by the orange and green bars of figure 1.2 for each study. The differences in studies derive from the circumstance that not all studies bring up both time horizons. However, one investigation even shows divergent results for urban and rural environments [23].

The quantification how much capacity will be filled up depends on many influencing factors, including the road structure, economic influences and statistical evaluation method. Induced demand also is subject to the size of investigated area, since diverted trips cause more effects on single routes than they do on a more spacious regional area [23, 34]. In addition, the prediction strength of different studies is not clear even if the models replicate the road conditions precisely, since the parameters on which these studies base on still need to stay constant over time for the results to be correct.

The uncertainty of the predictions is revealed by the example of two different investigations applied to the same data, which argue in somewhat contrary directions. In [45], the central statement predicates little improvements to a higher level of service through adding road capacity due to the high increase in VMT of 0.9% related to a 1.0% increase in lane miles (remark: induced demand = 0.9), according to the authors. But still, it

is pointed out in the conclusion that convergence to any individual highway project may not be the case. Quite contrary to this work, Mokhtarian et al. [42] find no significant coherence between increased capacity and newly generated traffic for the very same data, just by applying a different methodology. Moreover, the used database containing traffic data was extended by six years by the authors of [42], which have become available in the meantime. They disagree with the initial study and believe the reason for the divergence in results is overestimation due to wrong attribution of the new traffic to induced demand, rather than other uncontrolled factors. The authors compare the so-called Average Daily Traffic (ADT) of selected improved and unimproved road segments between 1976 and 1996 (in contrast to VMT, which is used by other studies), and find no distinguishable statistical growth rate in the observation period. They claim that capacity expansion has a negligible effect on traffic growth during the observation period.

This once more points out that the studies from literature reflect in each case a certain, specific situation and cannot be projected to any individual other environment easily, what is also emphasized by several of the cited works, regardless of their conclusions. The two hypotheses

1. *"Traffic will not be affected significantly, meaning the volume stays approximately constant and thus density decreases with the application of ITS."* and
2. *"Newly generated capacities do not improve traffic flow in the long run, but solely lead to higher traffic volume since the available capacities are filled up by generated traffic completely."*

will presumably both not hold. To a greater degree, the truth will lie somewhere in-between [38, p. 62].

In the end, however, an improved travel comfort can be achieved by a combination of the following fields of application [42]:

- **Expansion of infrastructure:** Although this is very cost-intensive, arguments that were already mentioned above such as an increasing world population and urbanization make broadening of roads, adding highway lanes and building of new roads necessary to a certain degree.
- **Traffic avoidance:** As a central instrument of transportation science, the stimulation of people's motivation to use transportation types different to motorized private transport (i.e. passenger cars) or carpooling plays an important role. More sophisticated land-use planning can be applied to decrease traffic demand. Of course, less individual vehicles cause relaxation and decrease congestion probability.

- **Optimization of the utilization of existing infrastructure:** Basically summarized as ITS, technical progress in car development, new communication standards and technical improvements of the infrastructure open up many new possibilities to improve traffic flow and increase efficiency. This can be changes in travel time, intended detours as well as different starts and destinations to avoid rush hours.

The main focus of this thesis lies on detailed investigations related to the third bullet point. Tremendous research effort is made in this field, and new technical possibilities such as autonomous cars will further increase opportunities. Without any doubt, the remaining topics are not at all negligible. Therefore, section 6.3 discusses constraints for the proposed methodology and analyzes it from a different perspective. Notwithstanding, the potential of a more efficient use of the existing road infrastructure is very high, as this thesis reveals and describes fine-grained in chapter 5.

1.4 Thesis Organization

During the work on this thesis I published several papers as first author or together with research colleagues as co-author. The content of most of them is discussed in this final thesis, also have some passages been quoted verbatim from the following papers and articles. In [46] and [47], the traffic simulator *TraffSim* which was used for all simulation experiments within this work is introduced. Those papers give an overview of the basic architecture of *TraffSim*, including available functionality and applicable models. Additionally, we developed a mechanism to generate virtual road networks, which can further be used to carry out vehicular traffic simulations [48]. The generation process uses a Lindenmayer system [49] and takes the environment such as the geographic terrain, rivers and woods as well as the population density into consideration to customize the road density. In [50], an intersection control is introduced for various types of road crossings and highway ramps and exits as well as multiple control strategies such as traffic lights, traffic signs or unregulated intersections. Subsequently, [51] presents isolated traffic control strategies within *TraffSim*. The concept for an extension to existing lane change models which enables cooperative behavior is explained in [52], while [53] analyzes the performance of the model. The PCMA* rerouting algorithm is presented and evaluated in [17], while [54] analyzes the ability of PCMA* with varying penetration rates. The robustness of dynamic routing algorithms towards non-ideal communication delays by example of PCMA* is analyzed in [55].

The following publications are not directly related to this thesis and therefore not included. We introduce an LTE system level simulator and present investigations based on simulation results of this simulator in [56]. Those comprise effects of inhomogeneous distribution of up- and downlink users, and the potential of Long Term Evolution (LTE) Time

Division Duplex (TDD) to adapt the capacities and react to this asymmetry. In [57], we analyze the side benefits of vehicular rerouting in the context of inter-vehicle communication. The local density of vehicles decreases due to detours, which further can improve communication reliability based on a lower local concentration of communication nodes. Possible heuristic optimization approaches related to vehicular traffic simulations are ranked in [58]. The medium access of Institute of Electrical and Electronics Engineers (IEEE) 802.11p is modeled and an algorithm to reduce the complexity of the communication network while retaining its properties is introduced in [59]. Finally, [60] treats human driving behavior injection into *TraffSim*.

The remainder of this thesis is organized as follows:

The next chapter 2 gives an overview of vehicular traffic simulation including backgrounds and routing capabilities, with special regard to the mostly used models. In chapter 3, the PCMA* algorithm is introduced and elucidated in detail. Chapter 4 gives insights into communication technologies, especially in vehicular environments as well as the applied message delay models. The outcome of the conducted investigations including an algorithm comparison as well as simulations with distinct penetration rates and unideal communication delay is presented in chapter 5. Chapter 6 concludes the thesis and contains thoughts for future work.

2

Elements of Vehicular Simulation

Modeling of vehicular road traffic is a broadly diversified topic. It has serious consequences for human drivers, residents of roads, animals and the environment how we manage to travel from one location to another. In order to investigate the influence of traffic management, simulations are a practical and often the only feasible instrument for prediction of the impacts of different deployed applications.

2.1 Simulation Theory and Background

Modeling of vehicular road traffic is a very complex topic. It has serious consequences for human drivers, residents of roads, animals and the environment how we use vehicles to travel from A to B. With respect to the steadily increasing traffic volume, it is essential to deal with the big amount of vehicles optimally to minimize the driving time, traveled distance and subsequently exhausted emissions. Traffic jams cause, in addition to the mentioned issues, huge public cost for cities or countries, and should therefore be reduced. For that reasons it is important to learn and understand how to deal with this problem, and to achieve an improvement by intelligent control and management of traffic.

In order to investigate the influence of traffic management and put the results into numbers, simulators are a practical instrument for trying to predict the impacts of different deployed applications. Various situations and parameters can be set up with the objective of prognosticating possible implications resulting of the input change. In many cases, real time experiments are infeasible or even impossible to perform, be it because of the high number of involved vehicles or the impracticality of reproducing the same situation with different parameters to show their influence. Generally, simulators for vehicular traffic can mainly be classified in microscopic or macroscopic types, depending on the granularity of investigation, temporal resolution and level of detail [61].

2.1.1 Macroscopic Simulation

Macroscopic models deal with the traffic properties in a coarse level of resolution as aggregated characteristics rather than single vehicles' properties. Traffic is modeled as a compressible fluid or gas with the main properties of interest vehicle flow, spatial density and average velocity [62, 63]. The equations are similar to fluid dynamics, at least in free-flowing conditions. In contrast, some fundamental differences can be recognized in congested conditions [64]. That is why in practice microscopic models are often used, from which the parameters for the macroscopic models are derived. Also, mesoscopic models, which analyze groups of elements of transportation (such as platoons) can be used to derive those parameters. In other words, this means that it is in some cases required to model concrete situations of interest in detail, if key aspects depend on exactly those. The representative results can consequently be used to configure and customize the macroscopic models. An advantage is the resource-efficient simulation of multilane traffic by effective one-lane traffic [65] and statistical modeling of overtaking maneuvers. Generally, macroscopic models allow much faster and computationally efficient simulations by encapsulation of vehicles to continuity equations, at the price of results with lower detail level. Additionally, it is tricky to describe nonlinear phenomena [64, 66] and to find one out of many existing macroscopic models that fits best to the specific kind of application [67].

2.1.2 Microscopic Simulation

In contrast to the aforementioned models, microscopic simulation models represent each vehicle as a single particle in the system. Each simulated unit has its defined counterpart in reality. Vehicle dynamics such as acceleration behavior, discrete lane change maneuvers, interactions between vehicles and intersection crossings are modeled in detail and individually. The complexity and computational effort for calculation is therefore many times higher than for macroscopic models. A huge amount of outside influences must be considered, which include assessment of speeds, braking and acceleration distances, interaction with other vehicles as well as consideration of traffic signs, traffic lights and traffic laws. Basically, a microscopic model needs to represent all abilities that a human driver learns at the driving school combined with the perception of the environment [68]. Depending on the model, different parametrization allows the application of various electronic systems starting with driving assistance via partial or full automation up right through to autonomous driving. All these technical supporting mechanisms and their influences can be represented in detail for simulations by microscopic modeling.

With respect to the focus of this thesis, it is important to enable investigations on ITS and Advanced Traffic Management (ATM), which is one of the main objectives of micro-simulation [69]. Detailed modeling of intersections as well as the combined application of urban and highway scenarios is required to enable fine granular results and reveal the reasons for differences in simulation results. Another key aspect is the precise modeling of fuel consumption. In view of the required information exchange between vehicles and the routing entity, the provision of results with non-ideal communication environments implies the usage of microscopic models, since both the point in time and the concrete vehicle where the problem occurs matter.

2.2 Models for Microscopic Traffic Simulation

In this section, models for the experiments that were carried out within the context of this thesis are introduced. Amid numerous investigated and countless existing models in literature, only those which are relevant for the presented experiments are introduced here.

2.2.1 Longitudinal Models

This kind of models controls the movement of vehicles along the road, i.e. acceleration and speed. The used longitudinal models generally base on the comprehensive work of M. Treiber and A. Kesting in [70] and are implementations of the car-following models Intelligent Driver Model (IDM) and Extended Intelligent Driver Model (EIDM) [71]. Those models are both complete, which means accident-free and are dedicated to produce

acceleration profiles that are plausible and also could stem from a human driver. They produce smooth acceleration curves and provide controllable stability properties [72].

The following basic requirements are defined for all models [70]:

- The vehicle accelerates to the desired target speed in free-flow.
- The chosen acceleration is dependent on the distance to the front vehicle, i.e. the acceleration decreases as soon as the distance does, and vice versa.
- In situation with dynamically approaching vehicles, the acceleration decreases as the approaching speed increases (e.g. in case of a slowing down front vehicle), and vice versa.
- A safe distance between two vehicles is defined, which must not be undershot.
- The braking maneuvers are soft in normal situations, which means the acceleration must not be less than a defined safe deceleration. Furthermore, the comfortable acceleration is exceeded in critical situation, but not longer than necessary.
- Smooth transitions between driving modes are guaranteed. The acceleration function is therefore continuously differentiable.

The basis of all those models is the IDM, which is the simplest of the mentioned.

Equation (2.1) describes the calculation of the new acceleration a_{new} value according to [70, p. 188].

$$a_{new} = a * \left(1 - \left(\frac{v}{v_0} \right)^\delta - \left(\frac{s^*(v, \Delta v)}{s} \right)^2 \right) \quad (2.1)$$

The current speed v is considered in relation to the target speed v_0 , analogous to the current distance to the front vehicle s which is compared to the target distance s^* , (equation (2.2)). The exponent δ represents the aggressiveness of the driver, that is how fast and intense he or she reacts to changes of the front vehicle.

$$s^*(v, \Delta v) = s_0 + \max \left(0, vT + \frac{v\Delta v}{2\sqrt{a * b}} \right) \quad (2.2)$$

The target distance depends on the current speed v and the speed difference to the front vehicle Δv . It includes the minimum distance between two vehicles s_0 , the travel time T since the last update. The 'intelligent' acceleration strategy also includes the comfortable acceleration a and safe deceleration value b .

As also emphasized by the authors, the original IDM model basically is applicable for single-lane roads and does not consider any external influences as are the case in intersections or multi-lane roads [70]. Therefore, the EIDM was introduced and avoids unnaturally strong braking reactions in case of another vehicle changing its lane and becomes the new front vehicle, which is called Constant-Acceleration Heuristic (CAH) by

the authors [71]. Additionally, this model is described to have characteristics related to modern Adaptive Cruise Control (ACC) assistance systems, and is therefore used for this purpose. For more details regarding it is referred to [71].

The EIDM model partially counteracts weaknesses of the IDM, but only those that are related to lane change maneuvers. The behavior modeling of vehicles in and before intersections or highway ramps and exits is a complex task, and is not covered by the proposed longitudinal models, neither is it by any existing longitudinal model of my knowledge. Comprehensive intersection modeling requires interaction between intersection control algorithms, lane change algorithms and lengthwise movement, which is basically out of scope of a basic longitudinal model.

2.2.2 Lane Change Modeling

The lane-changing rules in my experiments base on the model Minimizing Overall Braking Induced by Lane Changes (MOBIL) [73]. As the name suggests, the decision whether to change to a neighbor lane is calculated by considering both the utility of the current lane as well as the benefits or risks of a potential target lane. Additionally, the impacts of a lane change on vehicles on the target lane are examined. The latter feature is what differentiates MOBIL from other, egoistic lane change models, as other vehicles are considered to a defined degree.

The core functionality of MOBIL is the calculation of a balance between the current and a possible target lane in terms of acceleration. It considers the old front and back vehicle (OF and OB, respectively) as well as the new front and new back (NF and NB). Such a situation is illustrated in figure 2.1.

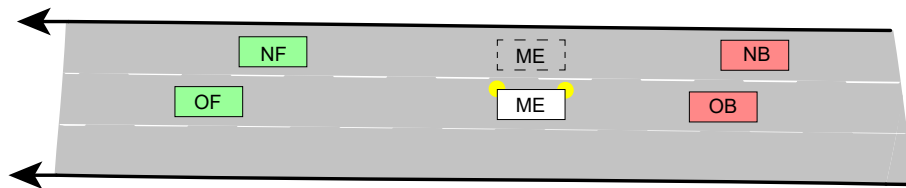


Figure 2.1: Lane change situation with MOBIL

In order to consider traffic rules where driving on the rightmost lane is mandatory, a *bias* is used to urge vehicles to do so, if possible. Additionally, the intensity of consideration of other vehicles' satisfaction with the situation after the lane change can be influenced with a *politeness* factor from 0 to 1. A value of 0 means completely egoistic behaviour, while 1 changes the behaviour so that other drivers' needs are considered at the same level as the own conditions. Equation (2.3) illustrates the calculation of the acceleration

balance according to [70], which is done for possible target lanes to the left and right. If any of the balances are greater than zero, the new target lane is defined. If both fit this condition, the greater of the two balances indicates the more attractive lane. A hysteresis *threshold* should avoid numerous lane changes within a short time.

$$balance = a_{new}^{me} - a_{old}^{me} + politeness * (a_{new}^{NF} - a_{old}^{NF} + a_{new}^{OF} - a_{old}^{OF}) - threshold - bias \quad (2.3)$$

The pseudocode in algorithm 1 describes how MOBILs acceleration balance calculation is implemented.

Algorithm 1 Calculation of prospective acceleration balance [73]

```

1: function CALCACCELERATIONBALANCE(vehicle, targetLane, politeness, bias)
2:   curLane  $\leftarrow$  vehicle.lane
3:   if vehicle has front vehicle then
4:     curFrontVeh  $\leftarrow$  GETFRONTVEHICLE(vehicle, curLane)
5:   end if
6:   if vehicle has back vehicle then
7:     curBackVeh  $\leftarrow$  GETFRONTVEHICLE(vehicle, curLane)
8:   end if
9:   if vehicle has front vehicle on targetLane then
10:    newFrontVeh  $\leftarrow$  GETFRONTVEHICLE(vehicle, targetLane)
11:  end if
12:  if vehicle has back vehicle on targetLane then
13:    newBackVeh  $\leftarrow$  GETFRONTVEHICLE(vehicle, targetLane)
14:  end if
15:  newBackNewAcc  $\leftarrow$  CALCACCVIRTUAL(targetLane, newBackVeh, vehicle)
16:  newBackOldAcc  $\leftarrow$  CALCACC(targetLane, newBackVeh)
17:  meNewAcc  $\leftarrow$  CALCACCVIRTUAL(targetLane, vehicle, newFrontVeh)
18:  meOldAcc  $\leftarrow$  CALCACC(curLane, vehicle)
19:  oldBackNewAcc  $\leftarrow$  CALCACCVIRTUAL(curLane, oldBackVeh, curFrontVeh)
20:  oldBackOldAcc  $\leftarrow$  CALCACC(targetLane, newBackVeh)
   $\triangleright$  Calculate differences for involved vehicles
21:  oldBackDiff  $\leftarrow$  oldBackNewAcc - oldBackOldAcc
22:  newBackDiff  $\leftarrow$  newBackNewAcc - newBackOldAcc
23:  meDiff  $\leftarrow$  meNewAcc - meOldAcc
24:  balance  $\leftarrow$  meDiff + politeness * (oldBackDiff + newBackDiff - threshold - bias)
  return balance
25: end function

```

2.2.3 Cooperative Longitudinal and Lane Change Behaviour

The consideration of different traffic conditions and incomplete knowledge of other vehicles intentions makes the development of comprehensive models for lane change and longitudinal movement more complex. Further, safety plays an important role, as well as smoothness of lane changes. Several microscopic models can be found in literature, which all are designed for specific use cases and have their pros and cons depending on

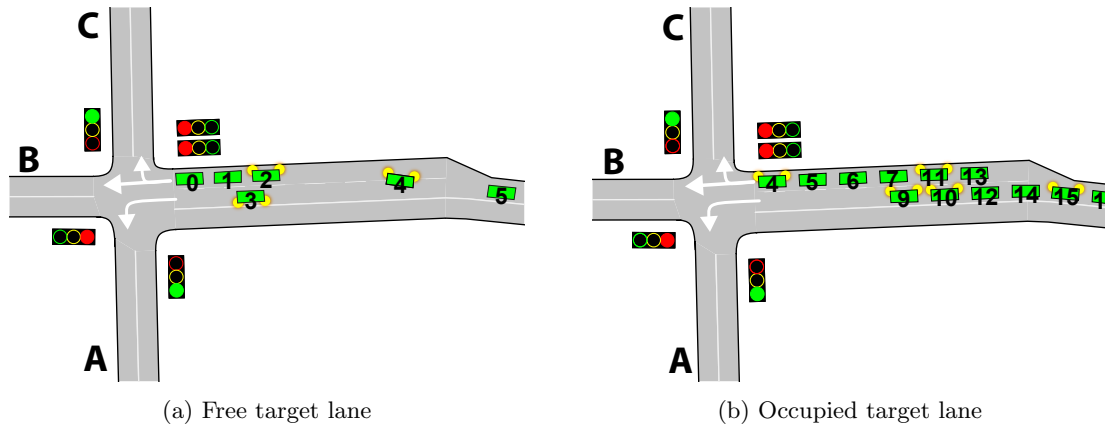


Figure 2.2: Solvable and problematic situations before multilane intersection

the defined requirements, the environment, density of vehicles or characteristics of the road network [74]. An essential capability of such a model is also to be applicable in different situations. A possible intention of changing a lane can be to follow the desired route, which would not be possible on the current lane, which is the main focus of this subsection. In particular, turn restrictions before intersections must be considered. The intention of drivers to switch to the correct lane which allows them to follow their desired route must be executed early enough before entering the intersection in order to enable automatic route guidance through the intersection. Especially in congested situations, individual lane changes are often not possible without the cooperation of vehicles in the neighboring lane, as figure 2.2 shows. In the left part (figure 2.2a, no problem will occur because the target lane for vehicle 4 is free and it can change without any problems. In contrast, figure 2.2b shows a problem situation where the vehicles 9 and 10 intend to move to the right lane that leads to exits B or C, but are blocked by vehicles 7, 11 and 13 which occupy this lane.

Vehicles 9 and 10 cannot stay on the current lane, because the upcoming intersection restricts turns to the left, which is not the intended direction. For this situation to solve, the lane change model on its own cannot achieve satisfying results. Therefore, an interface to the longitudinal model is defined, which can influence the acceleration and movement behavior to let the neighbor vehicle align and merge into the own lane. A comprehensive model also requires consideration of multiple vehicles in front of the subject vehicle, on both the right and left neighbor lanes. As soon as any of the front vehicles expresses its intent to change its lane to the subject lane, the model takes this into account when calculating its acceleration, speed and target lane.

A connection between lane change intentions and longitudinal behavior is inevitable, since the models influence each other [75]. Therefore, I developed *Cooperative Lane Change and Longitudinal Behavior Model Extension (CLLxt)* [52], which is a versatile extension

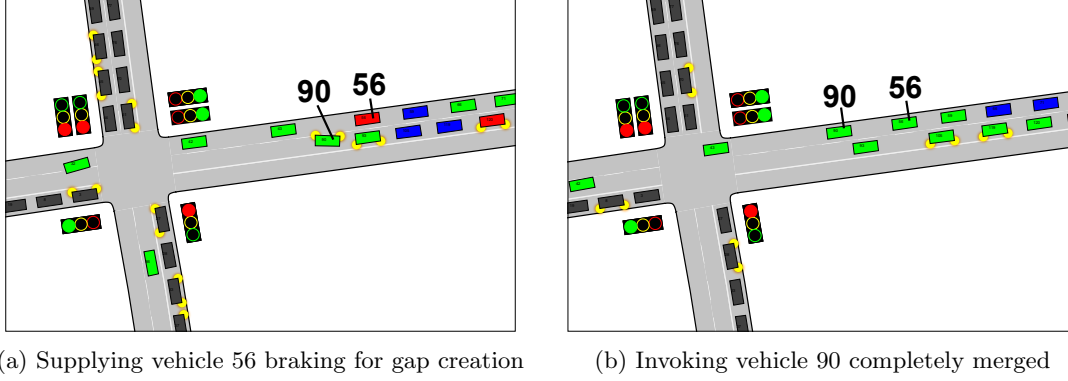


Figure 2.3: Snapshots of lane change maneuver before intersection

to existing longitudinal and lane change models and adds cooperative behavior that is especially relevant in congested situations. After determination of a target lane within a certain distance before the next intersection, an urgency function according to equation (2.4) is applied to quantify the necessity of a lane change, as the vehicle gets closer to the intersection. It depends on the current distance to the junction, denoted as d_{junc} . Additionally, a safety gap D is implemented, which specifies the minimal gap between vehicle and intersection border before the lane change must be completed. Equation (2.5) defines the maximum needed distance d_{change} for reaching the target lane. It is also applicable for more than one lane change by consideration of the difference in lanes between the current and target lane $n_{lanediff}$. The resulting urgency U in the interval $[0, 1]$ is used for slowing down and waiting for a chance to execute the lane change.

$$U = \min \left[1, 1 - \frac{d_{junc} - D}{d_{change}} \right] \quad (2.4)$$

$$d_{change} = (t_{exit} + t_{change} * n_{lanediff}) * v_{limit} - D \quad (2.5)$$

Figure 2.3 shows the applied model in action within *TraffSim*, where the left part (Figure 2.3a) shows the time of decision and the right part (Figure 2.3b) illustrates the situation after completed lane change. The colors of the vehicles denote the current acceleration value, where green means positive acceleration, red describes negative acceleration (braking) and blue and black imply zero acceleration (steady drive and standstill, respectively).

In order to provide better understanding of the influence of CLLxt, figure 2.4 shows history graphs of speed and acceleration over time for the affected vehicles 56 and 90, obtained from a traffic simulation. It's the very same situation as in figure 2.3. The blue solid line represents speed history, the red line shows the acceleration and time is plotted on the X-axis. The green dashed line $t1$ and the orange dotted line $t2$ mark significant

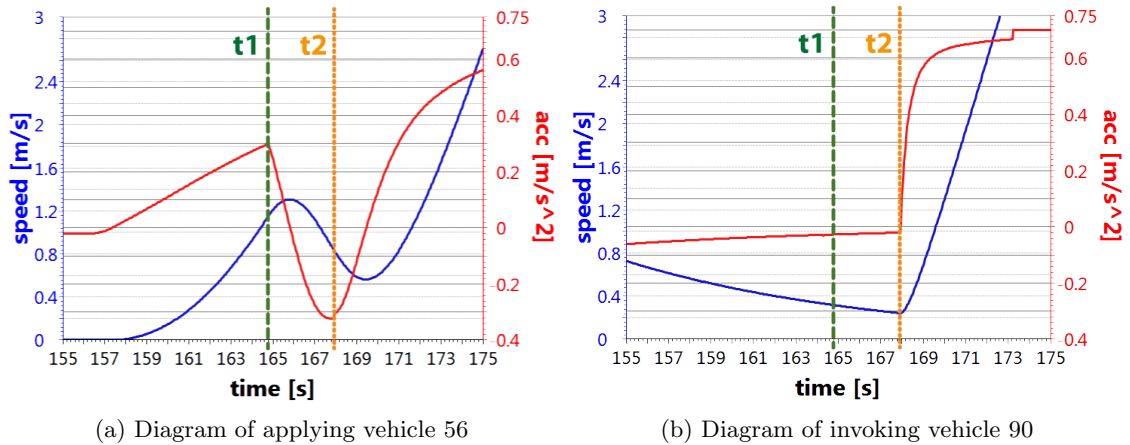


Figure 2.4: Speed and acceleration graphs for both supplying and invoking vehicles

timestamps. At time $t1$, the driver of the supplying vehicle (in this example number 56), recognizes the intended lane change of the invoking vehicle (vehicle 90). This behavior is reflected in a drop of acceleration, which becomes negative and the vehicle brakes. Thus, certainly also the speed drops and the gap between the vehicle 56 and its original front vehicle becomes larger. At time $t2$, the gap is large enough for the invoking vehicle 90 to merge. As a consequence, the acceleration and speed graphs in Figure 2.4b rise and the lane change can be completed. Figure 2.3a depicts the bird's view at exactly this point in time.

For further details regarding CLLxt, it is referred to [52].

2.2.4 Fuel Consumption Model

Since the simulation studies use the consumed fuel as one of the major performance indicators for comparisons and achieved improvements, the way how it is modeled plays a vital role. Especially the influence of acceleration and breaking maneuvers and how traffic jams and stop-and-go-traffic increase fuel consumption is important, and can be modeled by microscopic fuel consumption models [70]. Within all simulations, we use a physics-based model which basically calculates the required power to overcome all kinds of physical resistance.

Physical Fundamentals

The driving resistances are built up of several components and can be divided into steady-state resistances, which occur when traveling with constant speed and dynamic resistances caused by the inertia, which act when a vehicle is accelerating [76].

- Steady-state resistances
 - Rolling resistance F_R
 - Aerodynamic drag F_A
 - Climbing resistance F_C
- Dynamic resistances
 - Inertial resistance F_I

The total driving resistance is calculated by summing up all mechanical forces in equations (2.7) to (2.10), as defined in equation (2.6) [76].

$$F_{total} = F_R + F_A + F_C + F_I \quad (2.6)$$

$$F_R = m * g * \mu \quad (2.7)$$

$$F_A = 0.5 * \rho_{air} * cd * A * v^2 \quad (2.8)$$

$$F_C = m * g * \sin(\phi) \quad (2.9)$$

$$F_I = m * g * a \quad (2.10)$$

Equation (2.7) includes the variables for vehicle mass m , the gravity g of 9.81 m/s^2 and the rolling friction coefficient μ . The aerodynamic drag is dependent of the density of air ρ_{air} , a vehicle-dependent aerodynamic drag coefficient cd , the cross section surface A and the current velocity v . For modeling up- and downhill routes, F_C is calculated by the helps of the current slope angle ρ . The inertial resistance depends mainly from the current acceleration a .

Engine Power

In order to overcome the driving resistance, the engine has to raise power. In addition, the introduced model from [70] uses a supplementary base power P_0 for the rest of vehicle operations (lights, radio, air condition etc.), which is also necessary on standstill. The overall power is calculated according to equation (2.11) [70, p. 390]. No energy can be recuperated, but the fuel flow is cut off as soon as the mechanical force becomes negative, what is the case in all modern vehicles.

$$P(v, a)_{total} = \max(P_0 + v * F_{total}(v, a), 0) \quad (2.11)$$

The consumption rate is determined by considering the required power $P(v, a)_{total}$, the calometric energy density of the fuel w_{cal} and an efficiency factor γ . The consumed fuel C is calculated according to equation (2.12) by using the engine speed f , the overall power demand P_{total} and the efficiency factor γ . The engine speed f is calculated as stated in equation (2.13) and additionally to mentioned variables relies on the transmission ratio R_t and the dynamical tire radius r_{dyn} [70, p. 391].

$$C = \frac{P_{total}}{\gamma(P_{total}, f) * w_{cal}} \quad (2.12)$$

$$f = \frac{R_t * v}{2\pi * r_{dyn}} \quad (2.13)$$

Further details to fuel consumption models can be found in the very comprehensive work from Martin Treiber and Arne Kesting in [70].

CO₂ Emissions

As carbon dioxide is one of the most prominent greenhouse gases responsible for global warming [77], it is also considered in the simulation results. The relationship between consumed fuel (which is diesel in all investigations) and emitted carbon dioxide is assumed to be linear and translated according to equation (2.14) [77, 78].

$$1 \text{ l diesel} = 2.69 \text{ kg CO}_2 \quad (2.14)$$

This conversion factor is valid for a density of 0.87 kg/l fuel. For reasons of simplicity, deviations such as various fuel densities, gasoline cars, different combustion engine types or climatic conditions are disregarded.

Review

For all simulations that were carried out, I configured vehicles with diesel combustion engines and the introduced physics-based model without exception for the sake of keeping the focus on methods for optimization of traffic flow. I admit that this practice is slightly disconnected from reality nowadays. However, application of many different engine types such as electric powered, petrol and diesel combustion engines, hydrogen driven etc. would complicate the investigation, lead to a multiple of the already considerable amount of varying parameters and thus goes beyond the scope of this thesis.

Certainly, the described model also comprises some simplifications in several areas, but for the evaluations within this thesis further details are negligible. The detail level

is sufficient for showing differences between congested and smooth traffic flows which are not linearly related to the average speed, but reveal significantly higher fuel consumption for the former.

2.2.5 Model Validation

Calibration and especially validation of microscopic simulation models is a difficult endeavor in the development and application of them, especially but not limited to the possibilities for model adaption to empirical data [79]. A suitable approach to validate the behavior of such models is to compare to real-world experiments, where all relevant data such as trajectories, acceleration and speed as well as gaps to the front vehicle are recorded over time for all vehicles.

For the longitudinal model we apply for the conducted simulations, the chosen parameters were calibrated and validated to have realistic values and have a reasonable interpretation [80, 81]. Due to the fact that more vehicles are involved, the empirical investigation of lane change behavior is much more difficult compared to car-following models. Additionally, the intent for a lane change is manifold and overlaps strategic, tactical and operational behavior [82]. Nevertheless, the lane change models are validated by comparing with recorded real data, as is the case in [83]. Fuel consumption models are validated by comparing the calculated fuel consumption with driving cycle experiments [70]. While the determination of driving resistance in the applied model bases on fundamental physics, the consumption is strongly dependent on car-specific characteristics such as engine maps, aerodynamic drag or tire dimensions, which makes the validation more difficult and limits validations to a certain vehicle and engine.

2.3 Overview of TraffSim and Capabilities

All presented investigations and results are produced with the microscopic traffic simulator *TraffSim*, which is a proprietary development within the Research Group nemo at the University of Applied Sciences (UAS) Upper Austria, Campus Hagenberg. Basically, *TraffSim* is a modular microscopic traffic simulator with optional UI feedback and extensive possibilities for statistics analysis. The work on this software was started in 2012 with the initial purpose of investigating the research questions this thesis deals with. However, *TraffSim* has become a powerful tool in the meanwhile and was used in numerous published research works since then, some of which are mentioned already in section 1.4. The functionality of the simulator is extended continuously and is not limited to the results presented in this thesis any more.

In this section, the most relevant capabilities and functionality of the simulator for the investigations related to the presented results are explained.

2.3.1 Simulation Mode

Apart from the basic distinction concerning the level of modeling detail into micro- and macroscopic simulators, the applications of traffic simulation programs can be additionally classified based on different approaches [61, 84], which are continuous and discrete simulations for both time and space. *TraffSim* applies a time-discrete simulation, which means that all vehicles' states, acceleration, velocities and positions resulting therefrom are calculated for a defined point in time. The calculation interval is fixed and can be chosen arbitrarily low. Although very low intervals bring results close to time-continuous differential equations, the required computation resources go up accordingly. Furthermore, time continuity is no requirement for *TraffSim* - neither for the scope of this thesis, nor for any other application of the simulator up to now. Much more important is the continuity in space. In contrast to simulators which base on cellular automata, each vehicle can be located at any position on the road. This is important for modeling real transportation systems and perform investigations on traffic flow, where space-discrete models are not suitable [70, p. 237].

2.3.2 Data Recording

Depending on the investigation, different properties with varying time resolution and detail level can be required. Therefore, it is possible to record certain values of interest and generate the output data with a configurable level of detail. The statistics can be separated in two categories. The first category includes values related to a single vehicle which change in each simulation time step such as:

- Travel distance
- Position
- Velocity
- Acceleration
- Current fuel consumption

Other events of interest which emerge only occasionally can be assigned to the second category:

- Congestion detection or prediction
- Route changed
- Accident happened
- Vehicle entered or left simulation

Values of the first introduced category that are recorded in each time step lead to a huge amount of data, which increase with simulation length, number of vehicles in simulation and with lower resolution in time. This is the reason for the possibility to summarize values as so-called outline statistics. Especially relevant for the presented investigations are the average travel distance, travel time and fuel consumption. The overhead for summing up these values during simulation is negligible. In cases where information with higher level of detail are unnecessary this methodology saves both storage space and time for writing the data.

All result files are created in the open MAT-format [85] and ready for postprocessing within Mathworks MATLAB [86].

2.3.3 Intersection Regulation

TraffSim contains many types of road crossings and junctions occurring in real road networks, including unregulated intersections without prioritization, traffic light controlled ones, roundabouts, intersections regulated with road signs and combinations of them with different numbers of road segments inwards and outwards. Basically, an intersection is a connection between at least three road segments with one or multiple lanes, and contains lane-to-lane connections for all allowed driving directions. Also, special situations such as route changes before intersections and multilane situations are addressed. With the introduced set of rules and situations, a great majority of intersections of real road networks can be parametrized and simulated virtually and the requirements for traffic flow investigations through dynamic simulations are fulfilled. The system provides a decentralized logic, which is applied to each intersection individually and therefore performs very well due to the possibility of parallel execution [50].

The regulation algorithm uses the following levels of priority evaluation, which are applied one after the other:

1. Traffic light signals
2. Road signs
3. Right-before-left rule, priority for vehicles turning right or going straight on compared to left-turners
4. Closest vehicle (minimal driving time to intersection border)

Naturally, traffic lights are the major type of regulation, which always are applied as soon as they are active. If no traffic lights exist for a specific intersection or they are not active (e.g. yellow blinking), the next level of regulation becomes active. Road signs specify the priorities in the second level. In situations where no unique preferred vehicle can be determined, level 3 comes in. If even right-before-left rules leads to multiple equally

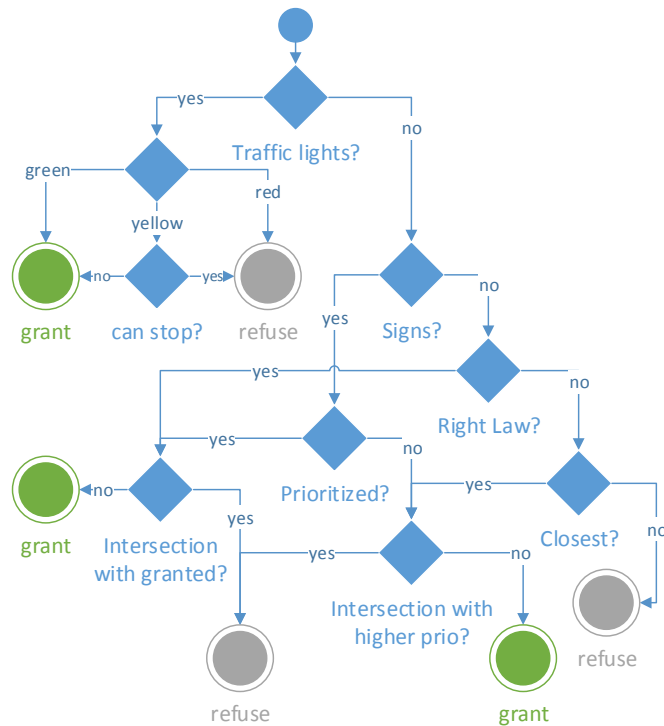


Figure 2.5: Decision graph from request for entry to grant or refuse

prioritized vehicles instead of a single one, entry is granted to the closest vehicle (minimal time to entry point). The diagram in figure 2.5 represents the decision process clearly.

Special care needs to be taken for situations which seem to be solvable straight-forward for human drivers, but actually reveal to be more complex. I picked two of the most common issues, as explained below.

Traffic Jam Situations: Independent of the regulation type, traffic may come to a complete standstill while passing the intersection. Thus, exits are blocked and vehicles cannot drive through because there is not enough space on the exiting road segment for the whole vehicle length, although it would have the highest priority. Figure 2.6 shows such circumstances. Vehicle $v1$ in figure 2.6b principally would have the right of way, but cannot enter because its exit lane is blocked. Thus, $v2$ may enter and if the exit of $v1$ is still blocked, also $v3$ may pass. This issue is solved by supervising the available space in the target lane and block entry for critical vehicles. Driving through the intersection is not granted before the distance measured from the front vehicle of the blocked one in the target lane to the intersection is larger than the length of the vehicle asking for access grant and the front vehicle reaches a speed above a given threshold. This speed threshold is necessary for ensuring smooth traffic flow in uncongested situations, because the decision whether or not a vehicle must stop due to a potential standstill has to be made

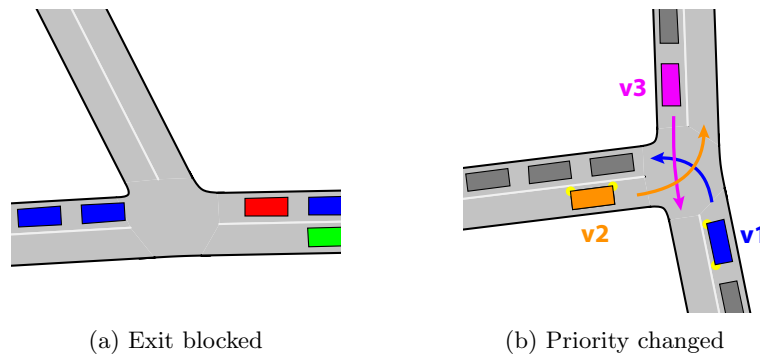


Figure 2.6: Different situations with a blocked exit connector

Table 2.1: Order of events leading to a deadlock

Time	Initiator	Event	Grants Int. A	Grants Int. B
t	$v1$	RE Int. A	none	none
t	$v1$	RE Int. B	none	$v1$
$t + 1$	$v2$	RE Int. A	$v2$	$v1$
$t + 2$	$v1$	RE Int. A	$v1$	$v1$
$t + 3$	$v3$	RE Int. B	none	$v1$

early enough in order to allow a safe braking procedure. Without using that threshold, traffic flow suffers because vehicles would always brake before a junction as long as another vehicle occupies the intersection or the appropriate exit lane, although speed of all vehicles is high enough so that no standstill is possible anyway.

Time of Decision Dilemma: A special deadlock situation as a result of intersection modeling and an unfavorable order of requests for entry grant can be observed. The sequence of events in table 2.1 leads to a situation where no vehicle can enter any more. In this example, vehicle $v1$ has an entry grant for intersection B , but is not allowed to pass intersection A . In further consequence, $v2$ enters intersection B before vehicle $v1$. Therefore, $v1$ can never pass intersection B because $v2$ is in its way. Finally, vehicles $v2$ and $v3$ wait for $v1$ to pass through, which never happens. Figure 2.7 illustrates the initial and deadlock situations.

This can be avoided by denying entry to intersections which are not the very next in a vehicle's route. Furthermore, we continuously check the granted entry permissions if the respective vehicle is the closest of the incoming lane. If not, the entry grant is simply removed and calculated from scratch to fix the deadlock situation.

An extensive description and further details concerning intersection modeling within *TraffSim* can be found in [50].

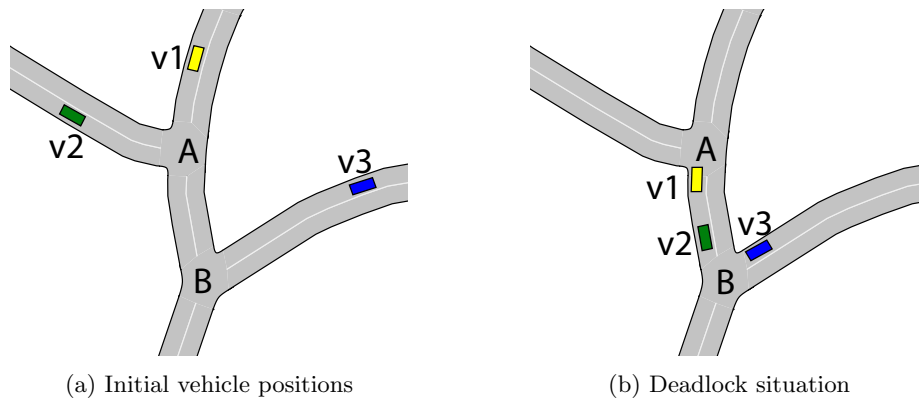


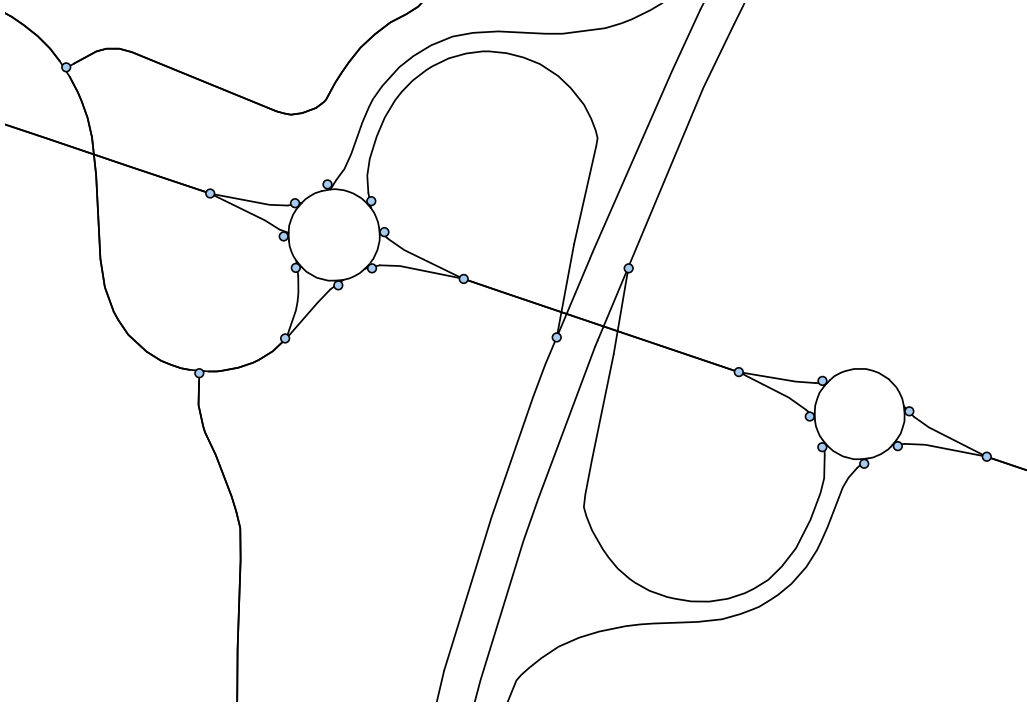
Figure 2.7: Vehicle layout before (2.7a) and after (2.7b) unfavorable decision

2.3.4 Road Infrastructure

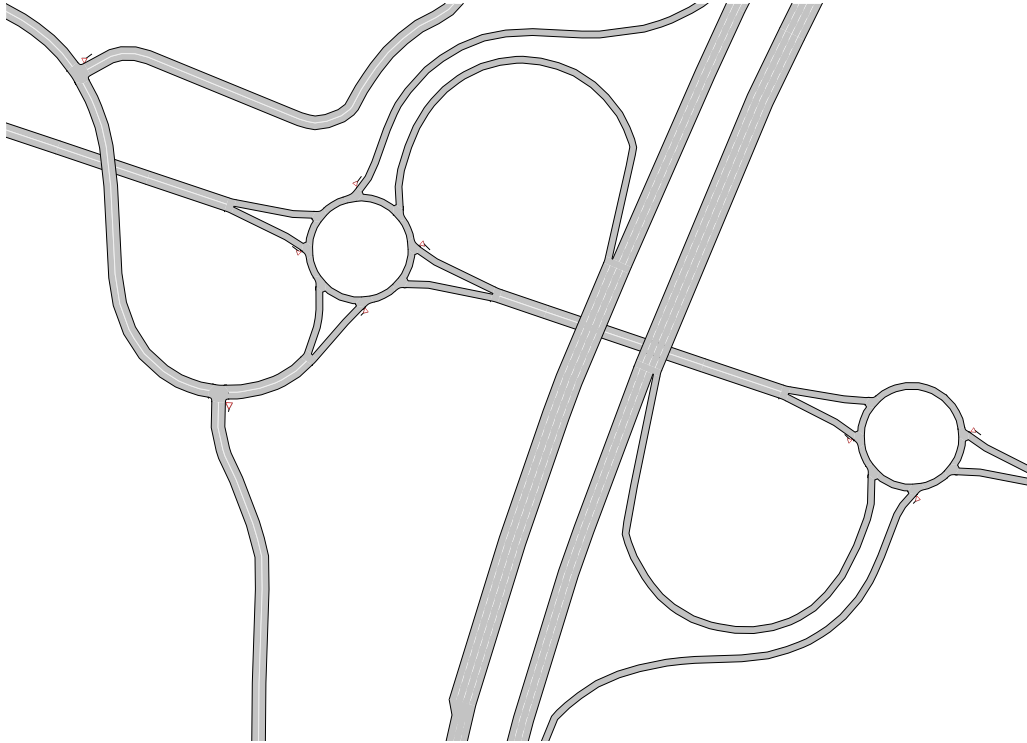
In order to apply both existing road networks from real life or artificially generated ones, *TraffSim* supports maps from OpenStreetMap (OSM) in the OSM XML format. This combines the advantage of using existing editing tools for the maps (such as JOSM [87]) with the possibility to use map data which is available for most regions all over the world.

The map data from OpenStreetMap in its available formats is not suitable for routing, nor is the geometry for all lanes available. Lanes with optional restrictions, intersections and ramp/exit lanes are created according to the information in the OSM data. The data basically contains a single polyline, which represents one road in both directions. Additionally, meta information such as the number of lanes in each direction, lane restrictions, speed limit, road name and type are available, just to name the most relevant tags [88]. Figure 2.8 illustrates an extract of a road network. The upper part (figure 2.8a) shows the graphical representation of what is available from OSM. In figure 2.8b, the processed geometries with multiple lanes, intersections and highway ramps and exits is depicted.

In addition to the road segments, also intersections need to be generated. This process is executed at each connection of more than two road segments. *TraffSim* creates a convex hull polygon for each intersection, which represents the intersection bounds. Within this area, connectors between lanes are generated according to the OSM metadata information regarding driving restrictions. Figure 2.9 shows an example for a generated intersection. The gray tracks indicate the centers of the lane connectors, which are bounded by the yellow borders. The solid white road markings in the middle of each of the intersection arms are located where the original single line polygon indicated the roads.



(a) Original map graph from OSM



(b) Map graph after processing

Figure 2.8: Original and processed map segment

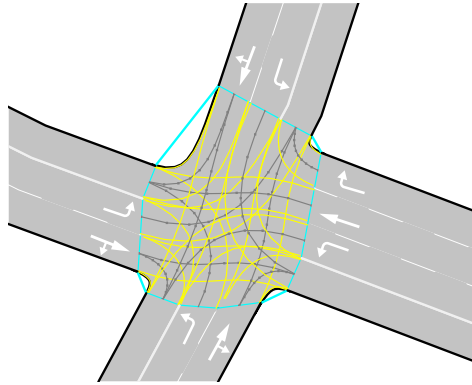


Figure 2.9: Augmented intersection

2.3.5 Routing

Simultaneously with processing of the road network source data, a routable graph is generated out of the roads. The graph is weighed with the initial cost which is based on the road length and speed limit of the road segments. Each existing connection between two intersection nodes has its unique routing ID, with which it can be referenced by defined routes. In turn, a route is nothing else but a list of IDs referring to the road segments in the order they should be passed.

Naturally, the decision which connector to take depends on the route of the affected vehicle. The fitting connector to follow the route is chosen automatically, as described in section 2.2.2. As *TraffSim* allows to update routes dynamically, it is also necessary to take care that a route update is avoided if a vehicle is in close proximity to the intersection and a change to a different lane, which would be required to follow the new route, is not possible anymore. In such a case, the simulator prohibits the route update.

2.4 Vehicular Routing Basics

As the vehicle routing problem is a very huge domain but still one of the core research fields of this thesis, short descriptions of the most relevant algorithms which are the background for this work are given.

The basis for all routes that are calculated is a single-directed graph. This graph is built up by the *osm2po* framework out of OSM map data. Its edges are the road segments and the vertices are intersections, where at least two road segments are connected to each other. As the graph is single directed, a road with lanes in both directions has two independent edges, one for each direction. The cost for a route is calculated by summing up the traversed segments from a defined source to a destination vertex.

2.4.1 Dijkstra Algorithm

One of the most common algorithms and also the basis for routing within this thesis is the Dijkstra routing algorithm, named after Edsger W. Dijkstra [89]. It is able to find the shortest path to any target for a given source node by traversing nodes and assigning the cost to reach each node from this start node. While traversing, the cost is summed up, and if the currently assigned cost of a node is higher than the just calculated node for an alternative path, this cost is assigned and the currently traversed path is the new shortest path to this respective node. This procedure is repeated until all nodes were visited and therefore the definite shortest path is found.

2.4.2 A* Algorithm

Due to the fact that all nodes are visited at least once, the algorithm follows multiple useless and unnecessary ways, which increases the complexity of the algorithm. Therefore, the routing engine bases on the A* algorithm, which is an extension of the Dijkstra algorithm and improves performance by using heuristics to guide the search [90]. The routing mechanism which is proposed in chapter 3 bases on the A* algorithm, as do all reference algorithms presented within this thesis. While the type of heuristics is problem-specific in the original definition, the Euclidean distance between two nodes is used within the scope of this work.

2.5 Categories of Traffic Optimization Systems

Multiple types of automatic, active traffic guidance and optimization systems exist. The available approaches can be separated into the following groups.

2.5.1 Dynamic Traffic Assignment (DTA)

Theoretical traffic optimization solutions are algorithms on dynamic traffic assignment (DTA) [91–93], which lead to user equilibrium. The optimization process usually runs in multiple cycles, until the optimal equilibrium is achieved. This means that after application of the DTA mechanism, not any single vehicle can achieve a better time to destination when changing its route and is described as Nash equilibrium in literature [94]. A significant drawback is the non-applicability in reality, due to the lack of providing real-time guidance, reaction to unforeseen congestion, high computational effort, and first and foremost multiple necessary calculation cycles.

2.5.2 Reactive Algorithms

This type of rerouting algorithms cannot react on traffic jams before they occur, and are also described as route guidance systems. In other words, those systems can calculate routes by taking into account the current traffic conditions, which can be detected anyhow by sensors [95], traffic surveillance infrastructure, report of humans or emergency vehicles. According to the current position and desired destination, the systems can calculate a route by considering known traffic conditions. Some examples are WITS [96], CDRG [97] or RETINA [98].

2.5.3 Predictive Algorithms

A number of approaches from literature predict traffic by using historical data. The forecast is carried out by making use of correlations between traffic flow, congestion and the time, day of week or month. Historical flow data from given locations on the roads is used for modeling future behavior in the same locations. They play an important role in traffic flow forecasting and are either univariate models [99, 100], which use collected flow data to predict the traffic for the very same location or multivariate models [101–103], which describe traffic flow simultaneously in various locations by using historical flow data [104]. Other approaches are the usage of Bayesian models [105] or neural networks [106] for prediction. The authors of [107] propose an algorithm which uses flow detection and prediction based on historic data and measurements through VANET as well.

However, the available knowledge of the road conditions is often incomplete or limited to highways and interurban roads, be it due to comparably high cost of surveillance infrastructure or because of insufficient reported incidents. The necessary traffic flow detectors, cameras or induction loops are expensive to deploy and maintain, and thus they are often not available, especially for lower level road networks. The strong dependency on accuracy and availability of the collected data and density of the sensors is a drawback of both reactive and proactive methods. Furthermore and also due to the aforementioned constraints, the mentioned approaches can mostly not directly avoid congestion or counteract this same congestion prior to occurrence. A reactive behavior provides the same guidance for all users depending on their destination in a certain point in time and can cause moving congestion to a suggested alternative route. Often, drivers have to decide themselves which information to trust. As a consequence, choosing a different route selfishly often may not lead to advantages in reality in terms of lower time or less distance to their destination. An egoistic approach is not feasible for achieving a satisfactory global optimum, but tends to move congestion to nearby spots. Moreover, bottlenecks in lower level roads cannot be detected at all by the mentioned approaches. An appropriate reaction in case of jams in those areas is not possible because road operators cannot notice those problems outside their sphere of supervision.

While reactive algorithms do not fulfill the requirements of timely jam counteraction, the predictive algorithms from literature have weaknesses for various reasons. They either base solely on historic data or present algorithms for prediction, but without elucidating how to utilize the prediction for decreasing negative effects of traffic congestion. This is essential since utilization of predictions for alternative route calculations influence the future conditions of the whole road network. Although complex models can provide good forecasts through multiple processing cycles, they are often not suitable for real-time applications. Furthermore, they cannot react to exceptional circumstances such as accidents or short-term roadworks.

Current traffic management systems also do not fully exploit capabilities of vehicular communication, which can be V2I or V2V communication, briefly designated as V2X communication.

For this reasons, in the next chapter 3 a combination of both congestion prediction and utilization of the currently gathered information, applicable for realtime guidance is proposed. The contribution on this topic is a novel method on reaction on expected future congestion by prediction of overloaded spots and timely counteraction, applicable in real-time. The approach is also proven by simulations using a microscopic traffic simulator [47]. Dynamic vehicular rerouting utilizing current road state information is extended by intelligent congestion predictions. I focus on short-term live forecasts in the range from a few minutes up to half an hour. The results show performance of algorithms from literature ([108], to the authors knowledge the best available predictive algorithm) compared to our PCMA* algorithm, including comparisons for differently parametrized jam detection and prediction mechanisms, weighting algorithms and also distinct environments.

3

The PCMA* Routing Algorithm

Beyond doubt, there are more than the arguments mentioned in section 1.1 for thinking of intelligent and at the same time practicable solutions to minimize or in the best case avoid traffic jams and standstill of vehicles, summarized as ITS. The focus is to make use of new technologies in car Information and Communication Technology (ICT) to identify the destinations of vehicles' routes to provide future predictions for road conditions and optimize the overall traffic situation in a road network in real-time.

3.1 Introduction

In this chapter, I introduce the comprehensive traffic optimization system including a novel prediction algorithm for future congestion, called PCMA*. The timely notification of potential stagnation is an essential benefit of this approach compared to other algorithms, especially for drivers with route targets far away from their current location. A spacious alternative route over a wide area has significant advantages if the congestion spot can be bypassed completely. An early reaction to potential jams thus keeps vehicles far away from the congestion wherever possible. By doing so, a potential narrow range alternative route around the traffic jam is not further burdened and can preferably be used by vehicles where wide-range detours are not possible any more [17].

The goal of the approach is to evaluate the expected future conditions of the road continuously, so that potential traffic jams and congestion can be counteracted timely. The algorithm identifies expected bottlenecks before a traffic jam emerges. This is important to allow bypassing these critical spots over a wide area, because the probability of getting into the very same jam is higher if the alternative route is too similar to the original one, as figure 3.1 shows. Vehicular communication is utilized to determine the traffic condition data as well as to transfer routing information to vehicles.

Furthermore, it is important to identify vehicles which should be considered for rerouting. The set of rerouted vehicles in the best case only contains those vehicles which pass the predicted congested spot in the relevant time. PCMA* makes use of such an approach, as explained in section 3.2.5.

Recapitulatory, the introduced PCMA* algorithm combines three important mechanisms of a comprehensive traffic optimization system:

1. The routing algorithm itself, taking into consideration the current road conditions and predicted future congestion (sections 3.1.1, 3.1.2 and 3.2.1),
2. a congestion detection and prediction component (sections 3.2.2 to 3.2.4) and
3. intelligent selection of vehicles to be rerouted in case of a already occurred or predicted congestion (section 3.2.5).

Bottlenecks in road networks can naturally be caused by road capacity drops along the route, but mainly traffic jams occur due to merging of multiple roads through an intersection [109]. In our investigated scenarios, this behavior was confirmed by simulations. Thus, the prediction of PCMA* algorithm focuses on intersections.

3.1.1 Basic Routing

The routing mechanism is based on the A* algorithm, which needs a weighted graph in order to facilitate routing. The initial routing graph uses minimum drive-through times

of road segments (RS) as weights (w_{RS}), which are calculated as preprocessing step by equation (3.1), where len_{RS} represents the length of the road segment RS and v_{max} is the speed limit.

$$w_{RS} = \frac{len_{RS}}{v_{max}} \quad (3.1)$$

The weight of each road segment is available in a static manner at this stage. Initially, each vehicle gets assigned a specific path to its target as if it was the only one in the whole network.

3.1.2 KSP Routing

A popular approach for calculation of more than one route to a defined target is the k-Shortest Paths (KSP) algorithm [108,110], an extension of basic shortest path algorithms. It calculates a number of k distinct and loopless alternative routes from a given source to destination, starting from the best to the second best until the k th best path. However, the KSP algorithm has fundamental weaknesses in real environments. As soon as a huge real road network is applied and the network is not arranged in a rectangular, grid-like structure, the alternative paths are often not very beneficial in order to overcome traffic congestion. The bigger the real network, the more paths need to be calculated and the higher k is essential to obtain a satisfactory alternative route. An increasing k leads to considerably higher computational effort. Often, the resulting paths again lead to the original one, and thus do not really avoid congestion, but move the same to another spot in the road network [111,112]. The reason are paths that are defacto unusable for new routes because they are too similar to the original one and do not provide any feasible alternative route, as figure 3.1 shows.

Figure 3.1a depicts the results of the KSP-algorithm with $k = 5$. Obviously, large parts of the k different paths overlap. The provided 5 shortest paths differ only slightly from each other. Therefore, the calculated alternatives carry a high risk of providing an inappropriate alternative due to being not spacious enough. A reasonable alternative route requires to be the best compromise of length and spatial difference to the original one. This can mostly be achieved by increasing k and calculating more alternative routes this way, so that the result contains at least one adequate alternative route. In figure 3.1c, the algorithm determines 10 routes and some of the resulting paths are satisfactory as a real alternative using a completely different route in the eastern part of the map extract. One of these eastern alternatives (e.g. dark blue or magenta colored routes) is therefore more likely not to be influenced by any traffic jam on the western route.

If k is chosen too small, the previously discussed drawback becomes significant especially in real road networks, where such branch points into a lower level road lead back to the main road very soon, as the example in figure 3.1b points out. The resulting small

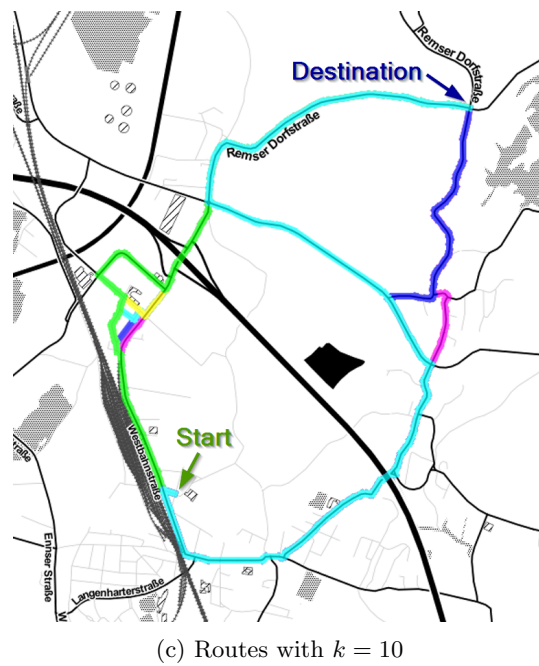
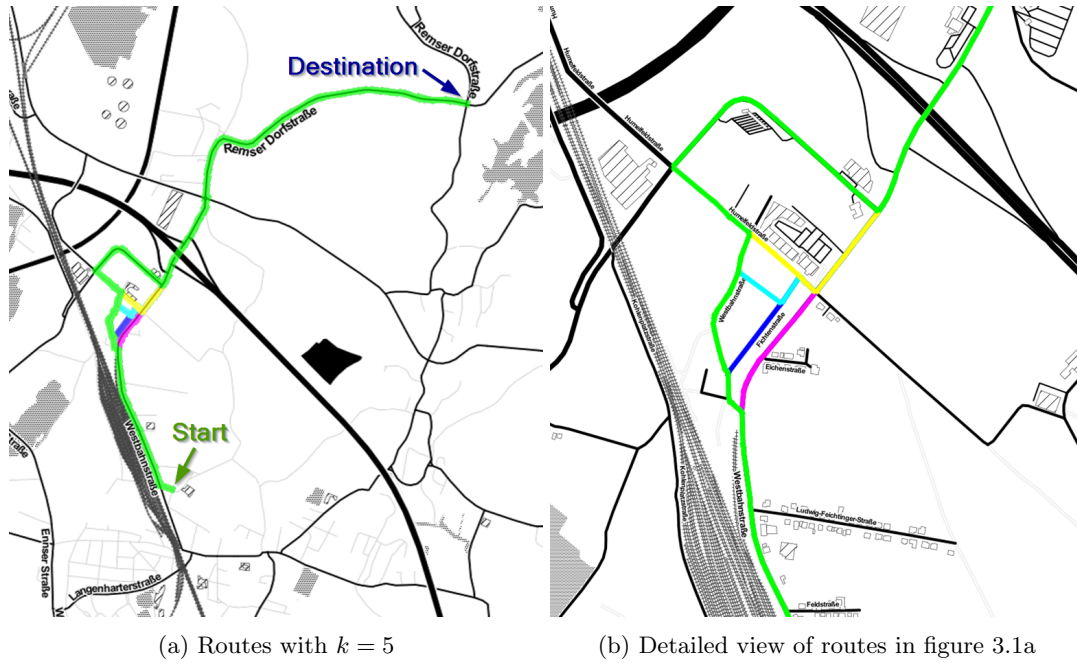


Figure 3.1: Alternative routes calculated by k Shortest Path algorithm with different sizes of K , colors indicate different routes

variations of the route appear as potential alternatives, although they do not really imply any benefit when using them. Often, just the opposite occurs: Vehicles use such an automatically calculated, apparently beneficial route. However, they drive a longer distance and in most cases do not bypass the congestion, but join the congested route just a few meters later via the side road. The result is a higher driving time and increased fuel consumption with zero gain for both oneself and other drivers.

Apparently, the static weight approach as well as the KSP algorithm are far from optimal, which raises the question of a dynamic and cooperative mechanism with a more intelligent optimization solution that also considers potentially upcoming traffic problems. To accomplish this, I propose a mechanism for evaluating the current and expected future congestion which makes use of the current road data in the next section.

3.2 Conception of PCMA*

3.2.1 Routing Graph Weighting

The used routing graph is initially weighted with the minimum passage time, as described in section 3.1.1. Certainly, the achievable true passage time and, by implication also the segment weight changes dynamically, depending on current load and potential traffic jams ahead of a road segment. Thus, the routing graph is updated dynamically. In order to accomplish this, different mechanisms are utilized (Speed Average Method, Greenshield's Model), as explained in the following. Those yield a value for a current passage velocity per road segment v_{RS} , which is used in the current routing graph as well as a value for segment weight w_{RS} . This weight is further considered as threshold for congestion detection.

Speed Average Method

A very simple but plausible approach is the regular update of the segment conditions in defined intervals, which we call Speed Average Model (SA).

$$v_{RS,SA} = \frac{\sum_{n=1}^N v_{V_n}}{NV} \quad (3.2)$$

$$w_{RS,SA} = \frac{v_{RS,SA}}{v_{max}} \quad (3.3)$$

Equations (3.2) and (3.3) elucidate the considered road segment speed $v_{RS,SA}$ and the calculation of segment weight $w_{RS,SA}$, respectively, where v_{V_n} denotes the velocity of the n^{th} vehicle (V_n) on the segment and NV is the number of vehicles on the road segment. To summarize, the weight of a single road segment is calculated by averaging the speed of all vehicles which are currently driving through this specific segment.

Greenshield's Model

An often used [108, 113, 114] approach for weighting and characterization of traffic flow is the Greenshield's Model (GS) [115], which is based on the ratio between free and occupied road space.

$$v_{RS,GS} = v_{max} * (1 - \frac{K_{RS}}{K_{jam}}) \quad (3.4)$$

$$w_{RS,GS}(t) = \frac{K_{RS}}{K_{jam}}, \quad \text{where} \quad (3.5)$$

$$K_{RS} = \frac{NV_{cur}}{len_{RS}}, \quad (3.6)$$

$$K_{jam} = \frac{NV_{max}}{len_{RS}} \quad \text{and} \quad (3.7)$$

$$NV_{max} = \frac{len_{RS}}{len_V + gap_{min}} \quad (3.8)$$

It makes the assumption that, under uninterrupted flow conditions, estimated speed v_{RS} , speed limit v_{max} and vehicle density K_{RS} are linearly related to each other for a road segment RS , as expressed by equation (3.4) [115]. The maximum vehicle density is denoted by K_{jam} , NV_{max} represents the maximum possible amount of vehicles on road segment RS with length len_{RS} and average vehicle length $\overline{len_V}$. The minimum gap between vehicles is gap_{min} .

3.2.2 Congestion Detection

Both described approaches, SA and GS allow the detection of congestion by defining a specific, dimensionless congestion threshold for the reactive algorithms $\theta^{(R)}$.

$$w_{RS,GS} > \theta_{GS}^{(R)} \quad (3.9)$$

$$w_{RS,SA} < \theta_{SA}^{(R)} \quad (3.10)$$

As soon as this threshold is exceeded in case of GS (equation (3.9)) or undershot in case of SA (equation (3.10)) for any road segment, a congestion event is risen containing the congested road segment. It is the rerouter's task to handle this event. For example, it could select affected vehicles and calculate alternative routes for them. At this stage, detection still happens reactive, which means that the algorithm can only react to already occurred jams and hence cannot consider any predicted future problems.

I utilize the described congestion detection approaches (SA, GS) as benchmark to compare them with the PCMA* algorithm.

Table 3.1: Structure of a node footprint

Δt index $j \rightarrow$	0	1	...	M
$RS_n \downarrow$				
RS_1	$NV_{RS_1,0}$	$NV_{RS_1,1}$...	$NV_{RS_1,M}$
RS_2	$NV_{RS_2,0}$			
RS_3	$NV_{RS_3,0}$			
...
RS_{NRS}	$NV_{RS_{NRS},0}$...	$NV_{RS_{NRS},M}$

3.2.3 Footprint Calculation

The footprint is a characterization of the road infrastructure, comprising a load quantification of the integral road system. It is an essential key component for the PCMA* algorithm to work. I define node footprints, which are maintained for each node. A node footprint contains a representation of the node occupancy, which is the number of vehicles that are currently passing and intend to pass the intersection node within the near future, discretized in time intervals Δt . Additionally, the node footprint includes information from which source road segments the vehicles are arriving. Table 3.1 roughly illustrates the contents of a single node footprint.

The summarized node footprint, denoted as $P_i^{(S)}$, is provided for node i and contains values for the current and all considered future time intervals $(\Delta t)_j$, $j = 0, 1, \dots, M$. It is measured by the number of arriving vehicles in node i during time interval $(\Delta t)_j$ according to

$$P_i((\Delta t)_j) = \sum_{n=1}^{NRS_i} NV_{RS_n,j}. \quad (3.11)$$

$$R_{eval} = M \times \Delta t, \quad M \in \mathbb{N} \quad (3.12)$$

Both the time interval Δt and the time range of future evaluation R_{eval} (equation (3.12)) are configurable. For calculation, we consider all vehicles $V_{RS_n,j}$ arriving during the j^{th} time interval $(\Delta t)_j$ at one of NRS_i adjacent road segments of node i . Then, we sum them up to achieve the total number of vehicles passing node i in time interval $(\Delta t)_j$. For further clarification, each cell of table 3.1 contains an indexed value $NV_{RS_n,j} \in \mathbb{N}$, which denotes the number of arriving vehicles from road segment RS_n in time interval j .

The aggregate node footprints are consolidated as network footprint, which exists once for each network. This quantification of the network load is essential in order to provide a possibility to detect congestion on the one hand, and as a consequence react to overloaded areas by changing the route of affected vehicles on the other hand. The network footprint is updated continuously as soon as a vehicle changes its route or propagates to another

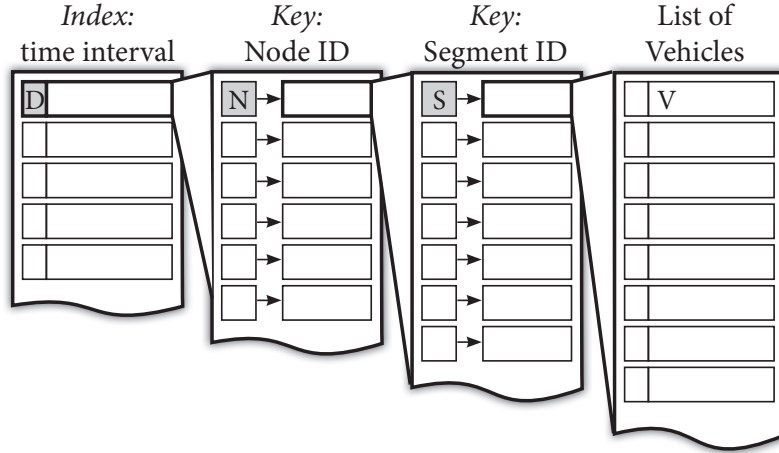


Figure 3.2: Logical structure of the network footprint

road segment, in order to provide a dynamic, time-dependent overview of the conditions of all intersection nodes.

By way of computing a node footprint, the travel time from the current vehicle location to this specific node i is required. For this to solve, the first value needed is the passage time of each road segment on the vehicle's way, in order to further determine the arrival timestamp of this vehicle at node i . The passage time is calculated by considering the algorithm-dependent passage velocity v_{RS} according to the following equation (3.13).

$$t_{p,RS} = \frac{len_{RS}}{v_{RS}}. \quad (3.13)$$

Subsequently, the overall travel time t_{travel} from the current vehicle location to a specific node i on the vehicle's route is calculated by summing up the calculated passage times $t_{p,RS}$ of all road segments where the vehicle travels through, as defined in the currently assigned route (equation (3.14)).

$$t_{travel} = t_{p,RS_{cur}} \times \frac{len_{RS_{cur}} - pos_V}{len_{RS_{cur}}} + \sum_{k=1}^{k_{max}} t_{p,RS_k} \quad (3.14)$$

Index k refers to the k^{th} road segment of the assigned route, RS_{cur} denotes the road segment where the vehicle is currently driving on and pos_V is the position of the vehicle on the current road segment, measured from the point where the vehicle first entered this road segment. Depending on the defined value of the time interval Δt , the network footprint calculation stores status information discretized for each time interval $(\Delta t)_j$ up to the future evaluation range R_{eval} . The network footprint is logically modeled as figure 3.2 illustrates. This way, one has full knowledge about which vehicle passes which node in which Δt , coming from which road segment. All this information is necessary for enabling comprehensive prediction of potential overloads of single nodes, as done by PCMA*.

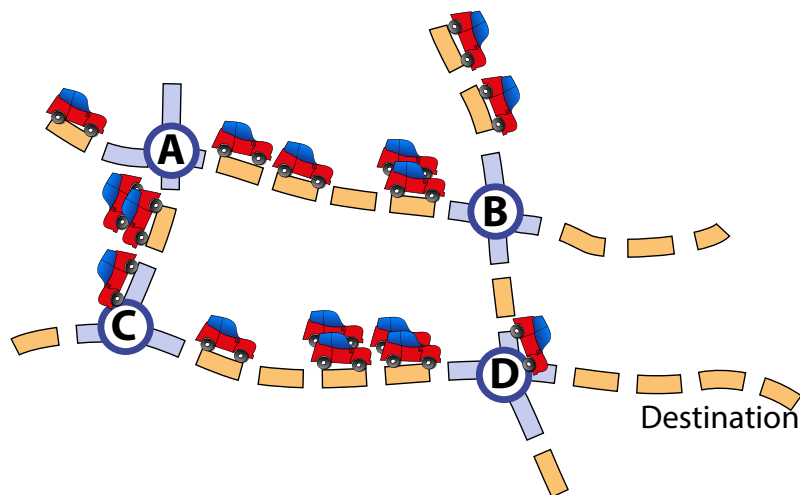


Figure 3.3: Example scenario for footprint calculation and time interval index 0

Table 3.2: Summarized node footprints for example scenario of figure 3.3

time interval index $j \rightarrow$	0	1	2	3	4	5	6	7	8	9
node \downarrow										
B	0	3	1	1	1	0	1	0	0	0
C	0	1	2	0	0	0	0	0	0	0
D	1	2	2	3	2	2	3	0	1	0

As an example, figure 3.3 shows a snapshot of a road network snippet. All shown vehicles are heading the same destination, either via nodes **B** and **D** or via nodes **C** and **D**. The dashed lines represent roads, whereas each dash represents a unit of time that is needed by a vehicle to drive through this passage. Likewise, the vehicles need one unit of time to pass a node. The blue dashes are considered as part of the node. To simplify the depiction, the vehicles are assumed to move with equal speeds of one road segment per time unit. Moreover, all road segments are assigned with the same speed limit. For reasons of further simplification, a summarized node footprint $P_i^{(S)}$ is defined as array of values, each of which denotes the number of vehicles passing this node in the respective time interval $(\Delta t)_j$. In table 3.2, a summarized node footprint therefore expresses as a single table row. In the explained example, the summarized footprints of nodes **B**, **C** and **D** over time are described in table 3.2.

By way of clarification, algorithm 2 gives insights in the calculation method. The update function is executed as soon as a route of a vehicle veh is updated, no matter if this is the initial setup of a vehicle or an update due to a rerouting procedure.

It takes the updated vehicle, its old route and the new route as parameters in order to clean old mappings for the vehicle and update footprints for new passed nodes. The passed

Algorithm 2 Calculation of footprint on a route update

```

1: function UPDATEFOOTPRINT(veh, oldRoute, newRoute)
  ▷ cleanup mapping for old route
2:   if oldRoute ≠ null then
3:     clear all mappings of veh
4:   end if
5:    $RS_{current} \leftarrow$  initial segment of newRoute
6:    $t_{arr} \leftarrow \frac{veh.position}{RS_{current}.length} \times \text{GETDURATION}(RS_{current})$ 
  ▷ traverse the new route and update footprint mapping
7:   for all  $r_{id}$  in newRoute do
8:      $t_{arr} \leftarrow t_{arr} + \text{GETDURATION}(RS_{current})$ 
9:     if  $t_{arr} > \text{maxForecast}$  then
10:      break
11:    end if
12:     $index \leftarrow \frac{t_{arr}}{\Delta t}$ 
13:     $RS_{veh} \leftarrow veh.RS$ 
14:     $node \leftarrow RS_{veh}.endNode$ 
15:    mapping[ $index, RS_{veh}, node$ ]  $\leftarrow$  mapping[...] + 1
16:     $RS_{current} \leftarrow \text{GETNEXTSEG}(r_{id})$ 
17:  end for
18: end function

```

vehicle is an object containing all necessary information such as the road segment currently driving on ($veh.RS$) and the current position on it ($veh.position$). The route parameters $oldRoute$ and $newRoute$ are number arrays containing a list of road segment IDs (each of which denoted as the loop variable r_{id}) which describe a route through the road network. t_{arr} represents the predicted arrival time and $node$ represents a specific intersection. After an optional cleanup of mappings for the old route (line 2-4) and initialization (lines 5 and 6), the passed in new route is traversed for the purpose of updating the footprint mapping (loop starting in line 7). The calculated index in line 12 corresponds to the relevant future time interval, analogous to the leftmost map in figure 3.2, followed by the determination of the node through which the vehicle goes (lines 13 and 14). After that, the footprint mapping which coincides with the combination of time interval index, originating road segment RS_{veh} and affected node is increased. This procedure is repeated for the entire new route, unless the predicted arrival time t_{arr} exceeds the maximum forecast time before (if the condition in line 9 is satisfied).

Congestion increasingly occurs near intersections which merge multiple high-frequently used road segments [109]. Thus, merely the total amount of vehicles passing a node within

a specific $(\Delta t)_j$ is not sufficient to calculate the load of a node. The knowledge about from which source segment a vehicle is entering is highly beneficial for calculating the likelihood of a future congestion in this spot. It makes a big difference whether 15 vehicles arrive at an intersection from three different source road segments or just from one single segment within a single time interval $(\Delta t)_j$. The upper part of the algorithm describes the cleanup of an old mapping in case of a route update. The mapping entry referring to the removed vehicle can be identified easily by the vehicle's ID, ensuring not to miss an entry in this mapping which leads to wrong decisions in further consequence.

The resulting network footprint then contains a full representation of the current and future road conditions in the resolution of the defined time interval Δt , which is further applied for congestion detection and selection of vehicles to be rerouted.

3.2.4 Prediction Methodology

In order to counteract congestion timely, PCMA* predicts future bottlenecks with the aid of the presented network footprint. A threshold for the prediction algorithm $\theta^{(P)}$ is defined per node (intersection) and determines how many vehicles can pass this node per second. We unify this threshold unit to vehicles per second, in order to be independent of the chosen time interval length Δt .

$$P_i^{(S)}((\Delta t)_j) > \theta^{(P)} \times \Delta t \quad \text{and} \quad (3.15)$$

$$\exists =^k NV_{RS_n} > 0 \quad | \quad k > 1 \quad (3.16)$$

Equations (3.15) and (3.16) describe the criteria for a detected congestion. The number of arriving vehicles from road segment RS_n is again represented by NV_{RS_n} , while k represents the number of distinct road segments from which vehicles are arriving. The reason for the constraint $k > 1$ is due to the fact that vehicles which come in from only one RS are unlikely to result in a congestion, independent of their exit lanes. To a greater degree, test simulations have shown that vehicles which cross the intersection approach from multiple entry lanes worsen the situation immensely (as also explained above in section 3.2.3). Put in simplified terms, six vehicles arriving from solely one direction are much less critical than three vehicles from two entry lanes within the same time interval. In the former case, the waiting times due to crossing trajectories within the intersection is zero, while the likeliness for delays in the latter case is higher.

Once a summarized node footprint $P_i^{(S)}$ of time interval $(\Delta t)_j$ exceeds the threshold $\theta^{(P)}$ and vehicles at the same time arrive from more than one source road segment RS_n , inequations (3.15) and (3.16) are satisfied. Thus, a congestion event containing congested node and the predicted time interval is risen for further processing.

3.2.5 Vehicle Selection

After a potential future congestion is predicted in time interval $(\Delta t)_j$, the next step is the selection of specific vehicles which should be considered for taking an alternative route. For this to solve, the PCMA* algorithm looks up all prognosticated affected vehicles in the network footprint with the concerned time interval and node ID as input. From the resulting list of vehicles, it chooses exactly the amount of vehicles which cause the threshold to be exceeded, ordered descending by Euclidean distance. The farthest vehicles are chosen first, as the probability for spacious alternative routes is higher for them than for those which are very close to the predicted congestion. Those selected vehicles are queued for rerouting and thus take a route which avoids the congested intersection node.

Avoidance of Self-Alternating Route Changes

In unfortunate cases, the rerouting algorithm may lead to a situation where N nodes, say that is node set S_N , are congested or short before exceeding the defined congestion threshold. After a congestion is detected in node $\mathbf{A} \in S_N$, vehicles may be redirected to an alternative route passing node $\mathbf{B} \in S_N$ in order to come below the threshold in node \mathbf{A} . This route change further causes exceeding the threshold in node \mathbf{B} . After detecting this exceedance, the algorithm tries to solve the situation in \mathbf{B} by assigning a route that again passes \mathbf{A} or another node of set S_N , that is currently not congested and so on. In other words, the routes consecutively exceed a threshold of a single passed node and tries solve this problem by using an alternative route that contains nodes of the same critical set S_N repeatedly. In fact, the situation is surely not resolved, but threshold violations are just alternating between the affected nodes of S_N . For that reason, we set a time hysteresis t_h due to the potential continuous and frequent switch of multiple vehicles' routes between nodes of a set S_N . Thereby these frequent route changes are prevented and a single vehicle cannot be assigned a new route twice within time interval t_h .

Route Filtering

Especially in overcrowded environments, the presented approach can rarely generate proposals for new routes which are unfavorable with regard to the potential of improvement. If a majority of intersections within a narrow area is identified as congested, an alternative route can in case of a disadvantageous layout of the road network be very long. In such a case, waiting for the situation to relieve can be a better option than accepting the extra travel distance.

In order to ensure that the detours which are implicated by the selection of an alternative route are in an acceptable proportion to the original route, a threshold can be defined which makes it possible to constrain the maximum allowed growth of travel distance between the original and newly assigned route. This threshold is independent of the

applied weighting and routing mechanism. It is denoted as η_s and calculated by dividing the accumulated distance of all road segments RS of the new route by the accumulated distance of the currently assigned route, according to equation (3.17).

$$\eta_s = \frac{\sum_{i=1}^{RS_{max}^{(old)}} \text{roadlength}(RS_i^{(new)})}{\sum_{i=1}^{RS_{max}^{(new)}} \text{roadlength}(RS_i^{(old)})} \quad (3.17)$$

Additionally, the estimated travel times of the currently assigned route compared to the potential new route can be related to each other, which further enables the limitation of unfeasible routes. This way it is ensured for the consuming vehicle that accepting the proposal for the new route is beneficial. This time threshold η_t is calculated according to equation (3.18), which brings the estimated cost in terms of travel time of the old in relation to the same of new route.

$$\eta_t = \frac{\sum_{i=1}^{RS_{max}^{(new)}} \text{traveltime}(RS_i^{(new)})}{\sum_{i=1}^{RS_{max}^{(old)}} \text{traveltime}(RS_i^{(old)})} \quad (3.18)$$

Choice of Vehicles with Regard to the Reactive Part

However, the PCMA* algorithm also makes use of the reactive algorithms described in section 3.2.1 as extension and additional source of congestion information. This is beneficial for the following reason: If a traffic jam cannot be avoided completely by prediction, vehicles can still be told to use an alternative route due to the reactive detection component. As soon as traffic comes to a standstill, PCMA* is not able to perform predictions any more since equations (3.2) and (3.4) yield zero because of zero vehicle velocity or a fully occupied road segment. As a consequence, the arrival times for all subsequent passed nodes yield infinity.

The reactive components (GS or SA) need to select the potential candidates for rerouting somehow different to the predictive component, since those mechanisms do not comprise affected vehicles at congestion detection time. Therefore, the range R_{seg} is used to define how far from the congested node to look for candidates to be rerouted. $R_{seg} \in \mathbb{N}$ denotes the number of segments that a candidate can be away to be considered for a new route assignment. Those vehicles which are traveling at a road segment that is reachable over R road segments from the congested node are selected for rerouting.

Recapitulatory, only the reactive algorithms make use of the range parameter R_{seg} for vehicle selection. In contrast, potentially predicted future congestion already contain the

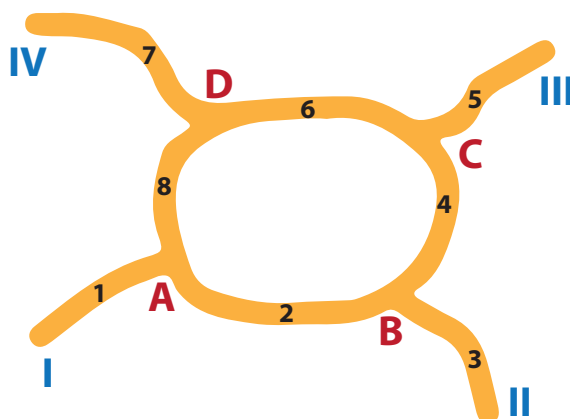


Figure 3.4: Simplified snippet of road network

information about involved vehicles. These possibly affected vehicles are not limited to be located near the congestion, but can be spread all over the road network.

3.2.6 Simplified PCMA* Example

The prediction and rerouting workflow is elucidated by the example in figure 3.4. We assume vehicles v_0 to v_3 , which will pass the depicted passage as described in table 3.3.

Table 3.3: Start order and times

Vehicle	Source \rightarrow Target	Route	Start time
v_0	II \rightarrow IV	{3 - 4 - 6 - 7}	0
v_1	IV \rightarrow II	{7 - 6 - 4 - 3}	0
v_2	III \rightarrow I	{5 - 4 - 2 - 1}	0
v_3	IV \rightarrow II	{7 - 6 - 4 - 3}	1

The vehicles start in locations II to IV, can use road segments 1 to 8 with segment cost $C_{seg} = 1$ for all segments and therefore may pass nodes A to D during their routes. The threshold $\theta^{(P)}$ of vehicles per second for this example is set to 1. For reasons of simplification, we further assume the speed of all vehicles to be equal to 1. Due to the initial assignment of routes as denoted in the third column of table 3.3, the threshold is exceeded in node C at time 2 (table 3.4). The algorithm detects this issue and calculates new routes for affected vehicles until the predicted congestion is resolved. In the example case, v_0 is chosen to assign the new route {3 - 2 - 8 - 7} and therefore bypasses node C (table 3.5). Finally, the thresholds for all nodes and all time intervals are satisfied and node C is relieved.

Table 3.4: Node state / time matrix with exceeding threshold

Time / Node	A	B	C	D
0	-	-	-	-
1	-	v_0	v_2	v_1
2	-	v_2	v_0, v_1	v_3
3	v_2	v_1	v_3	v_0
4	-	v_3	-	-

Table 3.5: Node state / time matrix with satisfied threshold

Time / Node	A	B	C	D
0	-	-	-	-
1	-	v_0	v_2	v_1
2	v_0	v_2	v_1	v_3
3	v_2	v_1	v_3	v_0
4	-	v_3	-	-

3.3 Validation

A validation of the routing algorithm is presumably connected with high effort. Not only would this require a possibility to transfer the routing information to cars and visualize it for the drivers. If the car itself does not (yet) have the communication ability, the information dissemination could take place via devices connected via an existing cellular network, such as common smartphones. Assuming the challenge of information dissemination is solved, a high amount of participating cars is necessary in addition to that, what is probably the most difficult thing to realize. Although the experiments concerning penetration in section 5.4 show effects even for low percentages, the amount of routable vehicles still needs to exceed a minimum threshold in order to reach a level where congestion occurs and routing is useful. Thus, an end-to-end validation of PCMA* is rather difficult and exceeds possibilities of our research group, though by no means impossible. However, validation of the applied models is arguably of even higher importance and treated in sections 2.2.5 and 4.5.

4

V2X Communication Modeling

Numerous technologies are already deployed or will exist in the near future to assist and manage vehicular transportation. Modern vehicles already have sophisticated sensing capabilities and carry powerful computing platforms. This chapter gives a short overview, introduces existing and standardized technologies, and how those are related to the investigations within this thesis.

4.1 Communication Technology Overview

4.1.1 Applications

Basically, the applications of communication technologies in vehicles can be categorized into the following three scopes [116, 117]:

- *Transportation Safety*: Applications concerning safety try to help to reduce the probability for an accident, or at least reduce the severity if it is still unavoidable. A wide range of intelligent systems is covered. Firstly, those are diverse types collision avoidance systems. The system can keep a safe distance by using built-in sensors and/or V2V communication to detect dangerous situations and reduce the speed. Also, intersection collision avoidance is an important application, which also requires V2X communication capabilities apart from built-in sensors for enhancement of the visibility range of a vehicle. Secondly, driver assistance such as notifications for road signs or speed limits and incident management are covered. Handling of accidents which still happen is the third type of safety application by sending warning messages to upcoming and surrounding vehicles. All these applications require communication between vehicles and/or infrastructure and low latency [117].
- *Transportation Efficiency*: This category includes applications which on the one hand gather information about the current conditions on the road and make use of this information by managing traffic flow, guiding vehicles and perform optimizations. Applications include tolling on the one hand, but also intelligent intersection control and route guidance of vehicles. Depending on the application, both V2V and V2I communication can be suitable. For reporting and route guidance, a good coverage, medium latency and low data rate would fit the needs. In contrast, for monitoring of short-term road conditions such as danger of aquaplaning, slippery roads due to ice or oil a fast local distribution of the information is necessary [117].
- *Infotainment*: All services related to passenger comfort are ascribed to this category. Although providing information, videos for passengers or news may have less time-critical aspects, it still can require lots of resources and communication capacities in case of video transmission, which must be taken into consideration. Additionally, contextual applications such as tourist information, local attractions, advertisements or parking booking can increase drivers' awareness of location dependent information. On the other hand, limited coverage and infrequent updates could be acceptable for non-safety applications, for example for news updates or download of entertainment videos.

This thesis deals with the second category of application, namely optimization of *Transportation Efficiency*. The following subsection introduces relevant communication standards, which can fulfill the requirements therefor.

4.1.2 Important Technologies

The basis of the mentioned applications for Cooperative Intelligent Transport Systems (C-ITS) is a functional infrastructure for both the mobile and also the base stations. In the following, short introductions into communication standards which are relevant for the application of increasing transportation efficiency are given.

A strong distinction needs to be made between ad-hoc communication between devices without any fixed infrastructure on the one hand, and communication from a mobile vehicle to a fixed Base Station (BS) on the other hand. The channel properties are fundamentally different, as BSs are usually placed above rooftop level, or at least elevated, while the placement of antennas for vehicles is limited to the car boundaries. This results in a different environment and scattering behavior. Additionally, the relative velocities in V2V channels are much higher, thus also the possible time span where successful transmission is possible limited [118].

Device-to-device Communication

Vehicular Ad-hoc Networks (VANETs) require only little or no permanent communication infrastructure. High mobility, few constraints regarding power or storage limitations due to the application within vehicles and fixed road networks are characteristics of VANETs. Ad-hoc device-to-device communication is basically designed for time-critical safety applications where the main goals are high reliability and short delays. Therefore, applications include lane change assistants or collision avoidance systems. Furthermore, applications that increase efficiency and traffic flow can require V2V communication. An example for the latter is platooning, where the gap between vehicles is reduced to a minimum and thus aerodynamic drag decreases, as well as space consumption on the road.

IEEE 802.11p: As one of the key technologies for V2X communication, the international standard IEEE 802.11p is part of the Wireless Access for Vehicular Environments (WAVE) initiative and based on the Wireless LAN (WLAN) standard as known from desktop and smartphone Wi-Fi networks. The low latency and design of 802.11p to support VANETs are among the strengths and design goals of the standard [119], which provides support for direct V2V communication [120] in absence of a network infrastructure. It is from the beginning designed for both V2I and V2V ad-hoc modes and the basis for Dedicated Short Range Communication (DSRC) in the 5.9 GHz frequency band [118]. Unlike other amendments of the 802.11 standard, the channel bandwidth is reduced to

10 MHz in order to make it more robust against fading. The defined ad-hoc mode enables devices to communicate in mobile environments outside a base infrastructure network. It uses Carrier Sense Multiple Access (CSMA) as its Medium Access Control (MAC) mechanism due to the lack of a coordinating entity. Because of the delegation of the authentication to layers above Physical Layer (PHY)/MAC, delays for the initial frame exchange are further decreased and are typically around a few seconds [121]. This is important due to very short timing in case of vehicles driving in opposite directions. Upper layers use the IEEE 1609 standard and its amendments for services. More details regarding layers can be found in [122]. The 802.11p standard was approved in 2009, and since then was intensively investigated in field studies and simulations [123–129]. It is gaining more and more attention, since it is ready for deployment by now (July 2017) - at least from the standardization and testing point of view.

LTE: This standard is described as the 4th Generation (4G) of cellular networks that is defined by the 3rd Generation Partnership Project (3GPP). Although the architecture of LTE is basically centralized with fixed BSs and movable Mobile Stations (MSs), it can on the one hand be the access technology for VANETs due to its high data rates. On the other hand, it is continuously extended and will support V2X communication in the near future. Already with Release 12, a device-to-device communication was introduced to the LTE standard in March 2015 [130]. The use cases are public safety applications in out of coverage scenarios and commercial interests. By Q1 2016, Release 13 was published which introduces LTE in unlicensed spectrum (LTE-U), such as the 5 GHz band as also used by 802.11 compliant Wi-Fi equipment. In contrast to the previous release, it introduces support for device-to-device communication also in areas out of coverage. In June 2017, the features for Release 14 were frozen, that introduces, among others, support for V2X services [131]. They promise support for relative speeds up to 500 km/h due to additional Demodulation Reference Signal (DMRS) symbols for channel estimation and also meeting latency requirements of V2V applications by a new arrangement of scheduling assignment. The standard supports two modes of scheduling, which can be assisted by an LTE eNodeB BS (Mode 3), or completely without permanent infrastructure based on distributed algorithms (Mode 4). Starting with Release 14, the LTE design is scalable in bandwidth, including also 10 MHz, as used by IEEE 802.11p [132].

Vehicle-to-Infrastructure Communication

Cellular communication infrastructure exists much longer than the necessity of thinking of communication directly between vehicles. While originally intended for speech communication in the Global System for Mobile Communications (GSM) standard, the usage nowadays more and more tends to be packet oriented data transmission. Especially due

to the increasing amount of applications for mobile data also in vehicular environments, V2I communication has gained more and more attention in the development of wireless infrastructure. The number of mobile subscribers in general has increased dramatically in the last two decades, resulting in a steadily increasing demand of higher data rates after the success of GSM/Enhanced Data Rates for GSM Evolution (EDGE) (2nd Generation (2G)) and Universal Mobile Telecommunications System (UMTS)/High Speed Packet Access (HSPA) (3rd Generation (3G)). Characteristics of current cellular systems are high capacities regarding data rates and communication speed as well as high coverage and penetration rate. Applications are information dissemination for traffic management as notification of congestion, dynamic events such as temporary capacity drops of roads or route guidance.

LTE: Due to its high market penetration over all the world, LTE cellular networks are already applicable also for vehicular purposes. Both the radio and core network for LTE were frozen with Release 8 in December 2008 with increased spectral efficiency, peak data rates as well as flexibility in frequency (from 700 to 2600 MHz carrier frequency all over the world) and bandwidth (1.4, 3, 5, 10, 15 or 20 MHz). LTE also supports TDD and Frequency Division Duplex (FDD) from Release 8 on. Orthogonal Frequency-division Multiple Access (OFDMA) and Single-carrier Frequency-division Multiple Access (SC-FDMA) are used as access technology in downlink and uplink direction, respectively [133]. Packet scheduling is done by the BS called eNodeB in LTE, which also manages the resources in each Transmission Time Interval (TTI) of 1 ms. 3GPP Release 9 adds Multimedia Broadcast Multicast Service (MBMS), which allows transmission of specific content to a closed subscriber group only once and can be used for high-quality multicast and broadcast (e.g. advertisements or video streaming) [134].

LTE Advanced (LTE-A): The 3GPP standardization further produced Release 10 in September 2011, which is an extension of LTE and allows higher data transmission rates up to 4 GBit/s in downlink and 1 GBit/s in uplink direction. LTE-A is backwards compatible to LTE, but has increased spectral efficiency, supports a higher number of simultaneously active users and better exploits Multiple-Input-Multiple-Output (MIMO) antenna technologies, which improves the performance at cell edges. Carrier aggregation is used to increase bandwidth. Certain areas may be covered by multiple serving cells, all of which are used as secondary component carriers what also increases the possible data rate and still maintains backwards compatibility [135].

Table 4.1: Wireless technologies for on-the-road communications (reproduced from [136])

<i>Feature</i>	Wi-Fi	IEEE 802.11p	LTE	LTE-A
<i>Channel width [MHz]</i>	20	10	1.4, 3, 5, 10, 15, 20	up to 100
<i>Frequency band(s) [GHz]</i>	2.4, 5.2	5.86 - 5.92	0.7 - 2.69	0.45 - 4.99
<i>Bit rate [Mbit/s]</i>	6 - 300	3 - 27	up to 300	up to 1000
<i>Range [m]</i>	up to 100	up to 1000	up to 30000	up to 30000
<i>Capacity</i>	Medium	Medium	High	Very high
<i>Coverage</i>	Intermittent	Intermittent	Ubiquitous	Ubiquitous
<i>Mobility support</i>	Low	Medium	Very high (up to 350 km/h)	Very high (up to 350 km/h)
<i>Broadcast / multicast support</i>	Native	Native	Through MBMS	Through MBMS
<i>V2I support</i>	Yes	Yes	Yes	Yes
<i>V2V support</i>	Native	Native	No	Yes (from Release 14)
<i>Market penetration</i>	High	Low	High	Potentially high

4.1.3 Comparison

The decision about which of the existing types of wireless communication standards to choose obviously strongly depends on the intended type of application. The main characteristics of the described technologies are shown in table 4.1 [136].

In case of safety applications, as described in section 4.1.1, reliability and timeliness are the two major criterions. Basically, time-triggered status messages and event-driven messages can be separated, as both standardization organizations IEEE and European Telecommunications Standards Institute (ETSI) have specified for the US and Europe, respectively [119]. The ETSI standard [137] describes the types of messages as those which are firstly intended for periodic transmission and contain status updates such as current position or speed and named as Common Awareness Messages (CAMs). In contrast, event-triggered messages are called Decentralized Environmental Notification Messages (DENMs) and are intended for alerts of any hazards or information. The IEEE has adopted these two central message types in 802.11p [119]. It was decided to use the same MAC and PHY layers, although using slightly different frequency bands. However, the fundamental type of application and way of functioning is comparable. Both messages are intended to be received within a limited geographic area in the neighborhood. CAMs are transmitted with a frequency of up to 10 Hz by each vehicle. Both mentioned message types have a critical latency constraint of maximum 100 ms [136]. Therefore, by now (July

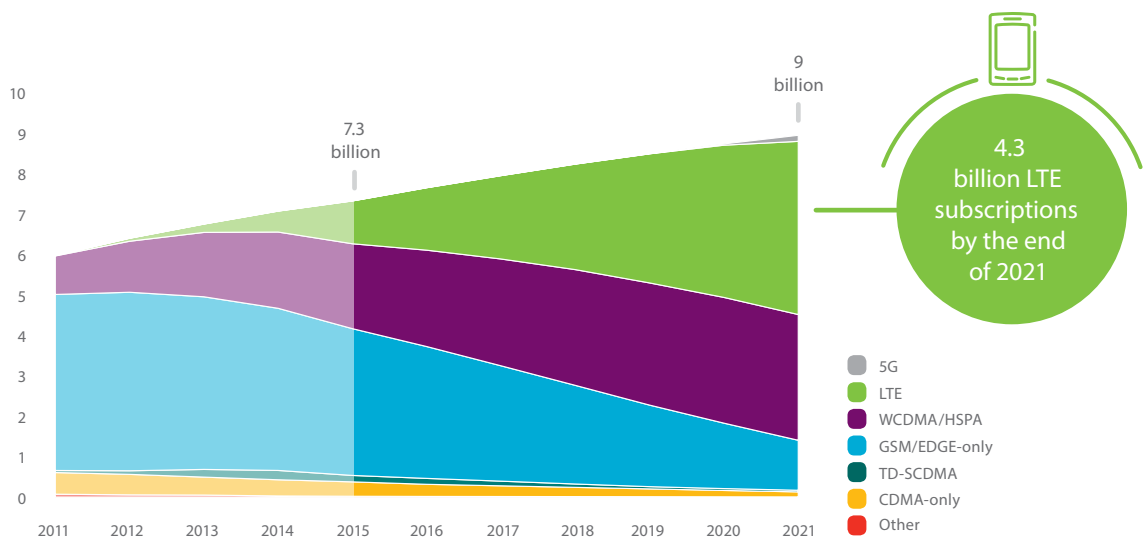


Figure 4.1: Mobile subscriptions forecast by technology [142]

2017), the capacity of existing centralized cellular infrastructure requires passing all this traffic through the network infrastructure, i.e. eNodeBs in case of LTE. The bandwidth capabilities are a problem with an increasing number of users [138], which is definitely an argument for technologies that support direct V2V communication for these applications (such as those introduced in section 4.1.2).

On the other hand, the cellular network has advantages for applications where time and delay is not so critical. LTE and LTE-A allow high payloads and have high coverage, what further allows data transmission over large areas. The distance between vehicles which can provide data and other which make use of it does not play a major role. Furthermore, in situations with low vehicle density the existing cellular networks are the only possibility to communicate. Therefore, ITS applications such as traffic management and forecast systems are well suited to use the cellular network for communication. Sensors in the road network and/or within vehicles can provide information that further can be combined and used for determination of the current or prediction of future situations on the road [139]. Furthermore, the fixed infrastructure can be used for collecting information about the current situation through Floating Car Data (FCD) [140]. What also should not be disregarded is the fact that LTE networks already exist, are among the most successful wireless standard of our time [141] and are used by billions of people around the world, with a rapid growth - as figure 4.1 shows [142].

4.2 Abstract Modeling of Communication

4.2.1 Background Overview

A widely investigated research area deals with centralized approaches related to traffic optimization and any manifestation of coordination system [103, 107, 143–148]. Independent of the applied algorithm to improve traffic flow and reduce congestion, the routing entity requires information of the current conditions on the road, the vehicles positions, their destinations or other constraints regarding the route itself or a vehicles' capabilities. Based on that information, it can analyze the situation and decide which actions to be taken to improve the situation. In the end, the proposed decisions for optimization need to be transferred to the affected vehicles. Various approaches from literature work in this or a similar way, and therefore require the availability of any communication system, be it V2V, V2I or a combination of them. The requirements of routing approaches further differ in delay and latency constraints, transmission capacities or number of supported users. Currently available communication standards such as 3GPP Release 14, which introduces LTE support for V2X services [131] or the Wi-Fi based IEEE 802.11p [120] imply different limitations regarding driving velocity, capacity, latency and other relevant properties (cf. section 4.1).

Standardization organizations naturally and with justification tend to improve existing communication standards and develop new ones, in the interest of fulfilling today's and tomorrow's requirements. Those have even shorter delays, latencies and higher capacities than their predecessors. However, the standards in case of LTE or IEEE 802.11p can merely define the maximum technically possible achievable transmission speed, latency, allowed driving velocities of communication partners and other crucial characteristics. The situative achievable average transmission speed is rather dependent on the environment, number of active subscribers, geographical properties, movement speed and capabilities of the subscriber's device. Nevertheless, while there are approaches to somehow guarantee the latency for 802.11p [149, 150] or LTE [151, 152], the question is whether the effort is worth the benefit resulting from it. Some approaches may have more restrictive requirements on the underlying communication network, while others may be more robust in respect of delays or transmission errors. In other words, the performance of intelligent cooperative vehicle routing algorithms can also depend on the quality of the information exchange by V2X communication. Ideal information exchange with no delays and perfect communication conditions does not exist in reality. In fact, the conditions can vary substantially depending on the infrastructure and environment [19] and therefore significantly reduce the functioning ability of an intelligent traffic routing. The border between achieved improvements that satisfy the operator of such an intelligent traffic optimization system to a bad performance is not hard, but to a greater degree follows a smooth

behavior. Exactly this topic is addressed by defining simple delay and loss models and applying them to PCMA*. The result is a precise quantification of improvements due to intelligent cooperative routing depending on the features and characteristics as well as applied parameters of the used communication system.

4.2.2 Basic Radio Propagation

The loss of signal strength in wireless radio transmission varies due to multiple effects, depending on temporal and local fluctuations. Even at constant distance between transmitter and receiver, the amplitude of the received signal varies. Fading can be distinguished in the following three generally distinct components [153]:

- **Distance pathloss:** The geometric pathloss describes the descent of signal strength as a consequence of a varying distance between transmitter and receiver. The loss follows a logarithmic behavior, depending on the distance.
- **Slow fading:** In addition to geometric pathloss, the propagation of a radio signal is usually not exclusively free space, but is subject to fluctuations due to obstacles in the environment. Especially in urban scenarios, this effect plays a major role. Due to buildings and vegetation in the way of transmission, signals are shadowed and thus also experience a decrease in amplitude.
- **Fast fading:** As a consequence of reflexion, scattering and diffraction, signals diffuse via many paths from transmitter to receiver. Due to this multipath propagation, the signals arrive at distinct times with multiple phase shifts at the receiver and interfere to a received signal. The interference of the parts can be constructive, when the signal strength is considerably higher than its mean value. However, in case of destructive interference, an extremely low signal is received for a short time.

In view of vehicular environments, the special characteristics and differences to the intensely investigated cellular communication channels must be taken into consideration. While the BS is fixed, mostly elevated and thus free of scatterers in the immediate surroundings in cellular scenarios, it is on the ground level in vehicular communications. The number of scatterers can vary notably in vehicular environments due to other vehicles in the near surrounding, and those are moving faster [118]. The time-frequency selective fading (i.e. fast fading) is significantly different between V2V and V2I environments due to the fact that both communicating entities are moving [154]. This also requires distinct models for these environments.

The radio propagation channel needs to be represented differently in simulations for varying propagation environments. Examples are urban streets with dense building blocks and high traffic density, suburban areas with a greater gap between the roads and nearby

buildings, highways with multiple lanes in each direction and no houses besides them and also rural roads with single lanes and a higher possibility for sources for multipath components such as hills, vegetation and lower traffic density [118].

Furthermore, the effects regarding antennas plays a vital role - especially in V2V environments. It is shown in [155] that especially the mounting position of the desired antenna omnidirectional characteristics greatly defines the performance and limits of the radio link. Mounting positions very close to the roof cause shadowing and thus also negatively influence the radiation pattern [118]. This is not a problem in cellular scenarios, since the antenna position of the BS can be chosen under consideration of the immediate environments, and due to the fact that it is not moveable also with a directional antenna characteristic.

4.2.3 Abstraction

For all the reasons mentioned in section 4.2.2 above, it is neither possible to specify a single model that is valid for all environments from urban to rural and from highly mobile to quasi stationary nor is it possible for all use cases, be it safety applications, infotainment or for the purpose of increasing efficiency on the road. Therefore, the influence of radio propagation channels on the performed simulations is abstracted in a way that the model is independent from the underlying standard, the environment or the used technology.

Many different channel models for various types of wireless propagation channels exist in literature [153,156,157], all of which have a special focus and area of application. In the field of simulation of wireless communication, common practice is to separate modeling the wireless channel characteristics on link level from the movement of the communicating devices on system level [158–160]. The link level includes detailed characteristics and modeling of the radio channel with microscopic time resolution including also a transmitter and receiver, apart from the fading channel. It aims to investigate impacts of algorithms on the physical layer and to quantify their robustness to fading in terms of an average Bit Error Rate (BER) or Frame Error Rate (FER). The system level uses the output of the link level, and models BS, movement and management of the radio resources among the users [161]. This separation is necessary due to the impossibility of modeling each radio channel with great level of detail while simulating a large extract of a communication system.

However, for the simulations of this work, I further abstracted the effects of the communication channel. The focus lies on the time delay in message transmission due to unideal conditions, as this is a major criterion for the presented ITS application. The reason for this abstraction is twofold: It harmonizes all properties of the communication channel to a single variable with few parameters of the statistical distribution. Thus, the applied communication standard and methodology is irrelevant, as long as it fulfills the defined

constraints. Put in other words, the performance of the presented approach is associated with properties of the message transmission. The second reason for the abstraction is patently simplicity, expressed by a minimum amount of parameters.

4.3 Message Exchange

For the determination of the current situation on the road and also prediction of potential future congestion, PCMA* naturally requires vehicles to provide information such as their position, speed, currently active route and destination. This information needs to be transferred somehow to the routing entity, which can be carried out by any V2X communication technology (cf. section 4.1). Apart from that, the router transmits the optimized routes to the corresponding vehicles. Basically, the time for transmission of a message from its origin to the destination is one of the most important performance characteristics of a data network [162]. In almost the same manner, delay is an important criterion for information propagation for PCMA*. Therefore, the messages are categorized into types since they have different frequencies of transmission, are either transmitted from or to the vehicle (or in both directions) and have varying triggers and content, as described in the following.

4.3.1 Types of Messages

Initial Message

<i>Frequency of transmission:</i>	Once
<i>Source:</i>	Vehicle
<i>Target:</i>	Routing system
<i>Trigger for transmission:</i>	The vehicle registers on the system in order to provide information and also receive route guidance in case of any congestion on the route.
<i>Content:</i>	Source and destination of desired trip

Vehicle Data Message

<i>Frequency of transmission:</i>	Continuously
<i>Source:</i>	Vehicle
<i>Target:</i>	Routing system
<i>Trigger for transmission:</i>	The defined transmission interval time is up
<i>Content:</i>	Current position and speed of the vehicle

Route Update Message

<i>Frequency of transmission:</i>	On Demand (just as route update is necessary)
<i>Source:</i>	Routing system
<i>Target:</i>	Vehicle
<i>Trigger for transmission:</i>	A new route was calculated for a selected vehicle as a consequence of a detected or predicted congestion.
<i>Content:</i>	The new route to take

Route Confirmation Message

<i>Frequency of transmission:</i>	On demand (new route successfully applied)
<i>Source:</i>	Vehicle
<i>Target:</i>	Routing system
<i>Trigger for transmission:</i>	A Route Update Message was received, and the vehicle has successfully applied the new route.
<i>Content:</i>	The applied route

4.3.2 Sequence of Communication

The messages are either transmitted in regular intervals, somehow comparable to CAMs as defined by ETSI or on demand, such as DENMs [163]. Vehicles which are configured to be able to provide information and receive route guidance actively tell the system initially from where to where the trip is intended to go. This information is used to update the PCMA* footprints for all nodes along the route. During the trip, the vehicle regularly reports its current position and speed, what results in an update of the footprint matrix on the one hand and refresh of the conditions on the current road segment on the other hand. Just as a congestion is detected or predicted by PCMA*, target vehicles are selected and the newly calculated routes are sent to them. Subsequently, the vehicle confirms the application of the new route and therewith also informs the router that the new route is valid from now on. If the message is not confirmed due to any communication problem, it is discarded. A possible sequence of messages could look as defined in figure 4.2. It includes regularly transmitted *Vehicle Data* messages, as well as two on-demand route update messages 1 and 2, from which only number one gets confirmed and thus is applied successfully as well.

4.3.3 Exceptional Cases

Several problems can occur during execution of the protocol above due to an unfavorable temporal flow of incidents.

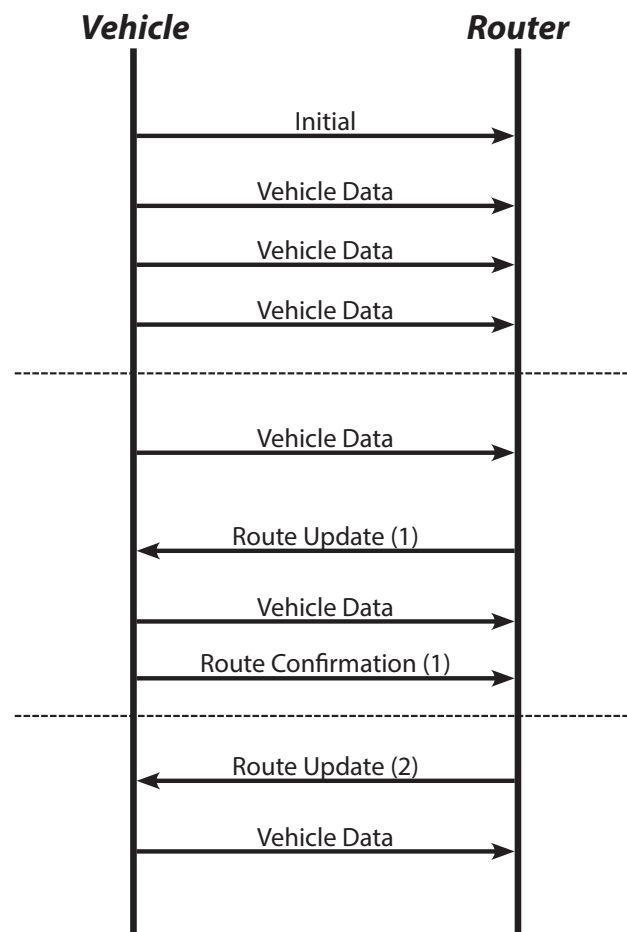


Figure 4.2: Possible communication flow between a vehicle and the central router

First, delay or loss of the regularly transmitted vehicle data may lead to inconsistent or outdated knowledge of the current road conditions on the part of PCMA*. As a consequence of a low p_{success} for periodic messages, the router's knowledge about possible velocities on certain road segments becomes inaccurate. This issue may not be serious enough to severely distort the known road network status as soon as the traffic density is high enough that at least one functional communication per road segment is possible in a reasonable time interval. If the success probability becomes very low, the router weighs its graph wrongly and uses this wrong basis for its routing decision. This has on the one hand strong influence on the reactive component of PCMA*, since congestion is recognized on the basis of the current load factor of an intersection. On the other hand, also the congestion prediction mechanism has a hard time, since the predicted times when a certain vehicle passes an intersection also depend on the currently detected average velocity of all passed nodes, and those time predictions are essential for congestion predictions.

Second, the impact of delays of messages related to route updates is threefold. The first influenced communication protocol is the initial registration of a vehicle on the system. A

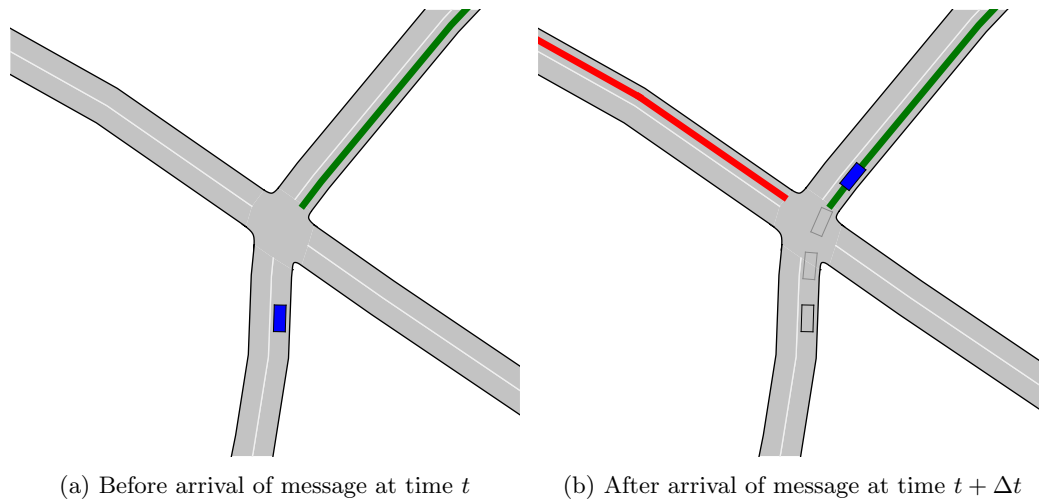


Figure 4.3: Snapshots before and after the new route (marked in red) was received by the vehicle

too late reception of this message shrinks the possibilities for the router for early reaction on possible traffic jams by spacious detours. Second, it can make the new route inapplicable in the worst case. This situation occurs if the message which contains the new route advice is received after the vehicle passed by the last possibility to change to the received route, as figure 4.3 illustrates. The routing algorithm comes to the conclusion that the original green route for the vehicle should be changed, and sends the message including the new red route to the vehicle at time t . Due a delay of length Δt , the message arrives after the vehicle passed the intersection, and needs to be ignored since the new route cannot be reached via this segment. And third, the confirmation message of vehicles that a new route is applied is delayed. This results in a discrepancy between the real assigned routes and those the router thinks that are assigned, which further has negative effects on the prediction mechanism due to a wrong calculation of the occupancy of intersections.

The third incident bases on the fact that the intersection regulation disallows changing the desired exit lane if the vehicle is in close proximity to the intersection entry. Otherwise, this could lead to overlapping paths between vehicles which already decided to drive through the intersection and would not have been intersecting, and the vehicle which changed its route before. Safe breaks are not possible in this case, and malfunction of the intersection control is the consequence. Figure 4.4 shows such a situation. Both vehicles $v1$ and $v2$ originally can enter and drive through the intersection without problems via the blue and green paths, respectively. On the contrary, a route change of $v2$ to turn left and follow the red path must be prevented if a standstill for $v2$ before entering the intersection is not possible safely any more.

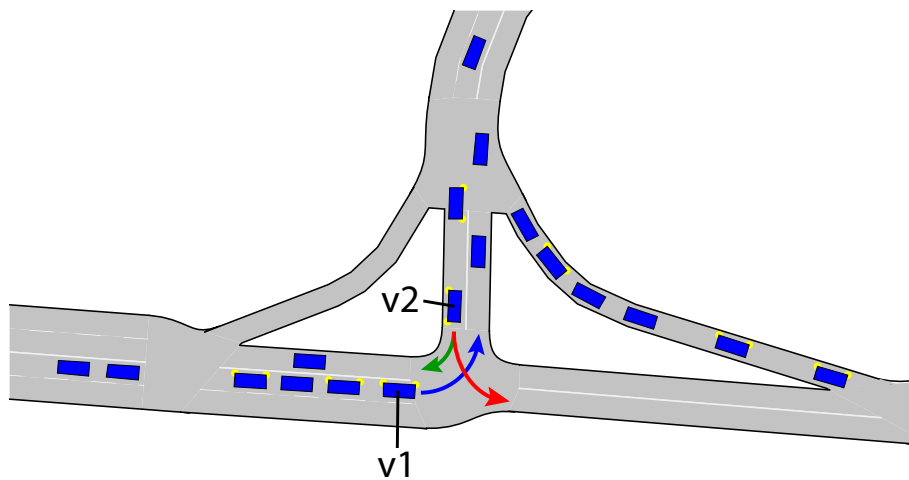


Figure 4.4: Problematic route change of $v2$ right before intersection

4.4 Delay Modeling

As delay is a major criterion for the presented approach for increasing traffic efficiency, the models for message delay must be able to provide the required times until the message is received successfully. Depending on the type of message, also complete loss of messages is modeled. These models comprise the whole protocol stack and reduce the output to either a certain time delay or a flag indicating a lost message, without modeling detailed channel characteristics, Automatic Repeat Request (ARQ) or Forward Error Correction (FEC) protocols or comparable mechanisms.

4.4.1 Geometric Delay Model

For messages which are not transmitted in regular intervals and are denoted as ODMsgs, the delay is modeled as a geometrically distributed random variable. It is assumed that potential unsuccessful transmissions are repeated until the full message can be interpreted by the receiver. The distribution itself is described by a single parameter λ in the range $0 \leq \lambda \leq 1$ which represents the probability of success. The influence of a varying parameter λ on the Probability Mass Function (PMF) is shown in figure 4.5.

The next message delay Δt is determined by calculation of the next sample of the distribution f , which defines the number of failures until the message is received successfully. Therefore, a second parameter is introduced, which defines the Roundtrip Time (RTT). This RTT is multiplied by the number of failures resulting from a realization of the random variable. In order to represent a potential fixed time delay which should be applied to each message transfer, an offset t_o is added. Therewith, an overall delay of zero, which would be the result of the distribution in many cases can be avoided, since this situation is impossible to achieve under real conditions according to equation (4.1).

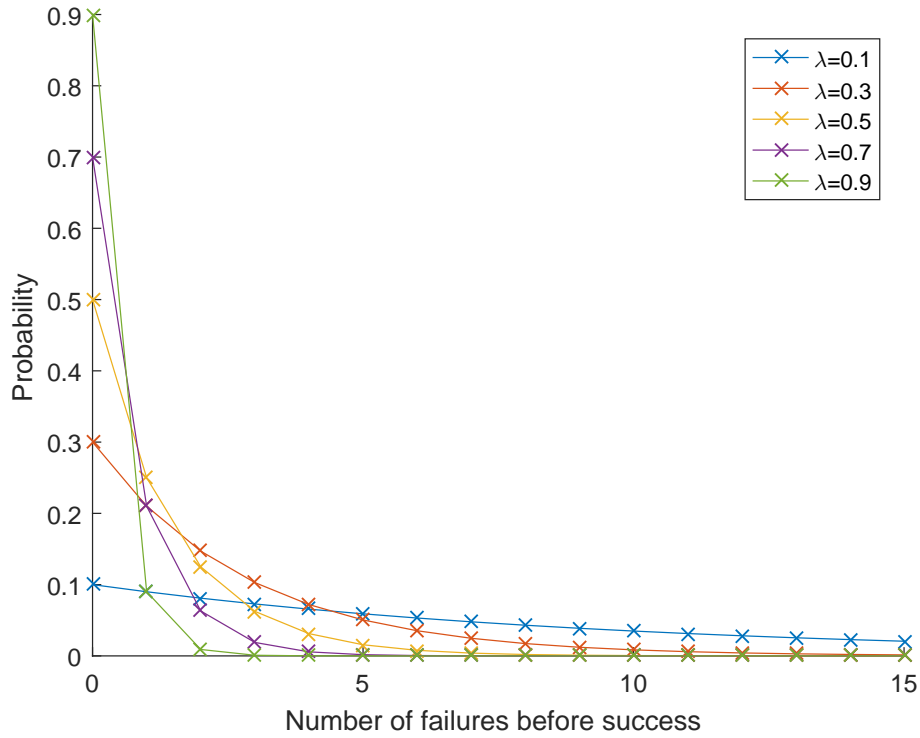


Figure 4.5: PDF of geometric distribution with varying parameter λ

$$\Delta t = t_o + f * \text{RTT} \quad (4.1)$$

The model also allows specification of the parameters t_o and RTT as normally distributed statistical variables with parameters mean m_{OD} and standard deviation σ_{OD} .

4.4.2 Uniform-loss Model

The communication of PMsgs which report current information and are transmitted in defined intervals is modeled differently than for ODMsg. It is assumed that the information transfer fails with a certain probability p_{fail} . As the content of all PMsgs has the same payload size, the distribution does not depend on the message size. If a single message transfer is decided to be successful by the model, a certain delay can be added. This delay is either zero or can also be specified by a Gaussian normal distribution with a mean value m_{PM} in milliseconds and standard deviation σ_{PM} of the delay distribution, analogous to the offset t_o of ODMsgs. An example of such distributions with varying failure probability is shown in figure 4.6.

The added delay is neglected for simplicity reasons ($m_{PM}=0$). The x axis shows the resulting delay, if the interval of transmission tries is set to 10000 ms. What becomes obvious is the fact that the view at delays also results in a geometric distribution. The figure represents a histogram of 10^8 realizations of the random variable. In order to improve

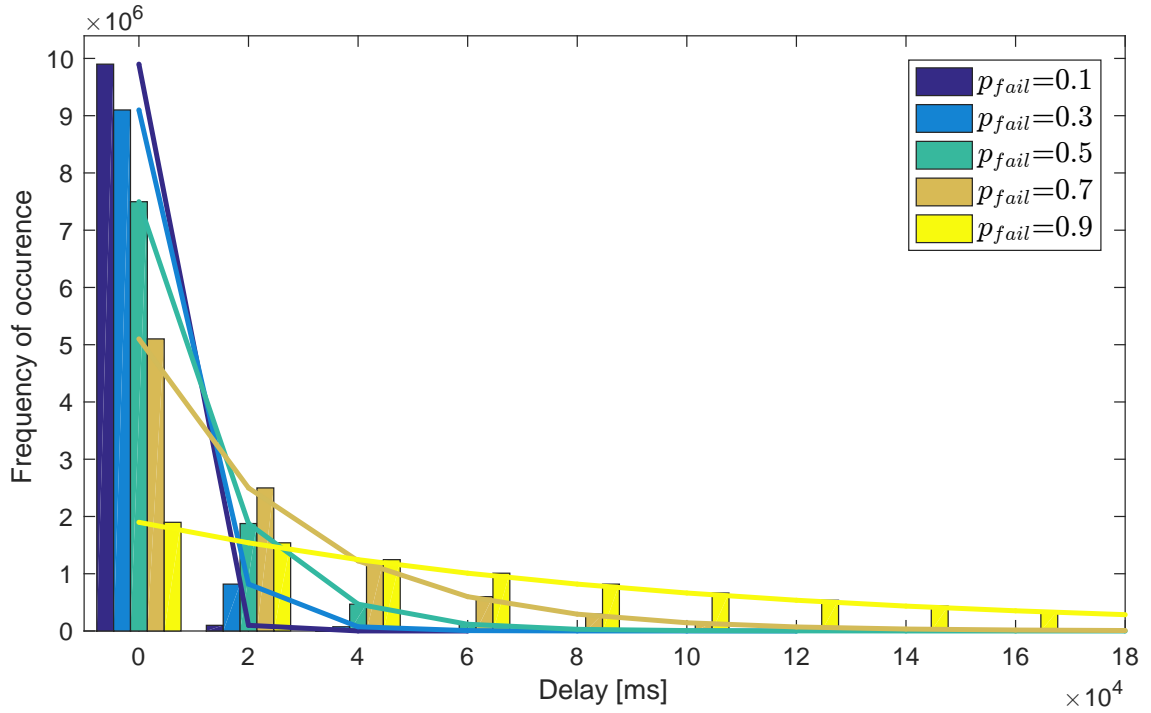


Figure 4.6: Delay distribution with the uniform-loss model and $RTT = 80000$ ms

the readability, the plotted lines connect the bars, interpolated linearly. The figure shows that failure probability scales the distribution accordingly.

This model is applied to messages containing vehicle data including the current position and speed of the vehicle. A consequence of failing message transfers is obviously outdated information on the receiver side. Any error correction is not considered explicitly, but is included in p_{fail} . Hence, the effects of powerful error correction mechanisms of the Modulation and Coding Scheme (MCS) are to be considered by setting lower probabilities of failure. This further means a message is either assumed to be fully error-free, or lost completely. Hence, partly received information is not possible, nor is it possible to get wrong information when using this channel model.

4.5 Validation

The selection of a geometric distribution for ODMsgs is based on the fact that the simple and widely used Gilbert-Elliot (GE) channel model [164–166], that allows to model the burstiness of a channel in alternating bursts of high and low error probabilities. Basically, the GE channel model consists of a two state Markov chain with states "good" and "bad". It is setup by four parameters, which are two probabilities $p1$ and $p2$ which define the transition probability from one state to the other and inverse probabilities $1 - p1$ and $1 - p2$, which specify the probability to stay in the respective state, as figure 4.7 indicates.

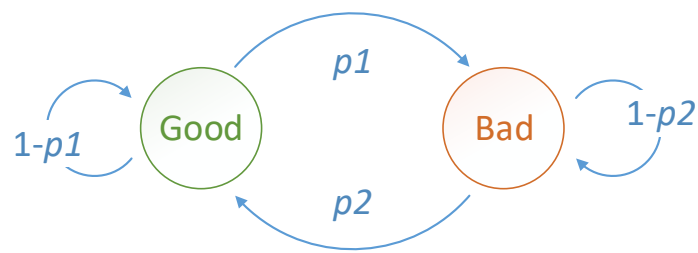


Figure 4.7: Gilbert-Elliot channel model state diagram

The GE model can be simplified to a geometric distribution [167], which is utilized in our model. In order to speed up simulation and simplify the model, we count the number of independent Bernoulli experiments until a "success", i.e. the transition to the "good" state occurs. This corresponds to a random variable X following a geometric distribution [167]. The validation of the often used GE model on which this assumption bases is frequently mentioned in literature [166, 168–170].

5

Evaluation Insights

The presented results include a copious study of the PCMA* performance, both compared to related algorithms from literature but also in different environments. In the first stage, the assumed preconditions comprise full knowledge of vehicle positions, route sources and targets, 100 percent penetration rate of the system and well-functioning communication. In the second stage, the scenario is chosen to be closer to real environmental conditions in terms of penetration rates of the system among vehicles to be less than 100 percent and non-ideal communication capabilities.

5.1 Simulation Environment

For the simulations, two scenarios are used, as depicted in figures 5.1 and 5.2, respectively. The first scenario is an artificial and pattern-oriented scenario, generated with the help of our network generator [48], which uses an environmental-sensitive Lindenmayer System [171]. Scenario 2 is a real-world scenario, extracted from OpenStreetMaps. It represents a snippet of the city of Linz in Austria, where the river Danube, a natural bottleneck to get into the inner city in the morning and out in the afternoon regularly is the reason for traffic jams.

The colored roads represent different road types, where orange equals high-level (freeway/interstate, speed limit of 80-130 km/h), yellow means medium-level (expressway, speed limit of 50-80 km/h) and dark gray marks low-level roads within the area of a city (village road, speed limit of 30-50 km/h). Both scenarios are depicted with equal scale, according to the ruler in figure 5.1. Additionally, start and destination area are highlighted with the green and blue ellipses, respectively. The locations are generated a priori for all vehicles from and to any dangling road segment within the appropriate area. They are immutable during simulation. Another precondition is that the network is empty before simulation start, and the simulation ends as soon as the last vehicle reached its destination.

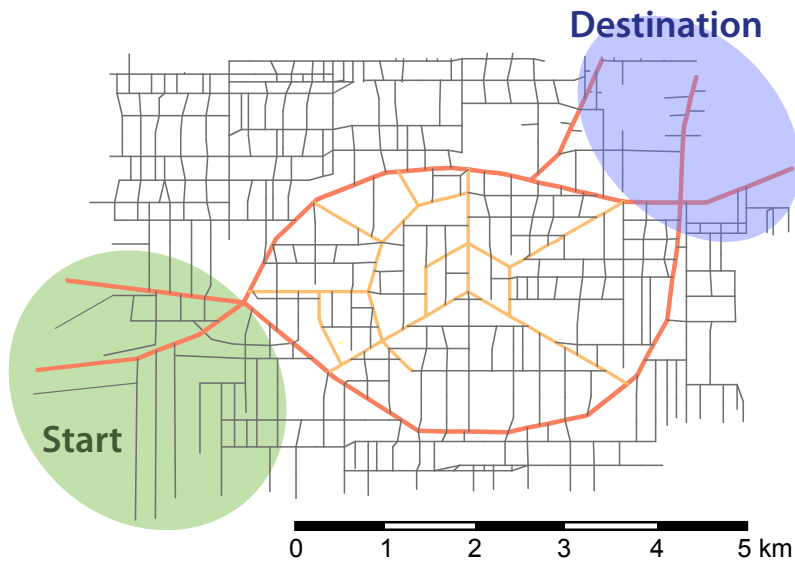


Figure 5.1: Scenario 1: Artificial Road Network

TraffSim uses maps from OSM as network source, which can be parsed directly within the tool by selection on the map but also by using downloaded OSM XML or PBF files [172]. This way, road networks from the real world as well as artificial networks, for example generated according to [48] can be used. Comprehensive network editors for OSM are available, such as JOSM [87], Merkaartor [173] or Quantum Geographic Information System (QGis) [174], just to mention a couple. Those tools provide full support for editing



Figure 5.2: Scenario 2: City of Linz

Table 5.1: Parameter set for all simulations

<i>Shortcut</i>	<i>Description</i>	<i>Value</i>
m_v	vehicle mass	1500 kg
C_d	aerodynamic drag coefficient	0.32
A_{cs}	cross section surface	2.2 m ²
P_v	vehicle engine power	66 kW
V_{cyl}	cylinder volume	1.4 l

geographic details of roads as well as meta information like road type, speed limit, lane count or access restrictions. Additionally, *TraffSim* provides an editor for extension of important meta information such as lane restrictions or road signs, if not provided or not automatically detectable from the OSM material.

The OSM road networks are basically not enabled for routing. Routable graphs require vertices to be between all edges, a direct connection between edges is not allowed [175]. A vertex can either be a traffic intersection in case more than two roads come together, or a simple node which solely connects two subsequent road segments. These preconditions are not fulfilled by basic OSM networks. For that reason, *TraffSim* uses an extended version of the 'osm2po' routing library [176]. This library supports generation of a routing graph out of OSM maps and is capable of calculating routes by application of different routing algorithms. For reasons of comparability, the parameters in table 5.1 are chosen equal for all algorithm configurations.

5.2 Prediction Efficiency

In order to evaluate the correctness of the made predictions, a test scenario was set up with the environment of scenario 2 (City of Linz). The simulation also chooses random start and random end points for routes of all vehicles, within the marked areas in figure 5.2 as is the case in all other simulations. While simulations which are intended to investigate the performance of the rerouting algorithm naturally have the calculation and assignment of alternative routes enabled, this functionality was disabled for the efficiency study within this section, as described in the following.

The routing cost and congestion evaluation mechanism was enabled to evaluate the correctness of predictions, while the rerouting mechanism (i.e. calculation and assignment of new routes) was disabled. This way, congestion is predicted, but instead of reacting appropriately by rerouting the affected vehicles, this simulation solely records the relevant events indicating a congestion prediction at a specific node and future time. With that, the correctness of the prediction can be proven. The extended congestion detection algorithm recognizes an actually arising congestion (since it was not avoided) at the time of occurrence, as described in section 3.2.5. In those cases where congestion really occurs, another event is recorded.

The number of overall congestion predictions is then compared to the number of correct predictions, i.e. the congestion that really occurred. For each intersection, the time of prediction is then confronted with the time of detection, and investigated whether any detection was recorded. For analysis, I chose a tolerance of seconds between predicted and detected time that mark the interval within a future prediction is treated as correct. For instance, a tolerance of 30 seconds means that if the algorithm predicts a congestion at a certain node at time 14:30:10 (HH:MM:SS), an effectively happening congestion is allowed to be within the interval [14:29:40, 14:30:40] to be marked as correct for the prediction. Figure 5.3 shows that the algorithm's performance regarding predictions is functioning very well.

The curves show the same simulation setup with a vehicle Inter-Arrival Interval (IAI) of 1300 ms, but with different congestion detection thresholds $\theta^{(P)}$ between 1 and 1.8. These are measured in vehicles per second, and define the virtual capacity of the node. As soon as more vehicles than this defined threshold pass a node per second, the situation is treated as congestion. This finding is further used as comparative value to check whether or not a predicted congestion did really occur. In other words, the procedure is as follows. A congestion is predicted for time interval $(\Delta t)_j$ and node i . While the simulation propagates to the predicted time interval with index j , the system looks at the node i if the congestion really happened at the predicted time. The situation is recognized as congestion if the above mentioned threshold $\theta^{(P)}$ is exceeded and hence too many vehicles try to pass the node in the specific time interval Δt .

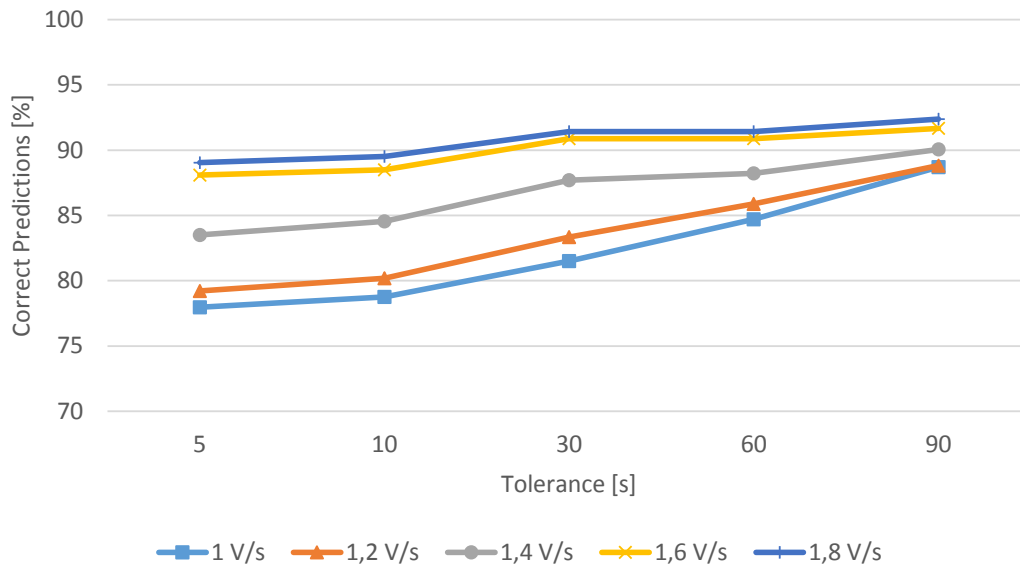


Figure 5.3: Percentage of correct predictions for different threshold values $\theta^{(P)}$

5.3 Assessment of Routing Algorithms

A major goal of this thesis is to evaluate the achievable gain of PCMA* and to compare it to other routing algorithms from literature. The requirements include real-time applicability of the algorithm. This means that it must be theoretically possible to apply the system in real conditions on the road, and therefore iterative processes with multiple required simulation cycles such as Dynamic Traffic Assignment (DTA) are not within the reviewed candidates, although they are capable of achieving user equilibrium [91, 92].

5.3.1 Procedure of Analysis

Two configurations of PCMA* are evaluated and compared to different methods from literature, among which are Flow Balanced k-Shortest Paths (FBkSP) [108], Single Path with Greenshield's weighting method [115] as well as with a situation without influence of any intelligent system and disabled routing. The investigated configurations consist of multiple components.

Terminology

The following listing clarifies the investigated composition of components and defines shortcuts that are used in the findings.

- **Routing configuration**

- Disabled: No rerouting takes place at all. All drivers use the shortest path, as if they were not influenced by any congestion or other vehicles.

- Single: Routes are updated continuously in regular fixed time intervals, which are 30 seconds long for the presented results. As soon as a congestion is recognized, vehicles which are affected by this congestion can get a new route assigned. Affected vehicles are those, which are in the range of a defined number of segments (denoted as R_{seg}) away from the detected congestion. The route is calculated by a standard A* algorithm.
- FBkSP: Similar to single mode, but instead of the standard A* algorithm, the flow-balanced KSP algorithm (FBkSP) [108] is used. The pretended best out of a number of k paths is selected by a heuristic function. This heuristic includes a weighted footprint counter, which basically considers the amount of vehicles which are assigned to paths passing a certain road segment. Out of the determined k paths, the one with the least footprint counter (i.e. the least amount of other vehicles that use a part of this route) is selected [108].
- PCMA*: According to the detailed description in chapter 3, the prediction component is activated. Future footprints are calculated, which extend the congestion evaluation component by the predicted future congestion. This implies usage of time-dynamic prediction.

- **Cost evaluation method**

- SA: Road weight of each segment of the A* routing graph is calculated by speed average method, according to equation (3.3) in section 3.2.1.
- GS: Road weight is calculated by Greenshield's model, according to equation (3.5) in section 3.2.1.

- **Congestion evaluation method**

- SA and GS: Threshold definition, according to description in section 3.2.2.

Parametrization

Apart from the algorithmic functionality of investigated approaches, a set of substantial parameters is relevant for each approach to achieve optimal results and adapt it to the needs of the simulated use case. Table 5.2 describes the most relevant parameters and points out which purpose they fulfill.

5.3.2 Parameter Survey

The behavior and power of the different presented approaches is influenced by each of the parameters to a certain degree. However, in order to find the best suited configuration for PCMA*, a comprehensive parameter survey consisting of more than a million simulations

Table 5.2: Parameter Specification

Abbr.	Definition	Description
n_{window}	Moving average window size for SA and GS	The weight for a specific road segment is low pass filtered by a moving average of this specific length
$\theta_{GS}^{(R)}$	Congestion threshold for the reactive GS method	An RS is considered as congested if the value is greater than that threshold, which is defined as the ratio between applied and available road space [115] (section 3.2.2)
$\theta_{SA}^{(R)}$	Congestion threshold for the reactive SA method	An RS is considered as congested if the value is lower than that threshold, which is defined as the current speed divided by the maximum allowed speed (section 3.2.2)
Δt	Time discretization interval	Time resolution of the footprint matrix and interval for which future congestion predictions are made (section 3.2.3)
$\theta^{(P)}$	Congestion threshold for predictive component	PCMA* detects an intersection as congested if more than the amount of vehicles defined by this parameter pass this intersection per second, in other words this represents the node capacity (section 3.2.4)
R_{seg}	Consideration range of segments	Number of segments to go over and look for vehicles if jam is detected; it defines the area around a congestion in which vehicles are taken into consideration for rerouting (section 3.2.5)
η_t	Route (RT) threshold: time	Travel time ratio between old and new route is limited by this lower bound to avoid unfeasible route assignments (section 3.2.5)
η_s	Route (RT) threshold: distance	Travel distance ratio between new and old route is limited by this upper bound (section 3.2.5)

Table 5.3: Parameter Survey

Param.	Variation Range	Influence
$\theta_{SA}^{(R)}$	[0.05, 0.4]	As one of the parameters with the most severe effects, this value changes results by about $\pm 6\%$ when varied within the given range. The artificial scenario tends to accept a wider range without any losses, what is not the case for the real world environment. This means a marginally higher tolerance for the reactive detection part.
$\theta_{GS}^{(R)}$	[0.4, 0.9]	Analogous to the SA threshold, this parameter is relevant when applying the Greenshield's weighting method. Its influence on the result is $\pm 3\%$ in both scenarios.
$\theta^{(P)}$	[0.8, 1.6]	The variation of the predictive congestion threshold results in travel time deviations of $\pm 3\%$. Both scenarios react similarly to changes.
η_t	[0.8, 1.6]	Changing the route time threshold leads to a $\pm 4\%$ variation of the results. Lower values are beneficial for both scenarios, which means that it is better not to limit new routes too strictly by estimated travel time.
η_s	[1, 5]	Low values mean low tolerance towards longer distances of new routes, which turns out to become worse the lower the threshold is chosen. A very restrictive value of 1 means 500 % higher travel times, while the results flatten when increasing the threshold. In other words, the best results can be achieved when this distance limit has no effect.

in total was carried out. All relevant parameters as presented in section 5.3.1 were varied in order to find the most suitable set. As some of them are dependent of each other or have a bearing on the results in contradictory directions, table 5.3 summarizes the values with the highest influence on results and gives a description of their characteristics. Within the framework of the simulation survey, of course all variations of the entirety of parameters were combined with each other in order to find the best compound, what led to the mentioned high overall number of simulations. For the sake of staying in a reasonable extent here, the stated influence on the results in table 5.3 of a single value is always related to the best known parameter set for 3000 vehicles and an intermediate IAI of 1500 ms. The percental deviation is shown for the resulting average travel time and a variation within the given range. Parameters outside this range either make no sense for the respective parameter, or the projection of the results out of the given range indicate no further positive effect, even not for any other parametrization.

Table 5.4 shows an overview of the simulation setups of all investigated configurations. It contains the parametrization as used in literature for Single and FBkSP approaches and

Table 5.4: Parametrization of simulations

	Single	FBkSP	PCMA* SA	PCMA* GS
Cost/Congestion Evaluation	GS	GS	SA	GS
Prediction Extension	No		Yes	
Segments Range R_{seg}	5			
Congestion Threshold $\theta^{(R)}$	0.7		0.3	0.6
Congestion Threshold $\theta^{(P)}$	–	–	0.9 V/s	1.1 V/s
Window Size n_{window}	–	–	10	
Discretization Interval Δt	5000 ms			
Time Threshold η_t	–	–	0.8	
Distance Threshold η_s	–	–	5	

the best performing set for PCMA* as a result of the survey. The deviations of the single parameters are evaluated by keeping all others at the particular best value. I skipped the configuration with disabled routing in table 5.3, as none of the parameters are applicable.

5.3.3 Preconditions

This comparison study of routing algorithms further assumes the following preconditions. All vehicles in both scenarios start from one of the dangling road ends within the start area, and have their destination within the blue ellipse, as depicted in figures 5.1 and 5.2. However, the start and destination nodes are immutable, defined prior to simulation start and are fixed for all simulation parametrizations. The optimization machinery is allowed to change the route by fulfilling this requirement. It is assumed that the network is empty before simulation start, and the simulation is continued until the last vehicle reaches its destination node. The penetration rate of the necessary communication and rerouting system in vehicles is 100 percent at this point. Another precondition for our results is that all vehicles follow the proposed guidance and do not overrule or ignore the decisions. The V2X communication is presupposed to function flawless with perfect conditions and quality. The message exchange works without any delays and no messages are lost.

In addition, it is mentioned here that *TraffSim* is capable of executing calculations in parallel computation threads wherever possible in order to increase the simulation performance. This is the reason for not achieving exactly the same output values for the same parametrization, compared to a configuration with single-threaded execution. Slight timing differences between executions of the same parameter sets can for example lead to a

situation where two vehicles enter an intersection in different order, what naturally affects the rest of the simulation. However, the discrepancy is compensated by a 3 to 5 times shorter simulation time in multithreading mode. Furthermore, each of the presented numbers comprises an average over (at least) three executed simulations in order to mitigate slight deviations (below $\pm 2\%$ at maximum) which arise from multithreading effects.

5.3.4 Time and Fuel Consumption

For the initial investigation, vehicles are generated in a fixed interval of 1700 ms for both scenarios. The IAI is chosen so that the algorithms have a chance to solve the jam situation. Therefore, vehicles arrive in an interval so that problems can occur, and the road network snippet is not hopelessly overcrowded where any rerouting would be pointless. Overall, 3000 vehicles are generated in both scenarios 1 and 2. Five routing configurations are evaluated, according to the description in section 5.3.1: Disabled, Single, FBkSP and PCMA* with GS and SA cost and congestion evaluation methods.

Scenario 1 (Artificial)

Figure 5.4 shows the simulation results for scenario 1, depicting two key indicators for traffic performance evaluation, i.e. average fuel consumption and average travel time per vehicle. The five bar groups indicate the different algorithms used in the simulations, where each group shows one algorithm. The right bar group shows the result with no rerouting activated at all, which brings to light that the proposed approaches heavily improve both travel time and fuel consumption. Results show close to three times more average fuel consumption in case of no rerouting (factor 2.85) compared to the best case with PCMA* SA. Furthermore, the average travel time per vehicle from source to destination is 5.21 times higher with disabled rerouting mechanism compared to when PCMA* SA is applied. This can be traced back due to the huge traffic jams, further leading to tremendous fuel consumption. Our assumption is confirmed by literature [177], which argues that long periods of standstill and stop-and-go traffic can rise up fuel consumption by more than 60 percent.

Also the single rerouting approach with no proactive component improves both travel time and fuel consumption compared to the egoistic, non-intelligent Disabled simulation setup. The average fuel consumption of 0.78 liters per vehicle and average travel duration of 29.61 minutes is still significantly below the values with disabled rerouting. However, due to the omission of cooperative behavior, in some cases this algorithm just moves congestion to another intersection in the near surrounding. Thus, some vehicles take a detour which does not decrease overall travel time and gain no advantage, and fuel and time consumption still are at least as high as if they took the original route. Additionally, the selection criteria for vehicles to be rerouted is based on relative distance from the

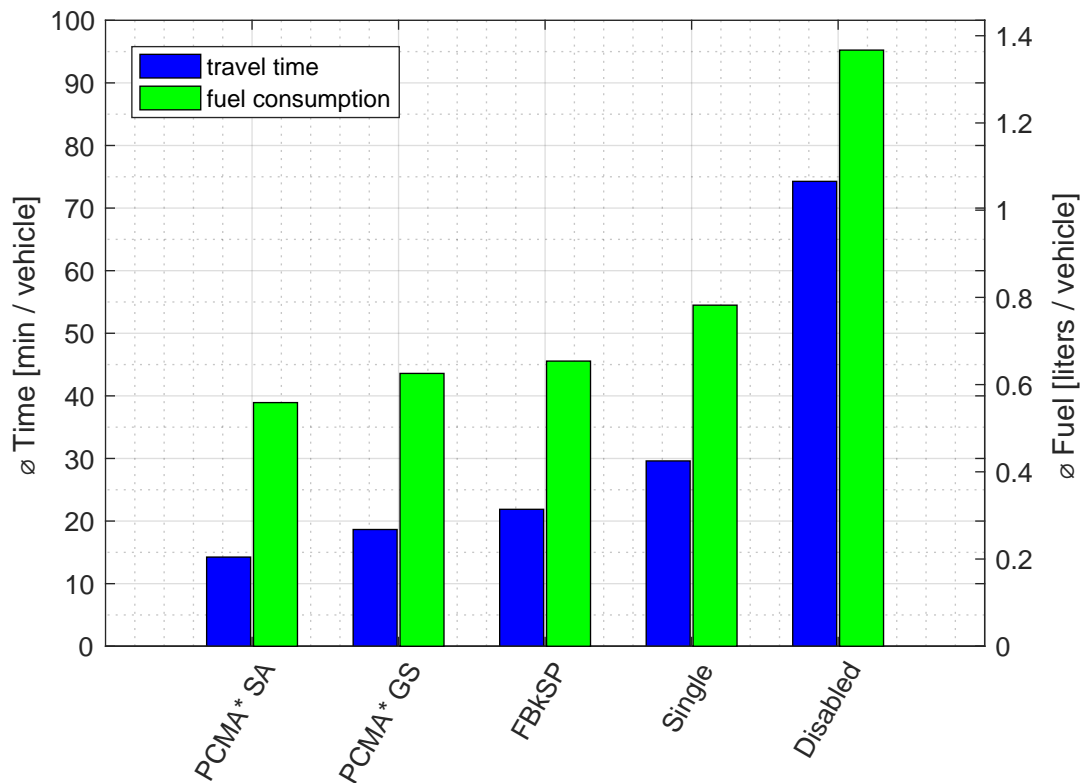


Figure 5.4: Average travel time and fuel consumption results for 3000 vehicles and IAI = 1700ms in scenario 1

congested spot (measured in number of segments R_{seg} , as explained in section 3.2.5). It is independent of the vehicle's destination, therefore also vehicles which would not pass the congested spot, but are in the near surrounding of same, are scheduled for rerouting.

The FBkSP algorithm, which utilizes both a reactive approach and kind of proactive methodology, intelligent route selection further leads to slightly better results due to the consideration of other vehicles' routes. It still detects congestion not before it occurs, but then selects the best out of k calculated routes by simple heuristics which consider the load of intersections. Although vehicle selection is also based on distance to congestion similar to the single approach, it achieves slightly better performance in this simulation scenario. I ascribe this improvement to the better route calculation algorithm and consideration of multiple alternative routes.

The best performance in scenario 1 is achieved by the PCMA* algorithm, configured with SA graph weighting and SA congestion detection extension. The proactive congestion detection allows to predict congestion and bottlenecks properly. Additionally, and this is a big benefit compared to the benchmark algorithms in figure 5.4, affected vehicles can be selected for rerouting very accurately. The time-component plays an important role in this concern, because if a jam is forecasted to occur in 10 minutes, there is no reason to

redirect vehicles which pass the respective node in 3 minutes or in 30 minutes. So, the big advantage is the target-oriented behavior. Especially in large simulation scenarios, where spacious routes are possible (as is the case for simulation scenario 1), the algorithm is very powerful. Certainly, the real world is not limited in area and thus can be seen as large scale scenario. Vehicles do not get into a traffic jam, because they get informed timely and so have the possibility to choose a spacious alternative route. Simulation results of scenario 1 reveal a factor of 1.54 between average travel duration of PCMA* SA (14.24 minutes) and FBkSP (21.88 minutes). Also fuel consumption decreases significantly, from 0.65 liters per vehicle (FBkSP) to 0.56 liters per vehicle (PCMA* SA) - that is 14.6 percent less.

As the results also show, a remarkable difference between GS and SA extension of PCMA* is recognizable. This indicates that prognosticated congestion quality depends also on the method of graph weighting and determination of current road conditions, which is better when using SA.

Scenario 2 (Linz)

The ranking of algorithms did not change in this real-world scenario (PCMA* - FBkSP - Single - Disabled), but the gap between the bar groups decreased, as figure 5.5 shows.

I intentionally chose this scenario to investigate whether the presented PCMA* algorithm still performs well in situations where spacious, wide-ranging alternative routes are rare. Less alternative route possibilities exist also due to the defined restriction of start and destination nodes. Nevertheless, the PCMA* algorithm outperforms all of the benchmark scenarios in both compared values, fuel consumption and travel time. It leads to 31.5 percent less travel time than FBkSP, about 35 percent less than single algorithm and more than 79 percent less compared with a situation with disabled rerouting algorithm.

Due to shortage of valuable alternative routes, the results of all algorithms get closer to each other. One can also observe the deterioration of the FBkSP algorithm, which is also caused by the weakness in non-grid-like real-world scenarios. The alternative paths are then often not satisfiable and not very beneficial, as described former in section 3.1.1.

5.3.5 Travel Distance

Obviously, the overall and also average traveled distance per vehicle rise as a consequence of rerouting and assignment of a route divergent to the original, shortest one. As figure 5.6 illustrates, the configuration with disabled routing algorithm unsurprisingly provides the shortest average travel distance compared to all rerouting algorithms. Travel distance tends to behave reverse proportional to the achieved gains in time and fuel. However, the absolute values still show the negligible rise in traveled distance. The minimal average traveled distance in the Disabled-scenario is 8336 m or 4948 m for scenarios 1 and 2,

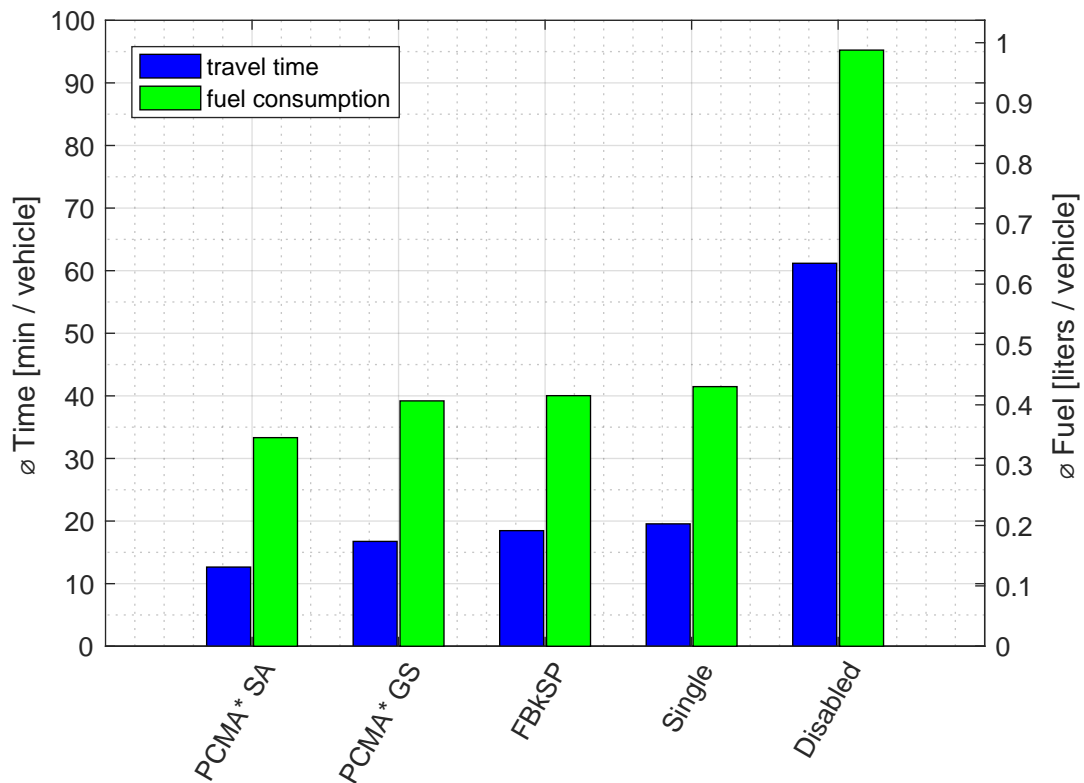


Figure 5.5: Average travel time and fuel consumption results for 3000 vehicles and IAI = 1700ms in scenario 2

respectively, whereas the maximum distance amounts to 9356 m or 5743 m. The difference of 12.2 or 16.1 percent between PCMA* SA and Disabled configurations is compensated by the gains in time and fuel consumption.

5.3.6 Vehicle Density Variation

In addition to the previous standard setup with a fixed arrival interval of 1700 ms and a constant total vehicle amount, supplementary investigations demonstrate the algorithms' performance with distinct vehicle densities and amounts. The vehicle density can be adapted by variations of the IAI as well as the vehicle amount.

Vehicle Amount

Figure 5.7 shows how the average travel time of vehicles is subject to the total amount of vehicles traveling through the network for both scenarios 1 and 2, which is setup between 1500 and 4000 vehicles overall.

Especially in the artificial scenario, with good possibilities for large-scale alternative routes, the potential of PCMA* turns into account. However, the curves of all algorithms in figure 5.7a follow a slight gradient when the vehicle amount increases, that indicates a

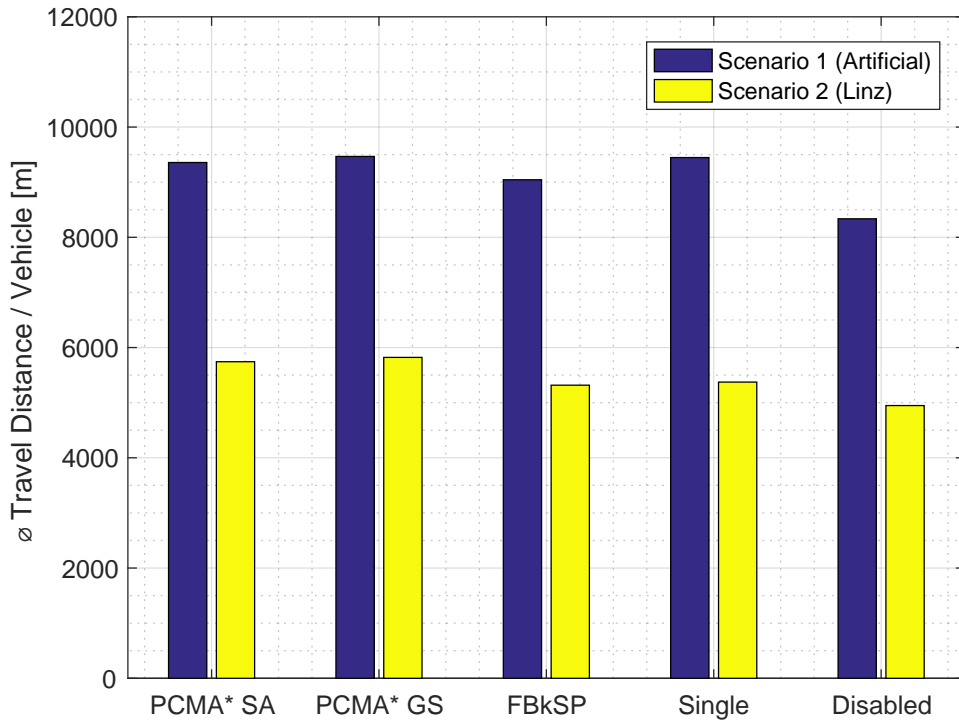


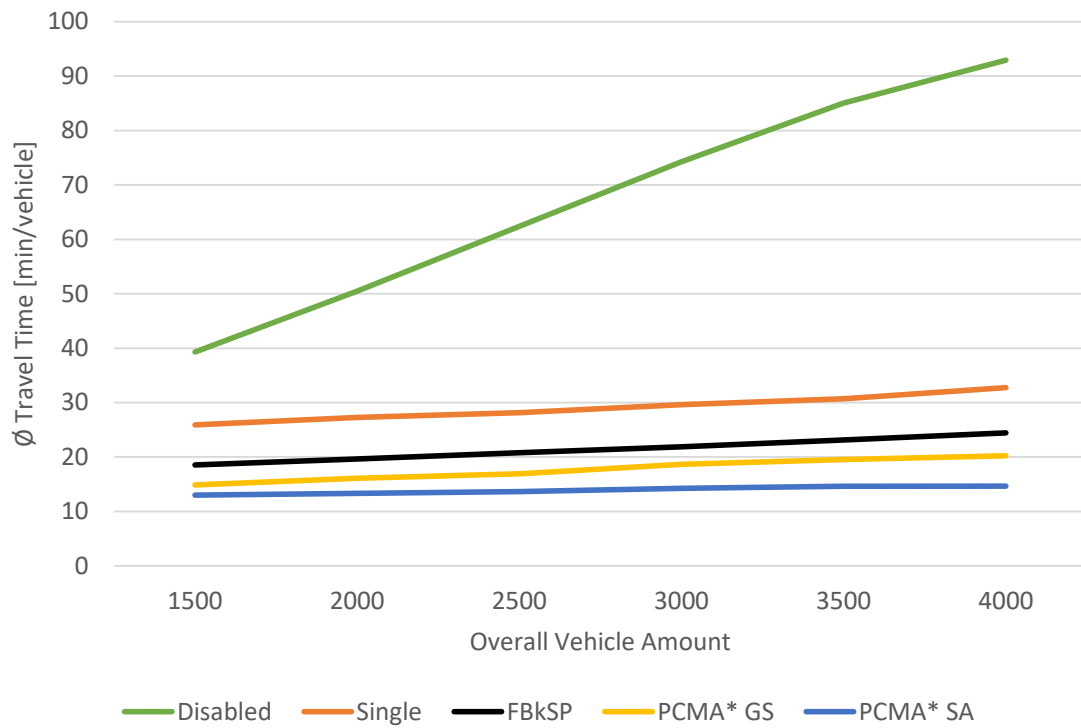
Figure 5.6: Average travel distance for both scenarios, 3000 vehicles and IAI = 1700ms

slight increase in average travel time. This is caused by unavoidable congestion and more traffic jams, which happen for any analyzed algorithm due to more vehicles. As expected, a decrease in vehicle amount leads to less difference in average travel time between the algorithms, since also less congestion arises. The largest slope can be observed by reference to the green curve, which represents the situation with disabled rerouting. It is caused by the unfavorable effects of the emerging traffic jams. Finally, figure 5.7a indicates the linear behavior of the presented PCMA* algorithms in respect of a varying overall vehicle amount, which performs satisfactory in all investigated configurations.

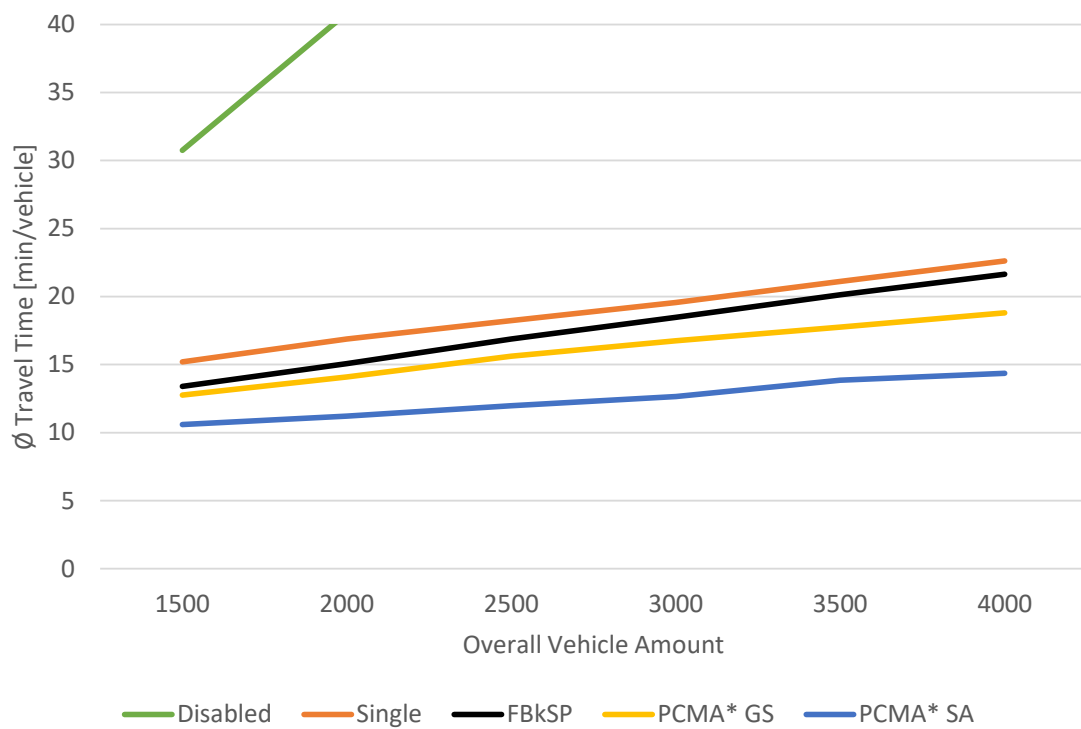
In contrast to scenario 1, the distinction between the algorithms is not as clear in scenario 2, as figure 5.7b shows. In order to point out differences between the rerouting algorithms Single, FBkSP and both PCMA* variants, the y-axis is zoomed in, which is the reason for the Disabled configuration to disappear. However, the latter curve reveals close to linear behaviour from about 30.8 s to 79.2 s average per vehicle. The reason for the slight differences between the rerouting algorithms is the same as explained in section 5.3.4, namely inadequate possibilities for alternative routes with sufficient capacity.

Inter-Arrival Interval

A supplementary option to vary the vehicle density is to change the inter-arrival interval (IAI) of vehicles at their defined start locations. Certainly, all start and end locations stay equal for all simulations, while only the arrival interval is changed. IAIs, i.e. the birth



(a) Scenario 1 (Artificial)



(b) Scenario 2 (City of Linz)

Figure 5.7: Variation of total vehicle amount and IAI = 1700ms

rate between 500 and 3300 ms are applied for both scenarios to point out the influence of density and also show extreme cases with very low and high IAIs. The influence of this variation is shown in figure 5.8. Both scenarios 1 and 2 reveal similar reaction to a variation of the inter arrival time. A lower value of the inter arrival time leads to more concurrently occupied space and therefore higher probability for congestion, hence higher travel time, and vice versa. This claim is proven by the provided simulation results, which indicate a dropping average travel time per vehicle accompanied by higher arrival time intervals.

The IAI investigation gains results coincident with variation of overall vehicle amount: With increasing IAI, which obviously leads to less vehicle density, the average travel time decreases. This behavior is pointed out in both scenarios. However, PCMA* still achieves the best results, but with much less distinction between the algorithms when setting the IAIs to extreme values, as visible on the left and right edges. Again, the curve with disabled rerouting was faded out to make the slight differences of the rerouting algorithms apparent. The curves have values of 98.7 and 89.6 minutes of average travel time per vehicle for scenarios 1 and 2, respectively.

What also becomes apparent here is the fact that the best improvements compared to other approaches are achieved for intermediate densities around an IAI of 1700 ms. When the traffic is very dense (lower values in x-direction in figure 5.8), the improvement compared to other approaches shrinks, especially in scenario 1. In contrast, the curves approach the curve with Disabled routing for low densities (right side of figures 5.8a and 5.8b), since the need for optimizations disappears.

Number of Vehicles over Time

In order to demonstrate how the IAI is related to the amount of active vehicles in the simulation over time, this coherence is shown in figures 5.9 and 5.10. Active vehicles are those which are currently along the way to their destination, in other words those which began their ride but did not yet reach the destination. Generally, a higher density is the result of short arrival intervals and/or a higher total amount of simulated vehicles, and vice versa. Although this relative dependency is basically true for all simulation setups, the absolute amount of active vehicles varies depending on the optimization power of the selected methodology. Naturally, a better optimization strategy results in less severe congestion and thus also means that vehicles reach their destination earlier. As a consequence, the average amount of vehicles over time is lower.

Figures 5.9 and 5.10 present the relation between the number of simultaneously active vehicles over time, comparing all investigated routing approaches with distinct densities in terms of IAI and overall vehicle amount, separated by scenario at first (figure 5.9 shows scenario 1, figure 5.10 contains results for scenario 2). The vehicle amount is set to 2500

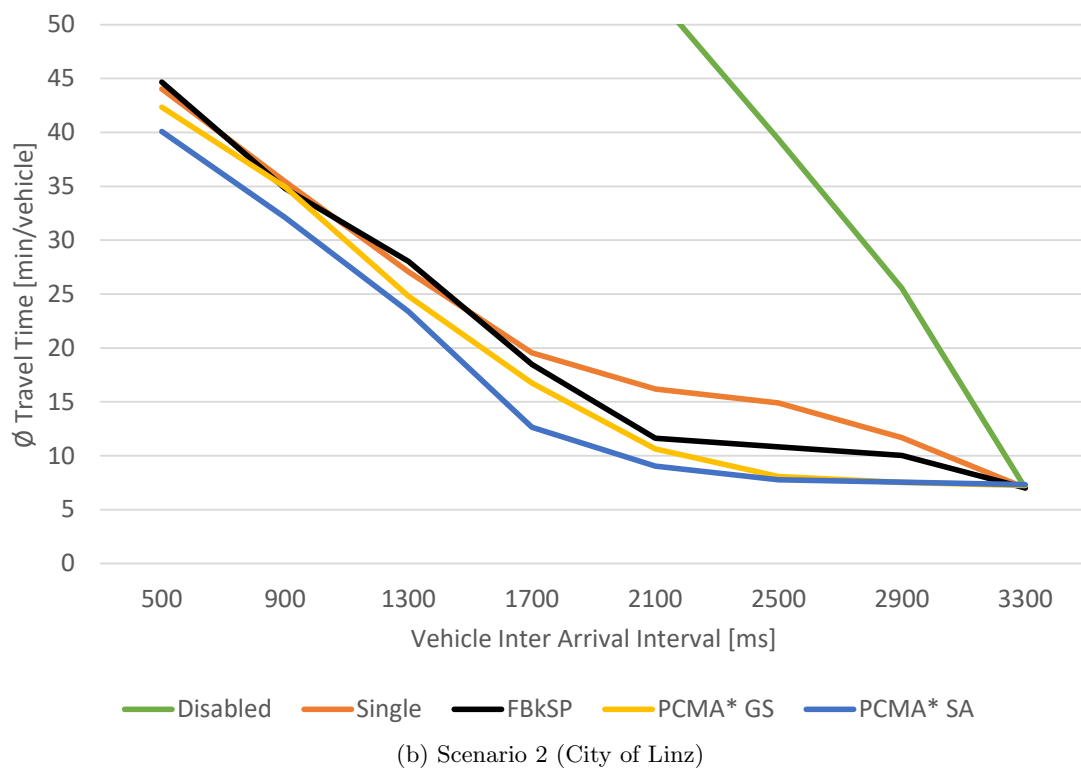
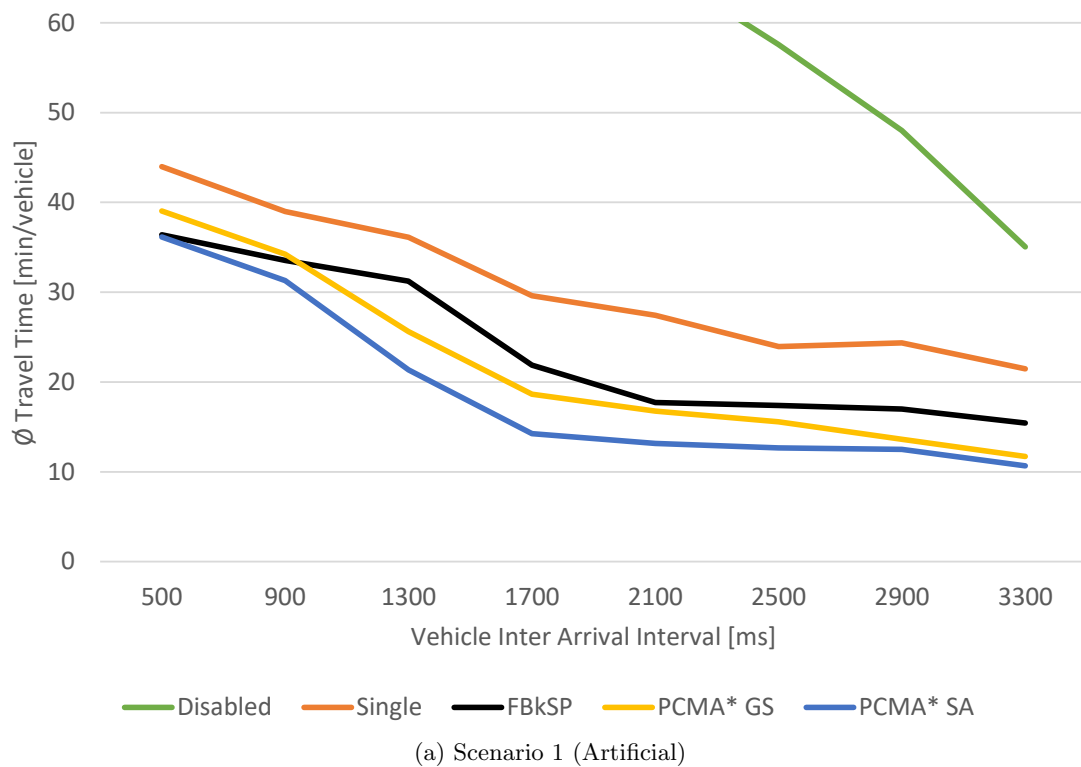


Figure 5.8: Variation of vehicle inter arrival time and 3000 vehicles in total

Table 5.5: Duration of vehicle generation process in minutes for both scenarios

		<i>Total Vehicle Amount</i>	
		2500	3500
<i>IAI</i>	700	29,2	40,8
	1700	70,8	99,2
	2700	112,5	157,5

and 3500 in total, which is represented by the columns in figures 5.9 and 5.10. The IAI is varied in row direction between 700 and 2700 ms. It has to be taken into account that the y-scales are not equal in the figures, for the reason of pointing out the relevant part of the diagrams. However, the time on the x-axis is fixed for each vehicle amount value.

Both scenarios show steep slopes for low densities in figures 5.9a and 5.9b and figures 5.10a and 5.10b. This means that the vehicles birth rate is considerably higher than the rate of vehicles which at the same time reach their destination. The highest peaks are reached by the green and orange curves which again represent disabled and single routing behavior, what means nothing else but enormous traffic jams. As long as vehicles are generated faster than they reach their destination, the gradient of the curves obviously is positive, what comes to light especially in the green curves with disabled routing behavior.

Table 5.5 shows the time spans how long new vehicles are generated, which can be calculated simply by multiplying the number of vehicles by the IAI. The end of vehicle generation expresses itself by maxima at the corresponding x-values of figures 5.9 and 5.10, which are incisive especially for the green curves. The local minimum and the following local maximum of the green curve in figure 5.9b around 50 minutes simulation time additionally indicates a jam at such a severe level that there is no space for new vehicles to enter. Instead, the generation process can be continued not until the vehicles set in motion again.

With lower densities, i.e. when looking at rows 2 and 3 of figures 5.9 and 5.10, the peaks for any approach that applies routing are significantly lower. This indicates a balanced state on the one hand, but emphasizes also the impact of the different routers. The overall vehicle amount is lower than any other approach in the area of interest for the whole period under consideration when applying PCMA*.

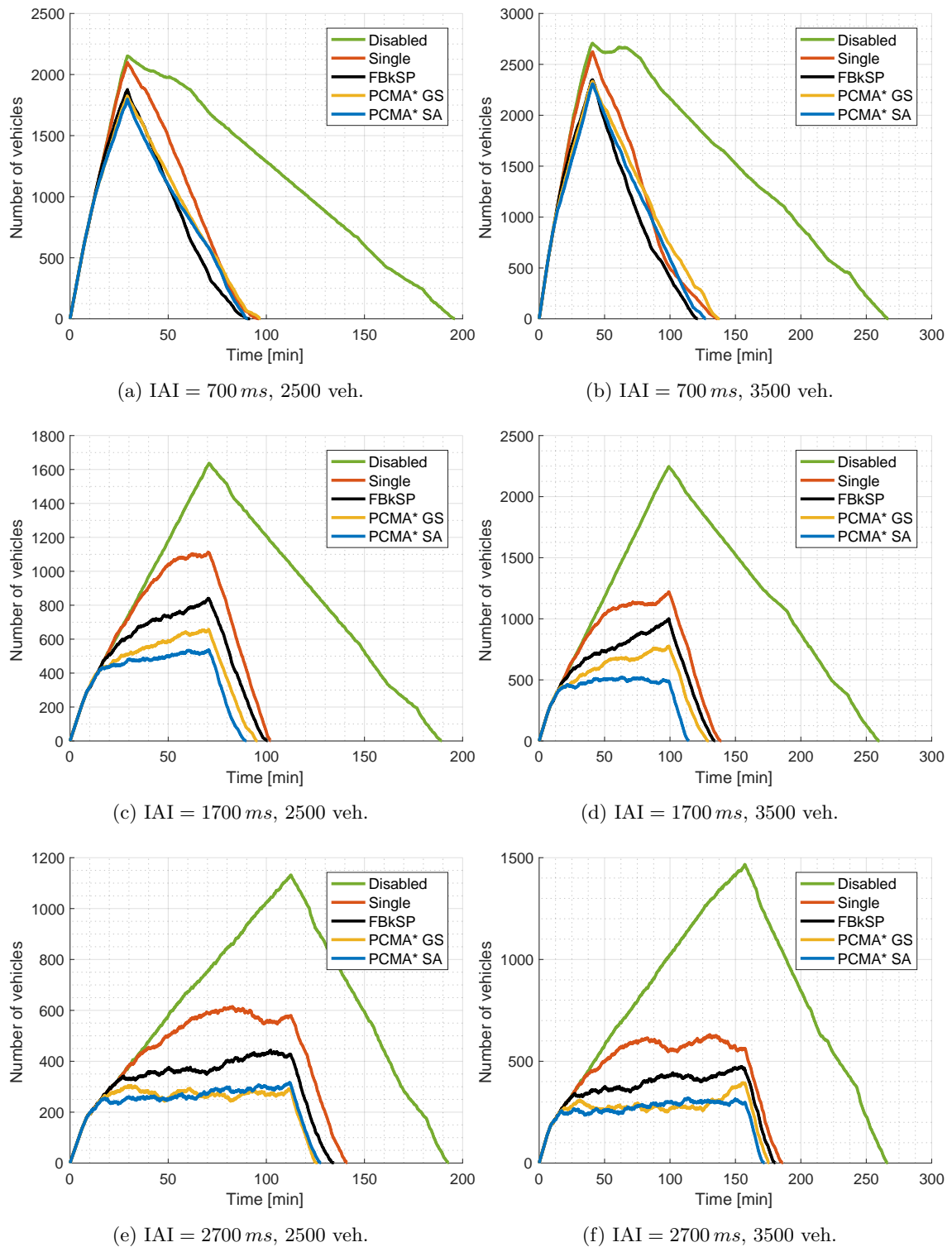


Figure 5.9: Number of active vehicles over time for scenario 1 (artificial) with distinct IAI and overall vehicle amount

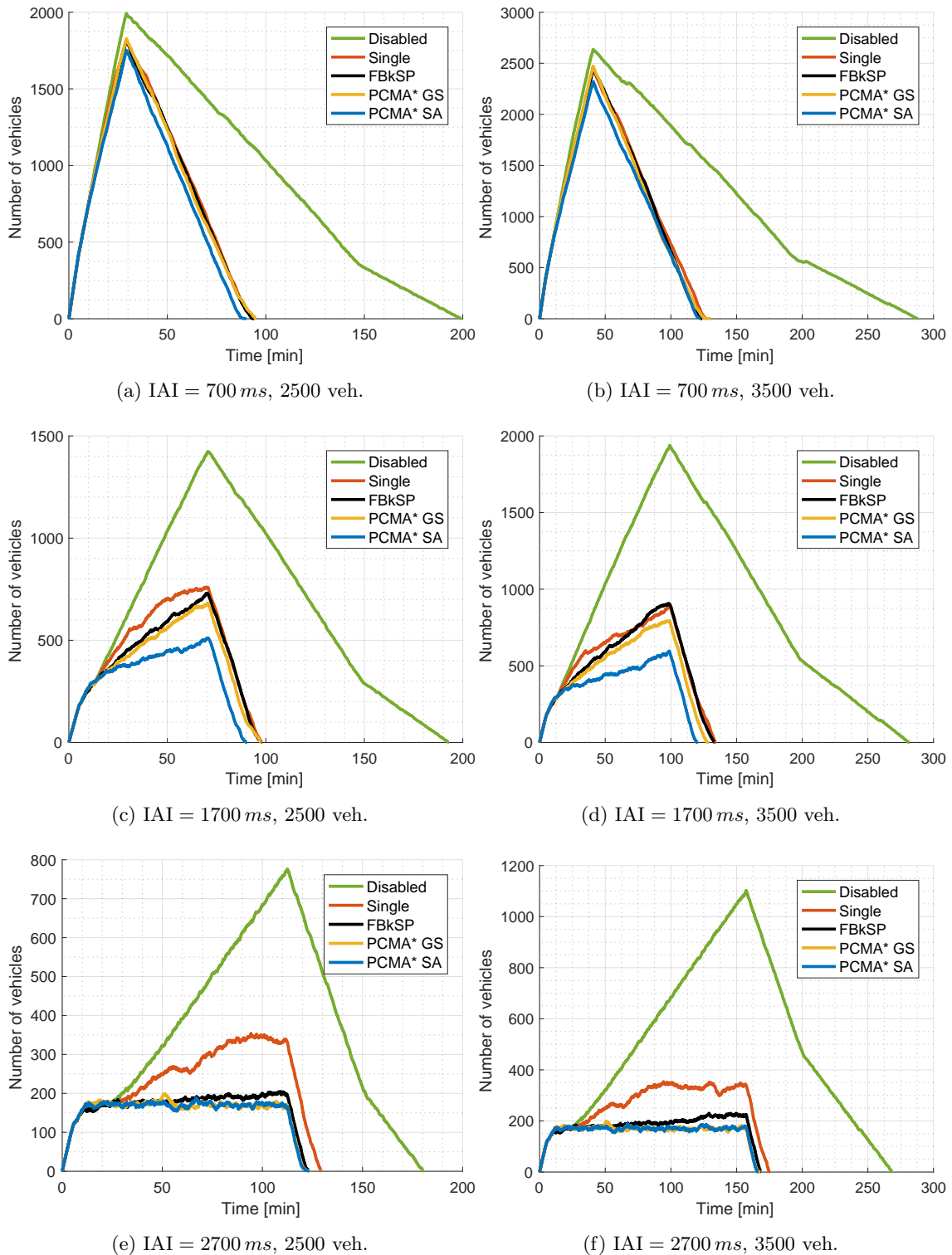


Figure 5.10: Number of active vehicles over time for scenario 2 (Linz) with distinct IAI and overall vehicle amount

5.3.7 Computational Cost and Complexity Analysis

An essential question is the one after the required computational cost (i.e. CPU time) of the proposed algorithm, and hence the real-time applicability. Obviously, the invested effort depends on multiple factors. The route calculation and footprint updates are basically the most significant part regarding computational cost and thus of great interest here. Therefore, the results presented below comprise all calculation effort related to routing. That are route calculations on the one hand, but also maintenance and update of the footprints on the other hand.

In order to answer the question on computational complexity, the complexity of the underlying routing methodology must be considered. That is the Dijkstra algorithm, which is used by FBkSP and the A* search algorithm by PCMA*, which is an extension of Dijkstra. The complexity of latter is $O(E + V \log V)$ [178], whereas A* has equal complexity but was demonstrated to be faster than Dijkstra [179]. The kSP algorithm calculates k paths and thus has a higher complexity of $O(kV(E + V \log V))$. This is valid for a directed weighted graph with E edges and V vertices and calculation of one path for a single source and destination. However, when looking at the system from a major level, the overall complexity depends on the number of necessary reroutings, which further depends on the amount of detected and predicted congestions and the severity (i.e. how many vehicles are involved). Additionally, the amount of calculated routes varies depending on the frequency of congestion emergence, since vehicles that are affected by multiple traffic jams still trigger only one route calculation when applying PCMA*. This can be traced back to the deployed time hysteresis for new route assignments, as explained in section 3.2.5. Notwithstanding, the overall time effort in the worst case rises linearly with the overall amount of vehicles within a simulation due to this hysteresis.

In order to show practical applicability, a CPU time analysis was carried out by an exemplary recording of all CPU effort related to rerouting. This includes the route calculations themselves, but also subsidiary tasks such as routing graph weighting or maintenance of the footprint data. Figure 5.11 shows a CPU time analysis for both investigated scenarios. The simulations for these results were carried out using a 64-bit machine with an Intel Xeon E3-1270 CPU running Windows Server 2012 at 3.6 GHz and 32 GB of memory installed. However, evaluations on other machines show similar ratios, although the absolute values are different. The presented recordings were created using *TraffSim*, which allows thread-based CPU time monitoring and filtering by functionality.

The column groups represent an algorithm configuration, the colors separate the scenarios. The CPU time on the y-axis is the sum of all thread CPU times needed for route calculation and related tasks of the respective algorithm. What becomes immediately apparent is the high CPU effort of the FBkSP algorithm. This is caused by the characteristic of this algorithm to calculate a number of k routes in order to finally decide for one and

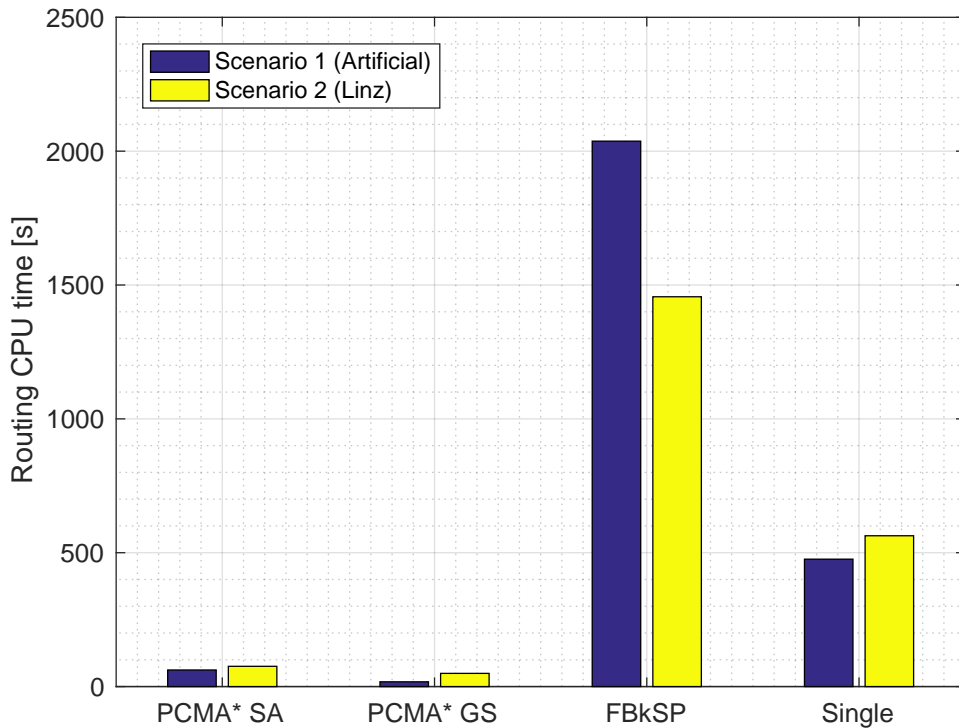


Figure 5.11: Rerouting CPU time for both scenarios for IAI=1500 ms

dismiss all others. Hence, also the calculation effort is that comparably high. Moreover, also the computational effort of the reactive method calculating a single alternative path is substantially higher. This is due to the inability of the approach to discover routes which pass by a traffic jam rather than creating a new one a few nodes away, which then again triggers new congestion and new route calculations as a consequence. The CPU time of both PCMA* algorithms is below or even far below 80 seconds for scenarios 1 and 2, respectively, as figure 5.11 points out. Considering that the overall real simulation time (i.e. from the simulated start time of the first vehicle to the leaving of the last one) is between two and three hours for both investigated scenarios, a real-time application of the PCMA* algorithm would be possible without any performance problems.

However, when looking at the relative CPU time variations for an algorithm between both scenarios, some anomalies become obvious. Basically, the consumed CPU time depends mostly on the number of calculated routes as well as the characteristics of the scenario. This value further depends firstly on the number of detected congestions, secondly on the number of involved vehicles in these congestions, but also on the quality of the computed routes. Presumably a large amount of routes exceeds the defined route thresholds η_t or η_s and need to be discarded, the route calculation effort increases due to those irrelevant calculations. Obviously, this depends on the scenario as well. I ascribe the relative differences of CPU time, that are notably visible for PCMA* SA, to this effect.

5.4 Variation of PCMA* Penetration Rate

With a view to applicability of a traffic management system in real conditions, the capabilities to deal with incomplete information and inability to provide route guidance for a certain percentage are important. Especially, the interaction of the routing algorithm with the applied methodology of information gathering plays a vital role for the transitional period to fully communicating road users. However, none of the approaches from literature consider varying penetration rates [96, 108, 180–182].

Due to the inevitable future situation of a mixed composition of vehicles which are equipped with modern communication devices and those who are not, this section analyzes how PCMA* behaves with varying penetration rates of vehicles that are able to communicate. This implies incomplete knowledge for the router as well as the impossibility to provide routing information for the unequipped part of the vehicles, which make routing decisions only on their own.

5.4.1 Procedure of Analysis

Basically, the capability to provide and receive information is parametrized diversely from 0 to 100 percent, in steps of 10 percent. On the one hand, this means that isolated vehicles are not able to send any position data, routing information or anything else to the routing entity. Their existence can only be recognized indirectly since other vehicles' behavior may be affected. On the other hand, obviously it is also impossible for those vehicles to receive information. No routing decisions or any other indications can be sent to them, neither can they be influenced in any way. The remaining percentage of the vehicles as opposed to the isolated ones is enabled to do both provide and receive information.

In contrast to the vehicles' start and destination locations (which are again kept unchanged), the ability to communicate is varied randomly between the vehicles in order to wipe out effects that occur due to local concentration of vehicles that are routable compared to others that are not. Each result value represents an average over at least five equal simulation runs, but with diverse local distribution of communication ability as a consequence of the randomization.

5.4.2 Penetration vs. Travel Time

The travel time is a major performance indicator for both the individual drivers and public road network operators. While the former intend to reach their destination as early as possible, the latter try to avoid congestion and dissipate traffic quickly.

Figure 5.12 depicts the results for scenario 1. The different colors in the line plot represent different arrival intervals of vehicles. On the x-axis, the penetration rate of

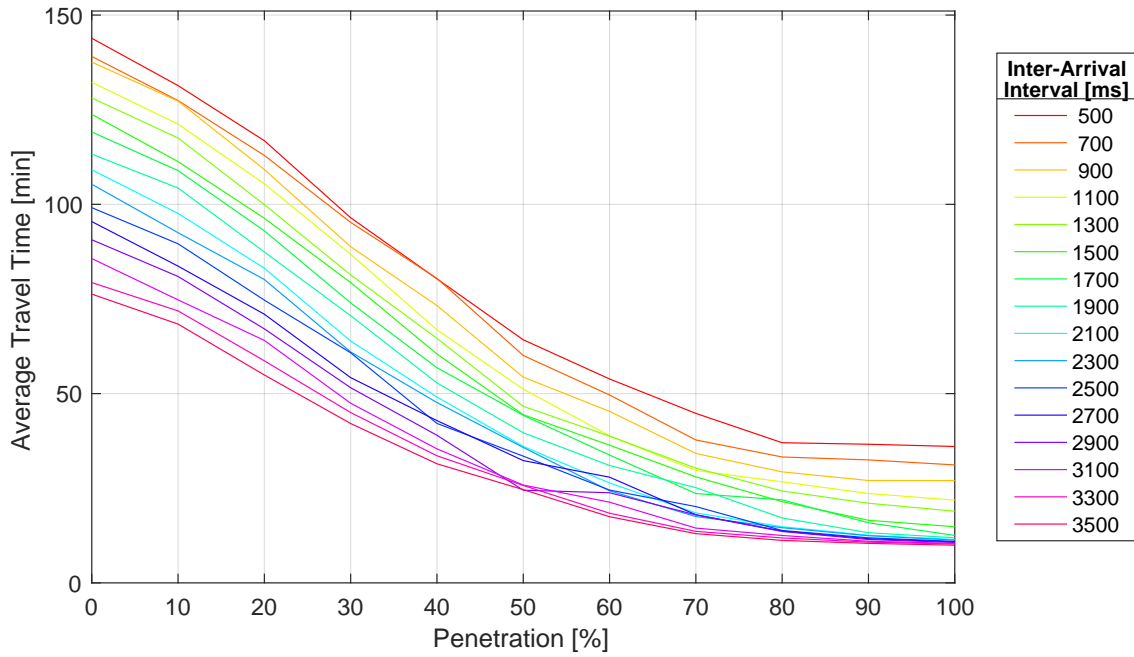


Figure 5.12: Average travel time vs. penetration for scenario 1 (3000 vehicles)

communication capabilities is represented from 0 to 100 %, where 0 means no routable vehicle at all. The y-axis illustrates the average travel time per vehicle in minutes.

In this scenario, the gradients for the different densities behave very similar. The greatest improvements are achieved between 10 and 60 percent penetration. Then, the curves flatten and there is only a slight decrease in travel time until full penetration of vehicles' communication capabilities. Fundamentally, the travel time decreases for all densities starting from very low penetrations. The reason for this is a good possibility for alternative routes in most parts of the network. The curves gradient decreases with higher penetration percentages and levels off between values 70 and 80 %, while higher percentages do not lead to great improvements anymore. As the majority of vehicles can provide and receive information, the disadvantages of few vehicles which are unable to communicate are compensated.

The surface plot in figure 5.13 again contains the average travel time, but normalized to a penetration of 0 % for each discrete IAI. The normalization is done by dividing each z-value by the travel time at penetration rate zero (i.e. the worst possible configuration). By doing so, the relative travel time gain compared to the least beneficial setup with zero possibility for routing becomes visible. It is noteworthy that this form of representation points out the area of operation where the PCMA* rerouting algorithm can accomplish the greatest improvements - that is the dark blue area with portions of travel times of around 15 % compared to total routing incapability.

In figure 5.14, the average vehicle travel times for scenario 2 are shown. As also

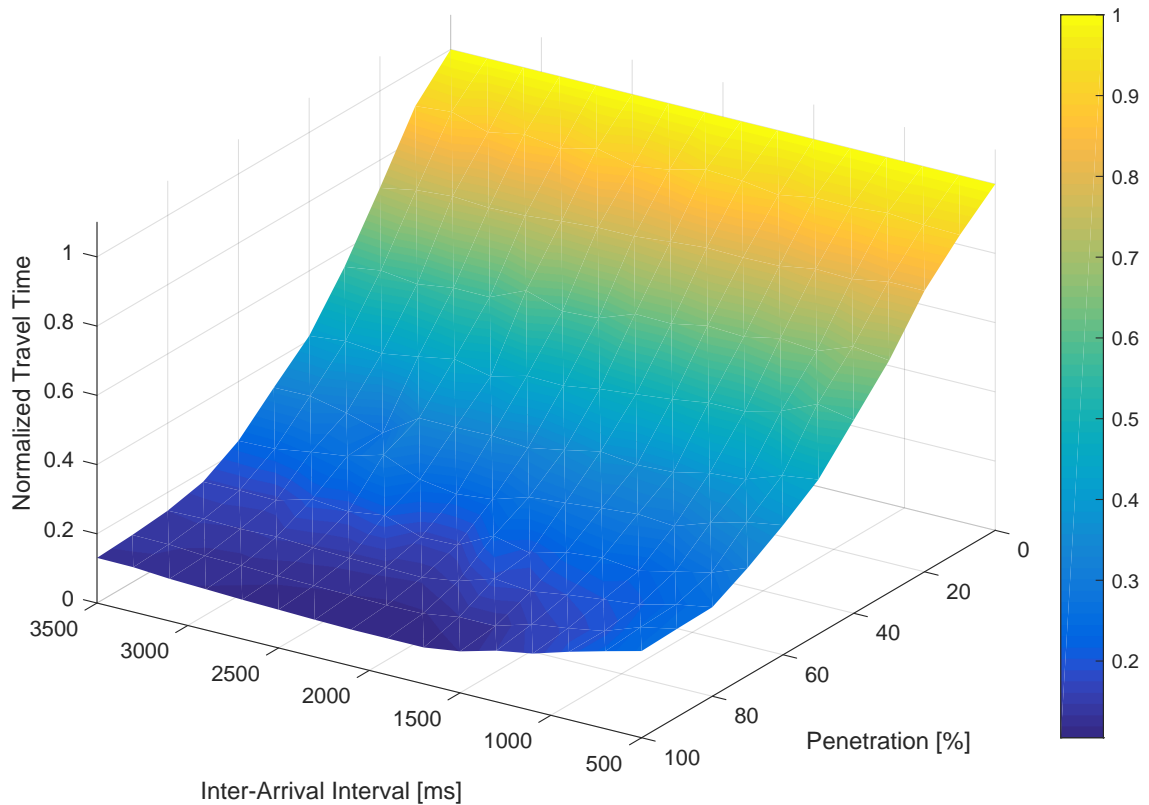


Figure 5.13: Normalized average travel time vs. penetration and IAI for scenario 1

observed in figure 5.12, gains in travel time can be achieved already for very low penetration rates. In contrast, for penetrations above about 60 to 70 % no significant decrease in travel time is possible anymore. This is on the one hand because of less appropriate available alternative routes in this scenario, which becomes visible by gradients of close to zero for penetration rates of greater than 60 %. Additionally, no advantageous effects in travel time come to light for very low traffic densities (inter-arrival times above 3000 *ms*), in contrast to scenario 1. This can be explained because almost no congestion occurs anymore, which further obviously needs no routing as a consequence.

Figure 5.15 shows the travel times normalized to zero penetration, analogous to what we saw in figure 5.13. What seems obvious is, in contrast to scenario 1, again the inability of improving the situation for very low traffic densities (i.e. high inter-arrival intervals), since no congestion occurs anymore and also rerouting is not necessary and beneficial in such cases. Notwithstanding, the gains in average travel time also become a little worse for very high densities. An explanation for this phenomenon is the lack of sufficient alternative routes in this scenario with adequate capacity, and that of course also potential wide-range alternative routes at some point become congested. However, the travel time can be reduced to even about 20 % of the value with zero penetration where only 60 % of the vehicles are capable to communication.

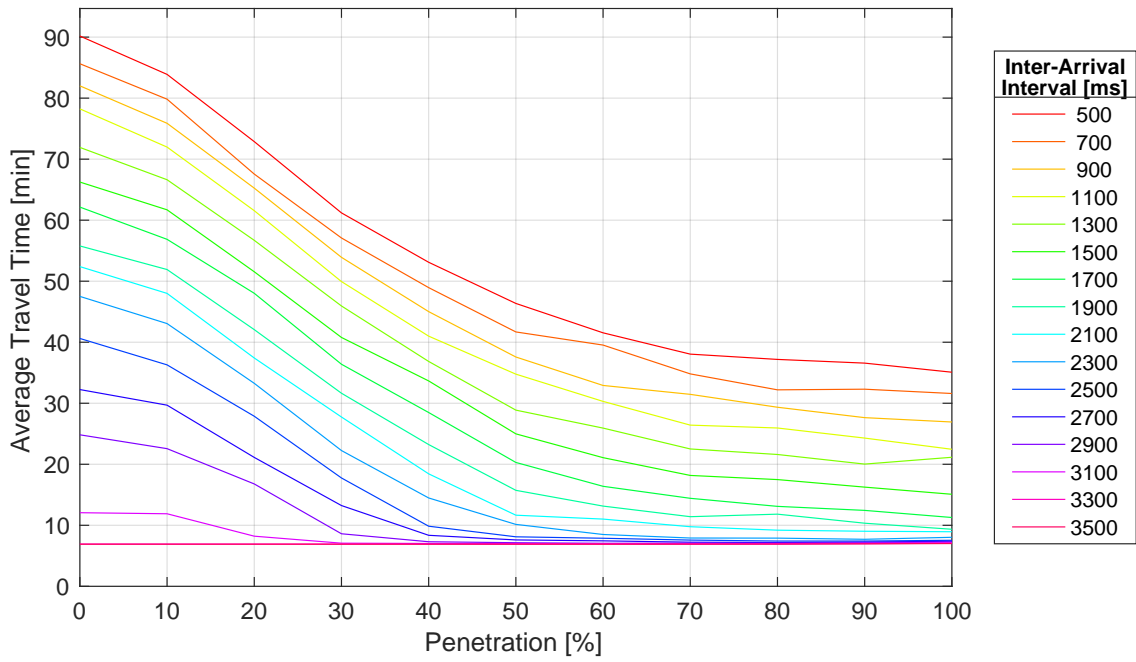


Figure 5.14: Average Travel Time vs. Penetration for Scenario 2

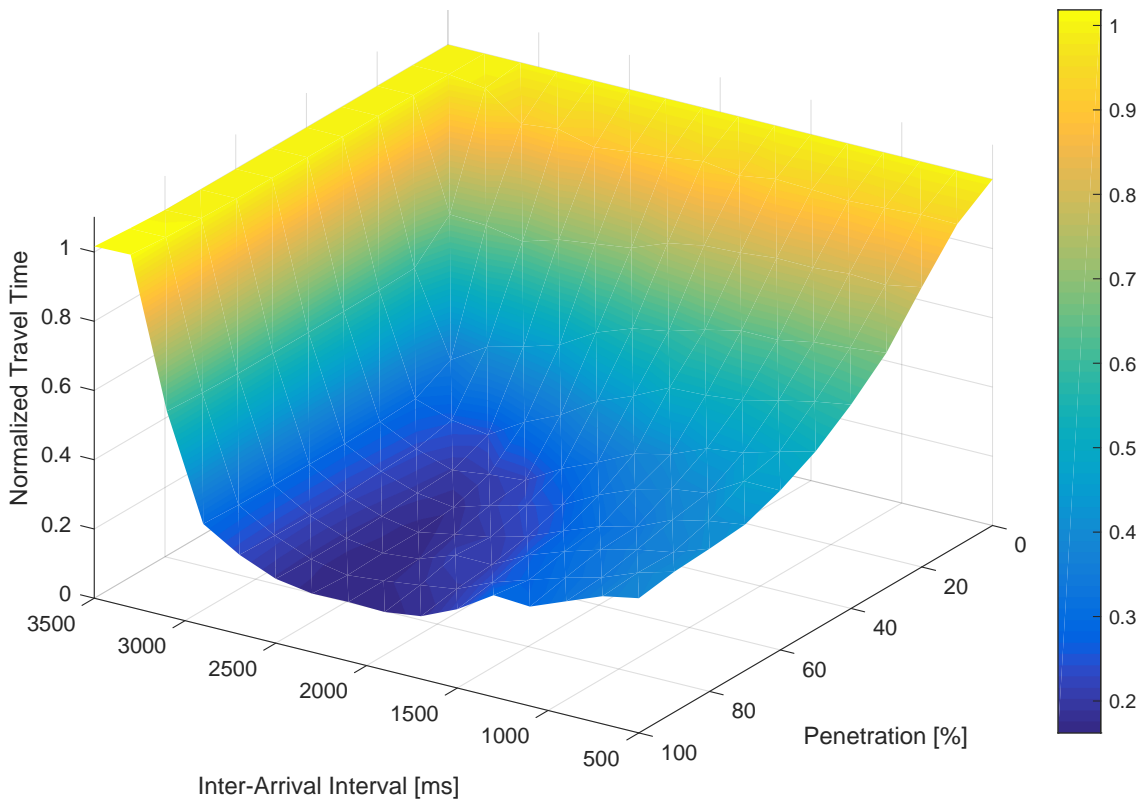


Figure 5.15: Normalized Average Travel Time vs. Penetration and IAI for Scenario 2

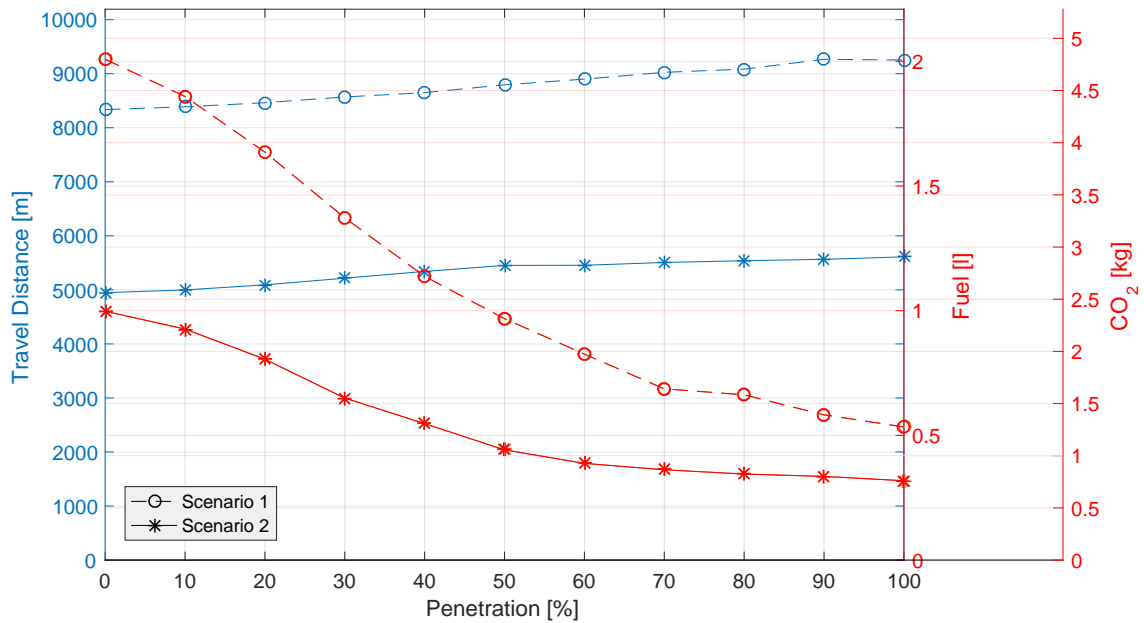


Figure 5.16: Average Fuel Consumption, CO₂ Emissions and Travel Distance for Scenarios 1 and 2 (marked with circle and asterisk, respectively) and IAI = 1700 ms

5.4.3 Fuel Consumption, Carbon Emissions and Travel Distance

In order to give insights into the fuel consumption, emitted CO₂ and travel distance, once more one representative setup with medium density (arrival interval of 1700 ms) was picked as demonstration, since the curves are characterized similarly for all vehicle densities. Figure 5.16 shows the mentioned parameters for both scenarios. The dashed lines with circle markers show results for scenario 1, while solid lines with asterisks as markers show scenario 2. The fuel consumption follows similar path shapes as the travel times do and bottom out with higher penetration rates of 80% and 60% and above for scenarios 1 and 2, respectively. As the calculation of CO₂ emissions follows a simple linear relationship to fuel consumption (assumption: 1 l Diesel = 2.69 kg of CO₂), the curves are equal but with a different y-scale. Obviously, the average travel distance slightly increases with higher penetration rate. The reason for this is that unrouted vehicles always take the shortest path, while detours due to rerouting result in longer travel distances, which becomes visible in the blue curves of figure 5.16.

5.5 Investigation on Unideal Conditions

This section focuses on the investigation of cooperative routing with non-ideal communication capabilities, in contrast to the previous section where such were presupposed. The effects of delayed or lossy message distribution on travel time and fuel consumption are presented, with varying configurations of the models which are introduced in section 4.4. Instead of assuming defined properties of the network and determining how well the routing algorithm can perform by applying them, the problem is redefined in a different light.

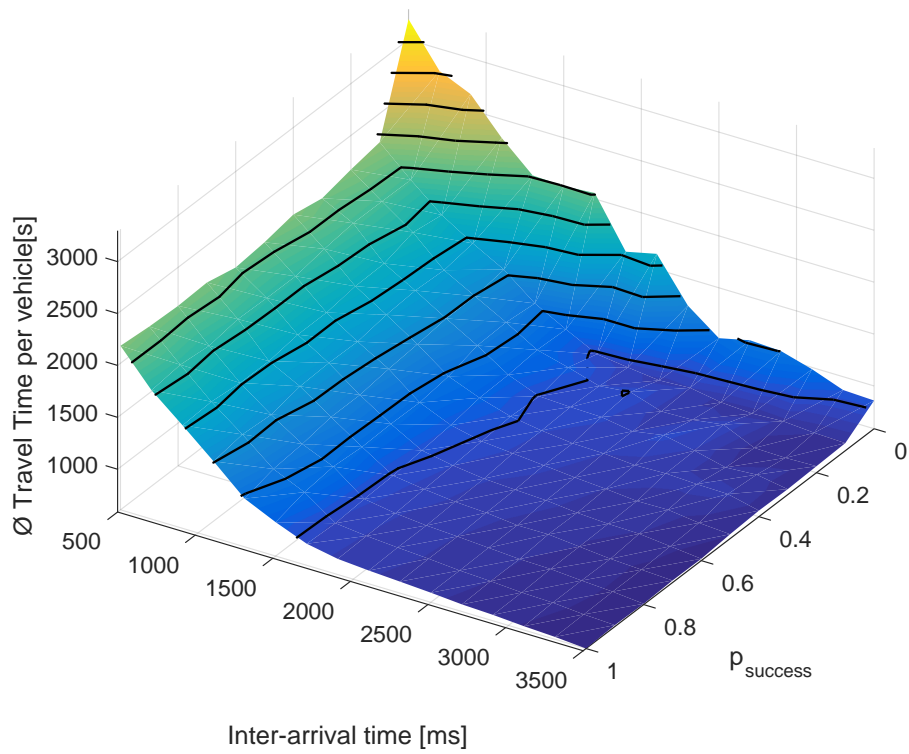
5.5.1 Success Rate of PMsgs

Initially, the success probability p_{success} of periodic messages was analyzed and set up to be from 0 to 1, in steps of 0.1. As described in section 4.3.3, low values for p_{success} can lead to inaccurate and outdated knowledge base of the current road conditions for the router. Figures 5.17a and 5.17b (scenarios 1 and 2, respectively) show the average travel time per vehicle over the success probability. As the shape of the surface basically behaves similar for the majority of investigated delay times ($0.1 \leq \lambda \leq 0.9$), we decided to choose medium values for the geometric model of $\lambda = 0.5$ and $RTT = 1000 \text{ ms}$.

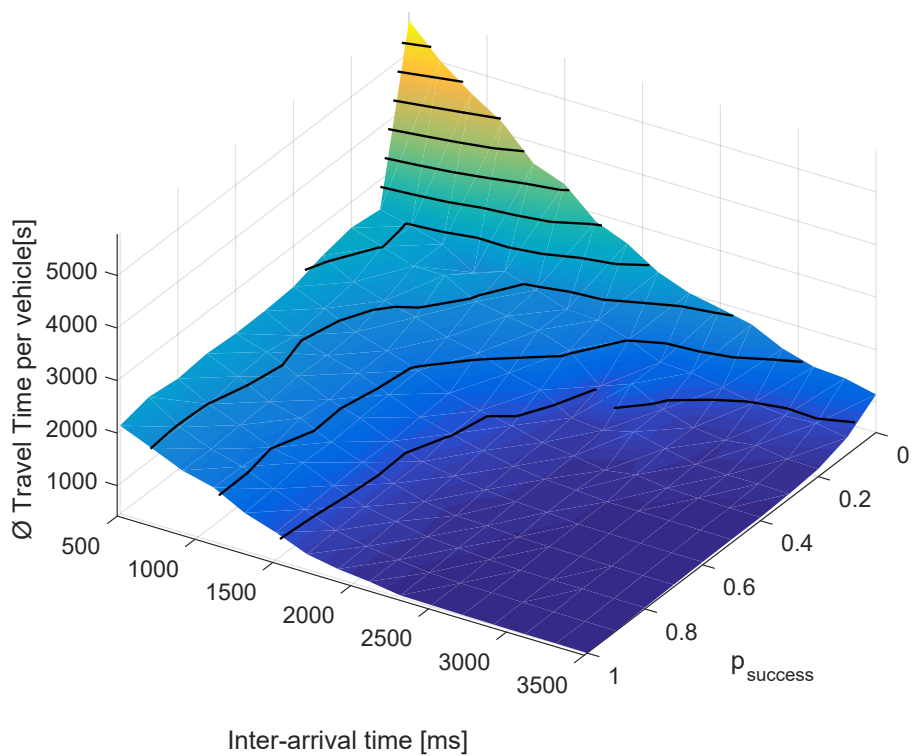
In both figures 5.17a and 5.17b, the travel time decreases slightly with higher success probability of the PMsgs. However, a huge portion of the gain is achieved already at success probabilities of 15 to 30 % in both scenarios. From then on, the improvements already attenuate until the minimum average travel times are unsurprisingly reached with $p_{\text{success}} = 1$, what is accentuated by the trend of the black contour lines. This fact emphasizes the strength of the algorithm in suboptimal environmental conditions. Obviously, the result values are negatively influenced with a higher traffic density, since congestion is much more severe and the potential for improvements shrinks.

While the surfaces in figures 5.17a and 5.17b basically behave similarly, they are still not identical. Minor deviations become visible in the right part of the diagrams, with $0.1 \leq \lambda \leq 0.3$. In scenario 1, the resulting average travel times are closer to the minimum much earlier, i.e. with low success rates. In other words, in this scenario the router can deal with sparse information better than in scenario 2. We ascribe this effect to the higher amount of possibilities for alternative routes in scenario 2. So while there are no more route possibilities for a certain situation in scenario 1, there might still be some in scenario 2. Therefore, a better information quality and density due to higher success probabilities of PMsgs does still lead to better results for $p_{\text{success}} = 0.4$ compared to a value of 0.2. The characteristics of these results can be associated with those with varying penetration rate in section 5.4.2, as the curves show similar behavior.

In contrast, the results are similar for the entire set of success rates (except from 0) for very low values of λ and, as a consequence therefrom, high delays for ODMsgs



(a) Scenario 1



(b) Scenario 2

Figure 5.17: Average travel times with varying p_{success} , $\lambda = 0.5$ and $RTT = 1000$ ms

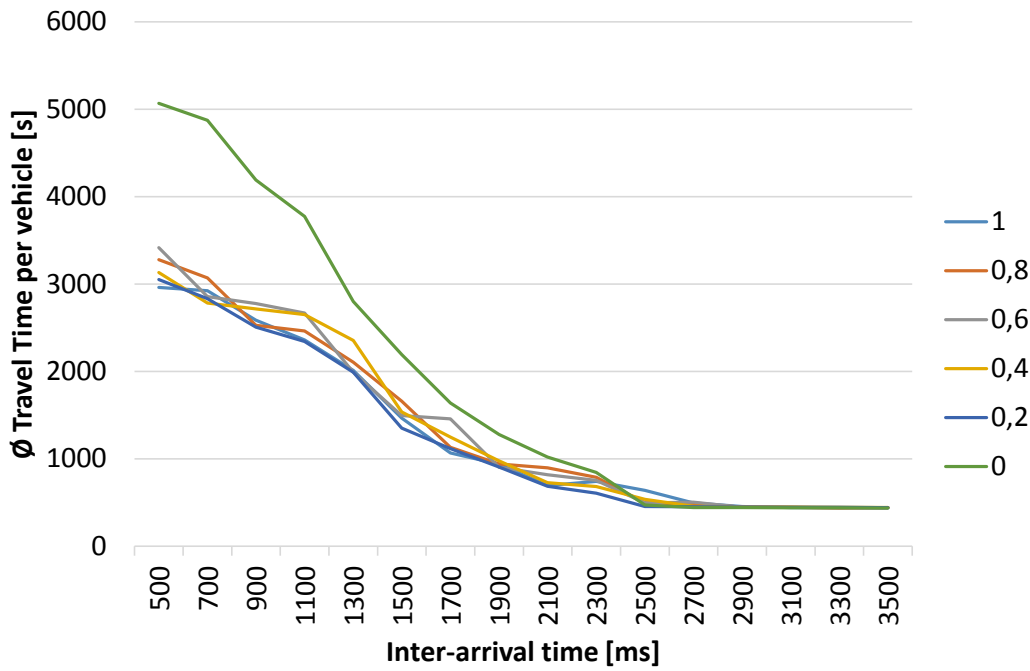


Figure 5.18: Average travel times with different line colors for multiple values of p_{success} for scenario 2 with very low $\lambda = 0.005$ and $RTT = 1000 \text{ ms}$

(average delay time $> 200 \text{ s}$). In such cases, only a miniscule minority of route messages reach their destination timely and are therefore not applicable any more. This explains the circumstance that the success rate is nearly independent then, which is pointed out in figure 5.18 and the close proximity of the travel time curves therein. However, a success rate of zero, which means no knowledge of the router about the road conditions at all still adds up in worse results. The still existing minority of ODMsgs that reach their destination (despite the low λ) is useless for the case $p_{\text{success}} = 0$, and explains the considerably higher results indicated by the green curve in figure 5.18.

5.5.2 Parametrization of ODMsgs

Both parameters of the delay model for on-demand messages, λ and RTT , were adapted for the purpose of analyzing the influence of message delay length on achievable average travel time. Basically, the parameters have an effect on the distribution of the overall delay for an ODMsg, as shown in figure 5.19. This figure shows the resulting average delay time per on-demand message for different setups of the geometric delay model. The delay naturally is independent of the vehicle density and equal for both scenarios. What also can be observed is that there exist parameter combinations which lead to equal average delays. Those pairs can easily be found by looking for columns which have similar values in y-dimension in figure 5.19.

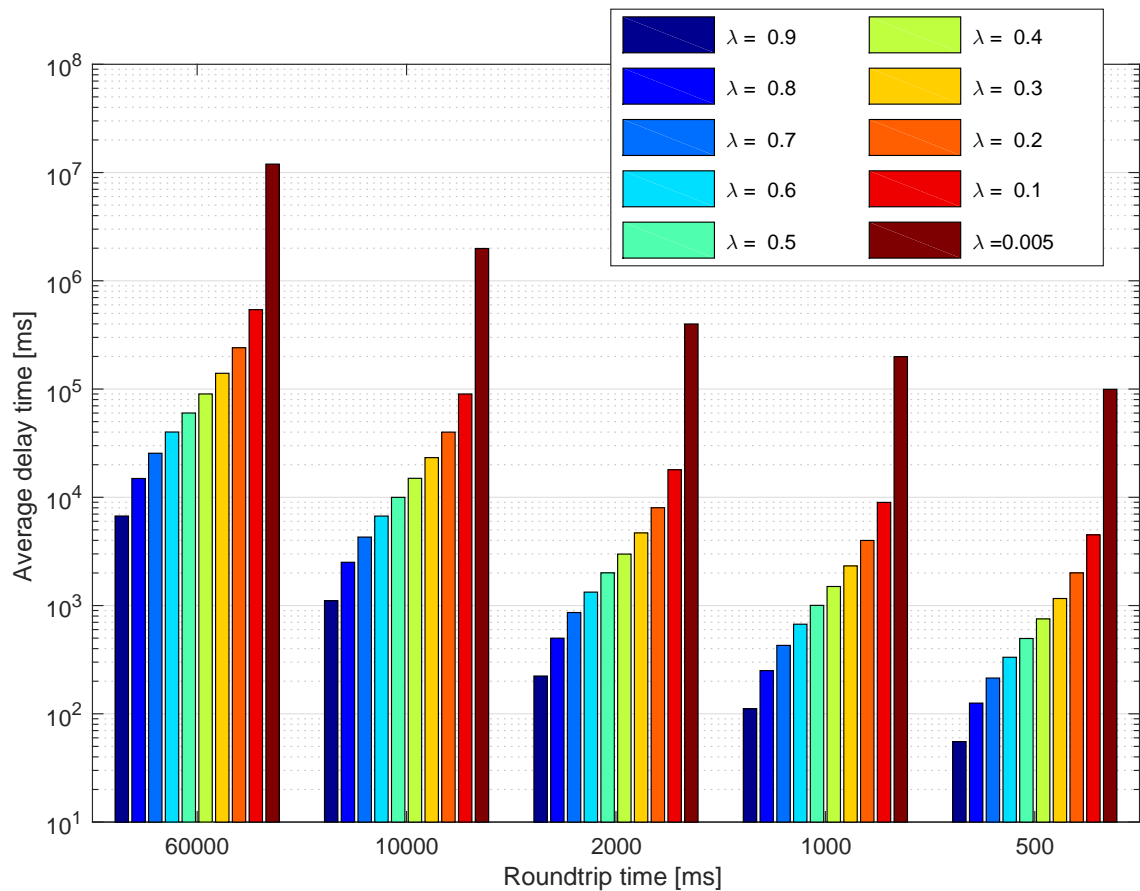


Figure 5.19: Average message delay times with different geometric delay model parameters λ and RTT

The consequences of delayed reception for ODMsgs is shown in figures 5.20a and 5.20b for scenarios 1 and 2, respectively. In these simulations, a 100 % probability of success for PMsgs is assumed in order to exclude the influence of them and be able to ascribe the changes in achievable travel time solely to described message delay variations.

As expected, the average travel time per vehicle increases with longer average delay, which becomes visible in the rear peak of the diagram (low lambda, high round trip time) in both scenarios. Accordingly, the decrease in average travel time per vehicle flattens with increasing lambda and decreasing RTT, while reaching its minimum at $\lambda = 1$ and RTT= 0 (i.e. zero delay). These extreme values were also added to the parameters for reasons of validation of the model. As expected, zero round trip time leads to a pretty straight distribution of average travel time. The same results become apparent for high values of λ . However, slight irregularities are visible in scenario 2 in figure 5.20b with RTTs of 60000 and 200000 and λ between 0.3 and 0.6: The achievable average travel time decreases although the message delay becomes higher. This effect can be ascribed to the fact that in these cases only very few messages arrive in a reasonable time, and the

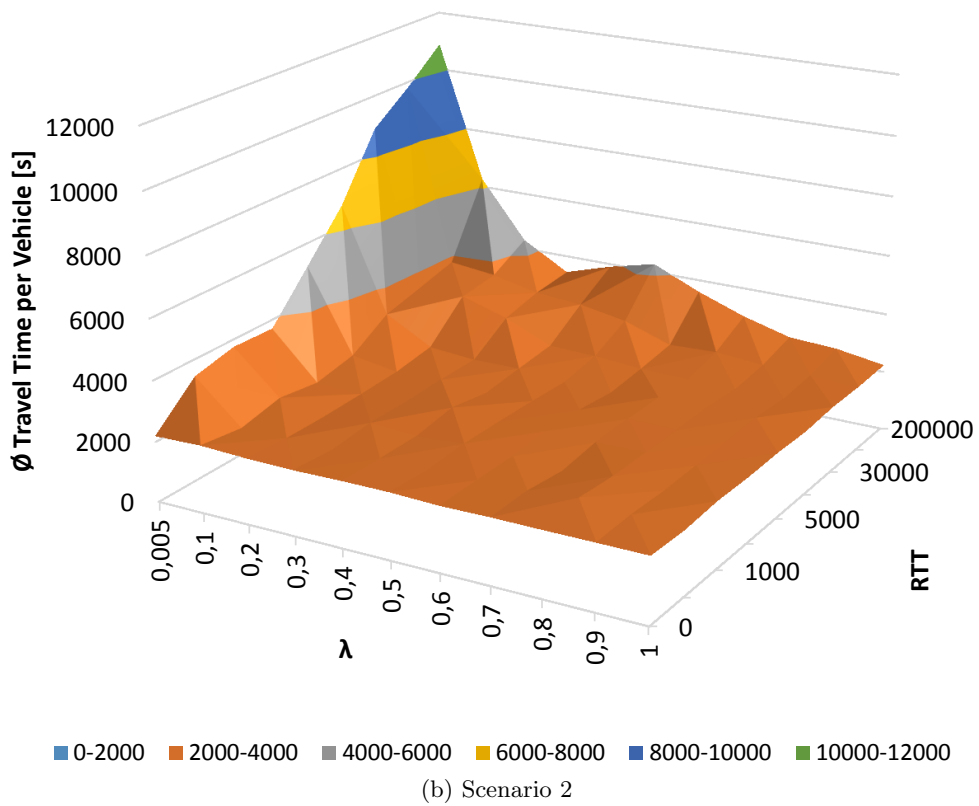
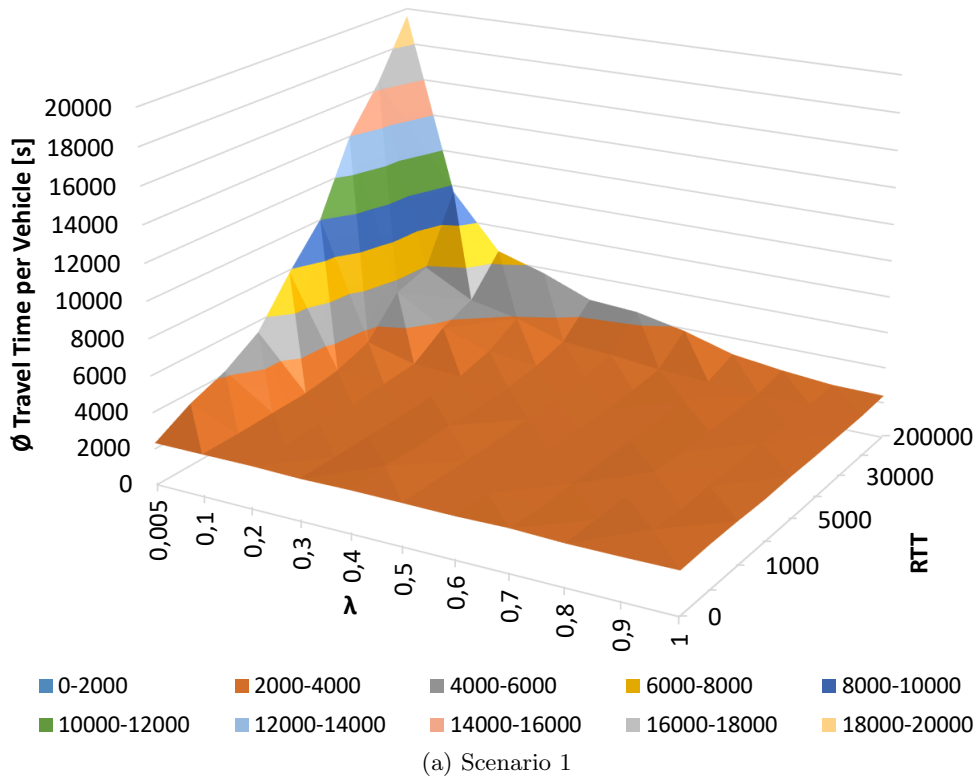


Figure 5.20: Average travel times with IAI = 1700 ms and varying λ and RTT

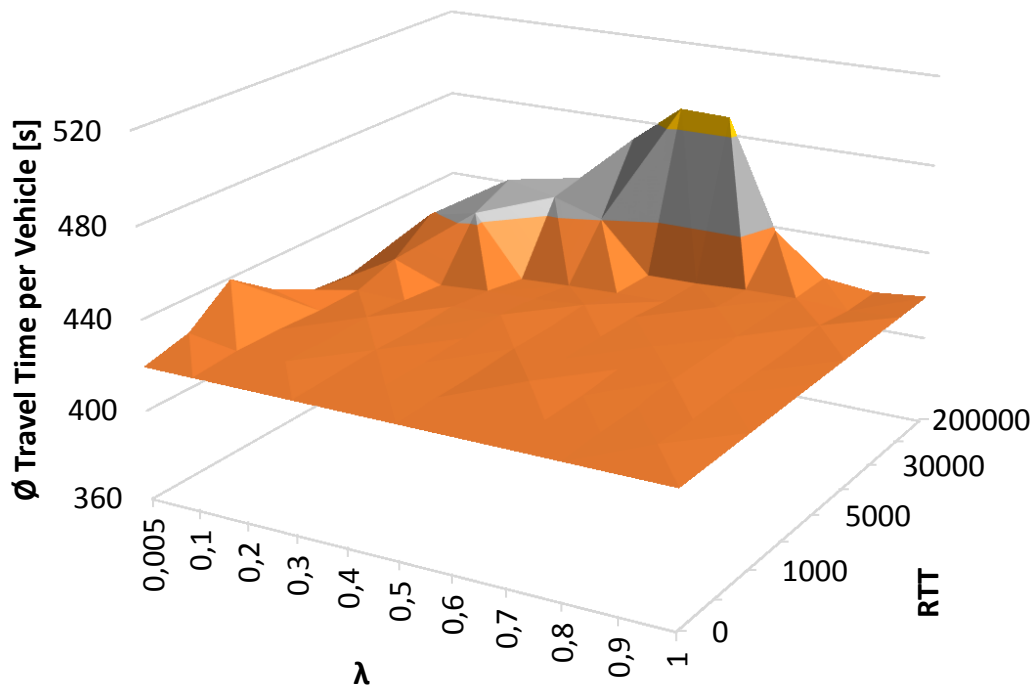


Figure 5.21: Zoomed view of average travel times with different geometric delay model parameters λ and RTT for scenario 2 and inter-arrival interval of 3500 ms

internal knowledge of the router regarding the vehicles' destination is scarce. Therefore, also routing decisions are made based on that outdated internal knowledge of the router. These routes lead to unnecessary detours and therefore increase the travel time with no gains elsewhere. This effect is becoming clearer when decreasing the vehicle density and setting the vehicle inter-arrival time to 3500 ms , as figure 5.21 illustrates. It should be noted that only the interesting range is extracted here. The peak disappears with low values for λ , since the probability of receiving wrong information is also very low then, and thus the negative impact therefrom is mitigated.

5.5.3 Fuel Consumption and Travel Distance

The consumed fuel basically is strongly related to the travel time for all investigated scenarios. However, one scenario was picked for visualization with medium success rate of 0.5 and medium value for λ of 0.5 as well. The RTT of the selected configuration is 1000 ms . As illustrated in figure 5.22, the fuel consumption also flattens at a medium density of about 2000 ms inter-arrival time, as does the average travel time. The travel distance does not change to the same extent as consumed fuel and time, but slightly decreases with lower vehicle density. The reason once more are the detours due to rerouting, which of course lead to longer distances since the alternative routes are longer than the original, shortest ones.

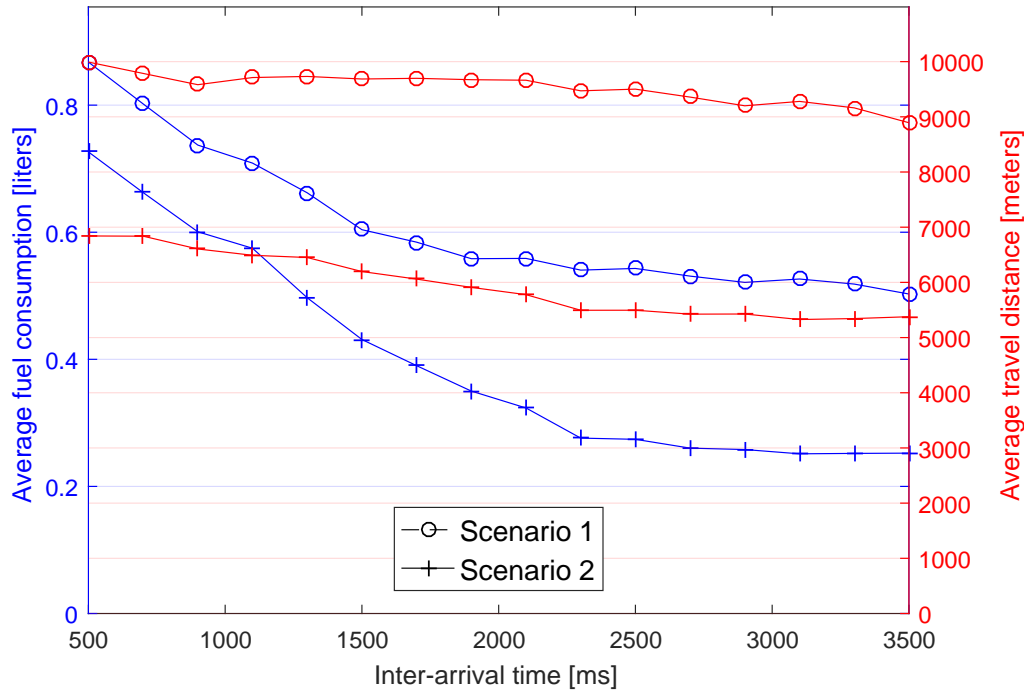


Figure 5.22: Fuel consumption and travel distance per vehicle for both scenarios and $p_{\text{success}} = 0.5$, $\lambda = 0.5$, $RTT = 1000 \text{ ms}$

5.5.4 Volume of Transmitted Data

Due to the relatively high regular update interval of 30 s , the amount of transmitted payload data is at a low level compared to the overall capacity of modern cellular communication networks [183, 184]. Tables 5.6 and 5.7 present the amount of transmitted messages (successful or not) during a complete simulation for both scenarios as well as the sum of transferred data for six selected vehicle inter-arrival time setups and a success rate p_{success} of 1. However, the data amount comprises only the payload itself, no overhead due to transmission protocols, error correction or similar mechanisms. The following payloads are assumed per message type (as defined in section 4.3.1):

- *Initial Message:* 4 bytes (source and destination positions, as pair of latitude and longitude, one byte each)
- *Vehicle Data Message:* 3 bytes (position and current velocity, one byte each)
- *Route Update and Confirmation Message:* 3 bytes + 1 byte \times length of route (position and velocity as for the initial and vehicle data message, in addition to 1 byte for each road segment which is identified by a unique number and referred by the containing route)

Table 5.6: Transmitted data volume and amount of messages in scenario 1

Inter-arrival interval	500 <i>ms</i>	1100 <i>ms</i>	1700 <i>ms</i>	2300 <i>ms</i>	2900 <i>ms</i>	3500 <i>ms</i>
Transmitted messages	276588	186669	117448	103383	92111	78871
Data volume [MB]	21.39	16.77	10.25	8.60	7.08	5.27

Table 5.7: Transmitted data volume and amount of messages in scenario 2

Inter-arrival interval	500 <i>ms</i>	1100 <i>ms</i>	1700 <i>ms</i>	2300 <i>ms</i>	2900 <i>ms</i>	3500 <i>ms</i>
Transmitted messages	270063	190774	96340	56351	52370	50279
Data volume [MB]	24.03	16.67	7.39	2.81	2.39	2.14

Basically it can be observed that the higher the density is, the higher is also the required amount of messages due to a greater need of intervention of the router and hence more messages containing new routes in both scenarios. Nevertheless, the data volume and also number of transmitted messages saturate faster in scenario 2 (table 5.7). The reason is that in this scenario, the improvements due to optimization are close to the best achievable already for lower densities, compared to scenario 1, what is expressed by figure 5.8b in section 5.3.6 as well. The blue PCMA* SA curve levels off already at an IAI between 2000 and 2500 ms, what is not the case in that manner in the artificial scenario depicted in figure 5.8a. This behavior is reflected in the amount of transmitted messages and data in the same way.

5.5.5 Perceptions

Generally, it has been discovered that the algorithm is very tolerant regarding both transmission delays and failures. This robustness is explained by several arguments:

1. Delayed transmission of ODMsg is not necessarily a problem in all situations. More specifically, it is not the case for a majority of situations, since the characteristic of the geometric distribution of delay time leads to few high values and a comparably higher amount of delays which have low values. So if it is still possible for targeted vehicle to apply the route because the road segment which would differ to the current route is not yet reached, the route is applied anyway. Figure 5.23 illustrates such a situation, where the vehicle continues its original route (thick, red) from position 1 to position 2, when it receives the route update. The delay does not matter in this case, since the routes do not differ until the point in time when reaching position 2, but at a subsequent intersection.

2. Situations where the intended receivers are not able to make use of the transmitted routing messages because of too high delays are resolved automatically by the routing

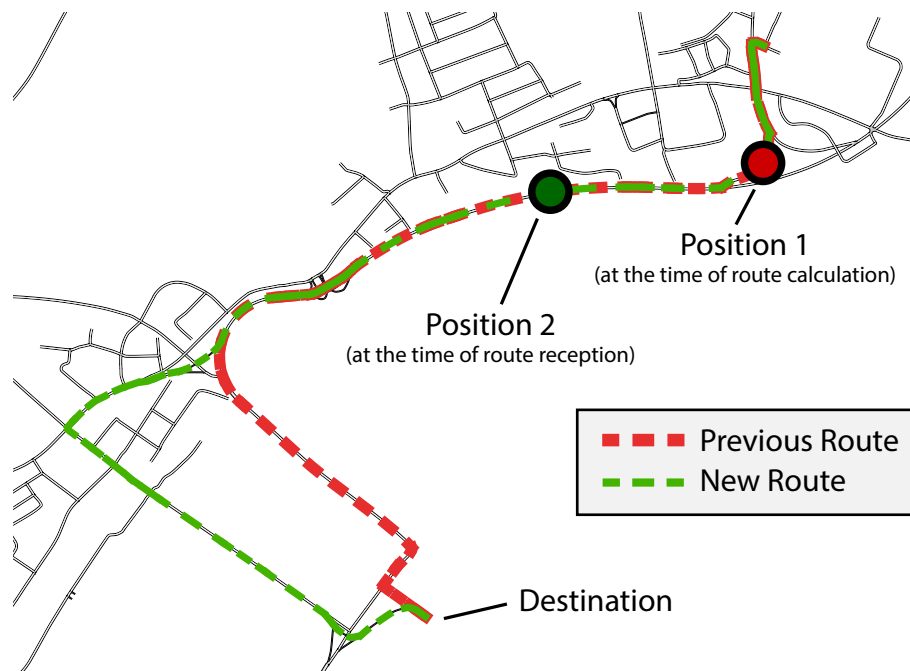


Figure 5.23: Unproblematic delay between positions of route calculation and reception

algorithm itself by the included method of vehicle selection (section 3.2.5). If the predicted congestion is not eliminated by the help of communication with the initially selected vehicles, the next potential vehicle out of the affected ones is chosen. This process is repeated and retried until the situation gets better, i.e. any of the vehicles which pass the congested node in the defined time interval finally manages to choose another route. In other words, the congestion still appears within the sphere of action of PCMA* if no vehicle changes its route, as long as messages are still received and can be processed successfully.

3. As the method of gaining knowledge about the current situation on the road is based on average speed (cf. section 3.2.1), it is less critical if some of the vehicles' reports containing their position and speed included in PMsgs is lost. The speed of all vehicles on the very same road segment is likely to be similar, so that it does not matter much as long as the percentage of correct reports per segment does not go down to zero.

6

Conclusions and Outlook

Encouraged by the ever more stringent traffic problems as well as increasing ubiquitousness of sensors and communication possibilities within cars, the main objectives of this thesis are to introduce a methodology how vehicular traffic can be optimized. The Predictive Congestion Minimization in Combination with an A* based router (PCMA*) algorithm for congestion prediction and vehicle rerouting is proposed in order to save travel time and fuel. The PCMA* algorithm mitigates congestion by addressing only those vehicles that are affected by forthcoming bottlenecks. The approach is evaluated comprehensively by simulations, which are carried out with the help of microscopic traffic models, using the *TraffSim* simulation framework [47]. Two different scenarios are considered, an artificial and a real-world scenario. In both investigated configurations, the PCMA* algorithm outperforms the benchmark configurations.

Besides the discussion about the introduced traffic optimization approach, another major field of research in this thesis is the investigation in environments with unideal conditions in multiple terms. This includes a study investigating the robustness against varying penetration rates of routable vehicles, as well as an analysis how the results are influenced in unideal communication environments.

In the following, the findings regarding the algorithm comparison as well as the evaluation with non-idealized environments are concluded.

6.1 Performance

PCMA* provides highly accurate predictions and reroutes vehicles such that they circumvent the congestion via a congestion-free alternative route. Extensive simulation results support these claims. Two different configurations of the proposed algorithm are introduced.

The proposed algorithm has its strength especially in cases where information of potential traffic jams is required. The shortcomings of other approaches are that this relevant information is simply not or not early enough available. Based on the predictions, vehicles are proposed an alternative route, ideally with minimal overlapping segments to the originally chosen, congested route. For being able to choose a spacious route, early traffic information and forecast is a key factor. Continuous evaluation of the current and subsequently the expected future conditions of the road enables this precise tackling of upcoming problems. Moreover, purposeful selection of vehicles to be rerouted is a great benefit.

An essential precondition for the predictive approach is undoubtedly the correctness and reliability of the forecast. This prediction efficiency, i.e. the number of correct predictions over the total number of predictions as sum of correct and wrong ones is analyzed. The result of this investigation shows a very good performance regarding this field. The results naturally depend on the methodology how they are gathered, since the rerouting of vehicles needs to be disabled in order to prove whether a predicted congestion really arises in the future or not. Of course, this fact further influences the whole simulation. Furthermore, the analysis depends on the accepted tolerance between prognosticated congestion future timestamp and real occurrence time of the congestion. Nevertheless, the prediction efficiency was revealed to be above 75 % already for very low error tolerances for the prediction time of 5 seconds and above 85 % for tolerances of 60 seconds. These numbers are valid for all investigated assumed node capacities (section 5.2), what is a good and very important basis for further routing actions.

The performance of PCMA* is determined by comparing on the one hand with the worst case, which means unrouted vehicles that are unaware to react to problems. On the other hand, the approach is contrasted with a simple, reactive approach and a more sophisticated approach from literature - the Flow-Balanced KSP (FBkSP) algorithm [108].

It turned out that PCMA* is able to improve travel time and fuel consumption considerably for both scenarios and outperforms the comparative approaches. The measured reduction of travel time is greater than 80 % compared to a situation with no central routing, and even more than 30 % in relation to the FBkSP approach. Also the consumed fuel decreases by 65 % and 16 %, respectively, in both investigated scenarios. The degree of improvement naturally depends on the traffic density, which is varied by changing both the amount of simulated vehicles as well as the inter-arrival interval. What became obvious is

that the major figures of merit, which are average travel time and fuel consumption, decrease in either investigated case. The algorithm is very effective in mitigating congestion while adapting dynamically to the current situation on the road. However, the potential is higher for situations where the network is not hopelessly overcrowded. In such a case, the capacity of the network and also the potential alternative routes are exceeded, even with any optimization strategy. Thus, the offset to the reference algorithms decreases. Moreover, it seems obvious that less density leads to reduced road congestion and enables vehicles to use the original, direct and shortest route with hardly any delay. This has also been proven by simulations (section 5.3.6).

6.2 Robustness in Suboptimal Conditions

Whatever approach is selected for the purpose of optimizing road traffic, it is for those which utilize any kind of cooperation necessary to interchange information between vehicles and/or the infrastructure by V2X communication. The robustness against fragmentary penetrations of the system, communication delays or transmission data loss is of vital importance.

Firstly, I examined a simulation setup with a varying penetration of vehicles which are able to utilize the system. Other cars are neither able to provide information nor to receive any route guidance. The results show that the degree of improvement is not related linearly to the penetration percentage. Instead, the average travel time curve over increasing penetration follows a regressive shape. It levels off at penetrations between 50 % and 80 %, again depending on density and scenario. A huge proportion of the total possible improvement is already achieved for penetration rates between 40 and 60 %, although the average travel time still decreases slightly with higher penetration. This strong nonlinear behavior is remarkable, since a comparably small amount of intelligent vehicles already has the potential to achieve major gains in travel time.

Secondly, the effects of delayed or lossy message distribution with varying delays and message error probabilities are studied. Instead of assuming defined properties of the network and finding out how a routing algorithm can perform by applying them, the problem is redefined in a different light, as the routing entity requires information such as the vehicles positions, destinations or velocities. The simulation setups comprise parameter variations for communication properties for both introduced types of messages, that are status messages which are sent from vehicles to the router periodically as well as on-demand messages with routing information. The results basically show that PCMA* performs very well for a large set of setups and even high delays and high loss probabilities. A high robustness against message delays comes to light, with negligible or even undetectable effects on travel time for message delay times of 10^4 and even 10^5 ms. On the

other hand, message success probabilities for continuously transmitted status messages of down to 0.3 are acceptable for losses in travel time of not more than 10%.

The presented findings can also help operators to decide how much communication capacity is required for a well-functioning intelligent rerouting mechanism. From another point of view, the preconditions for the underlying communication standard which must be fulfilled to reach a defined or required improvement are defined, while the rest of the capacity can be used for other services. It may not be necessary to further invest in lower delays and latencies and an increase of the network capacity, if the current features of the communication network already fulfill the desired requirements.

6.3 Critical Evaluation of Transport Planning Issues

While this work has made valuable contributions to dynamic optimization of vehicular road traffic, it on purpose shortens or leaves out certain aspects, especially related to induced traffic, which is a well-known issue in transport planning. As being a wide research area, the fact that at least parts of additionally generated capacities are eaten up by new traffic, denoted as induced traffic, is out of the question. It is standing to reason that extension in terms of new built infrastructure behaves similar to any other kind of capacity enhancement, like optimization and hence better utilization of existing infrastructure, as in this particular case. This topic was introduced and elucidated comprehensively in section 1.3. However, the presented results and achieved improvements are based on the assumption that the induced traffic is zero.

Notwithstanding, although investigations and particular quantification of induced traffic for the investigated situations do not show up per se, the results can still be interpreted in view of this research area. By the help of analysis results with varying density and number of active vehicles it can be determined how much induced traffic is acceptable in order to still benefit from enabling the proposed system.

For this to show, figure 6.1 initially reproduces the results for a certain configuration (IAI = 1500 ms with 3000 vehicles) with an additional measurement apart from unrouted (disabled) and PCMA* routed setups. This indicated value represents the lower bound, i.e. the absolute theoretical limit of time, distance and CO₂ that can be achieved. One can find no solution to undercut this limit. In this configuration, each vehicle drives to its particular destination individually using the fastest possible route, without any influence of other traffic. Put in other words, the road network is empty apart from the vehicle of interest, and the next vehicle does not start before the prior one reached its destination and the network is empty again. This lower bound is represented by the cyan columns in figure 6.1. It is emphasized that this is self-evidently possible only theoretically. However, it relates the simulated lower bound including start time constraints to the minimum

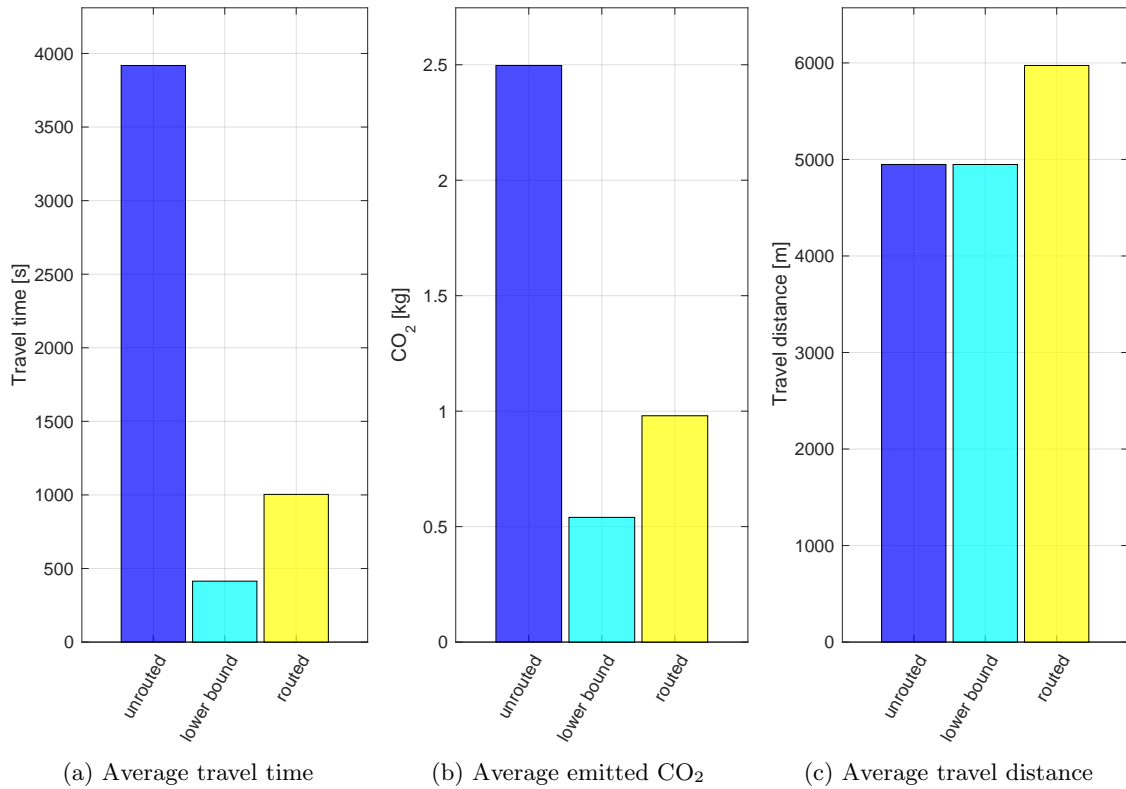


Figure 6.1: Comparison of figures of merit for unrouned, theoretical lower bound and routed simulation configurations (IAI=1500ms, 3000 vehicles, scenario 2)

achievable figures of merit. Those are travel time (figure 6.1a), emitted CO₂ (figure 6.1b) and travel distance (figure 6.1c). While again considerable differences in travel time and CO₂ between the unrouned and routed configurations can be observed, the travel distance is slightly higher in the routed case and equal for both the unrouned and the lower bound configuration. The reason for the latter is that the routes are the same in either case, just the departure time is different, what further makes no difference for the distance of course. Supplementary, this figure shows the comparison to the theoretical lower bound with a maximum amount of simultaneously driving vehicles of 1. Thus, this values can under no circumstances be undershot, and can thus also help to decide whether or not further improvement effort is worth the investment.

For the purpose of estimating the acceptable induced traffic before the improvements are eaten up, figure 6.2 compares travel time directly between configurations with a different number of vehicles and density. The evaluation also includes the best case configuration, which is represented by the black bars. Unsurprisingly, those values are independent of the overall vehicle amount, since they are normalized to the average per vehicle and thus of equal height. If examining the diagram in horizontal direction, configurations which result in similar average travel times per vehicle become obvious. Especially comparisons

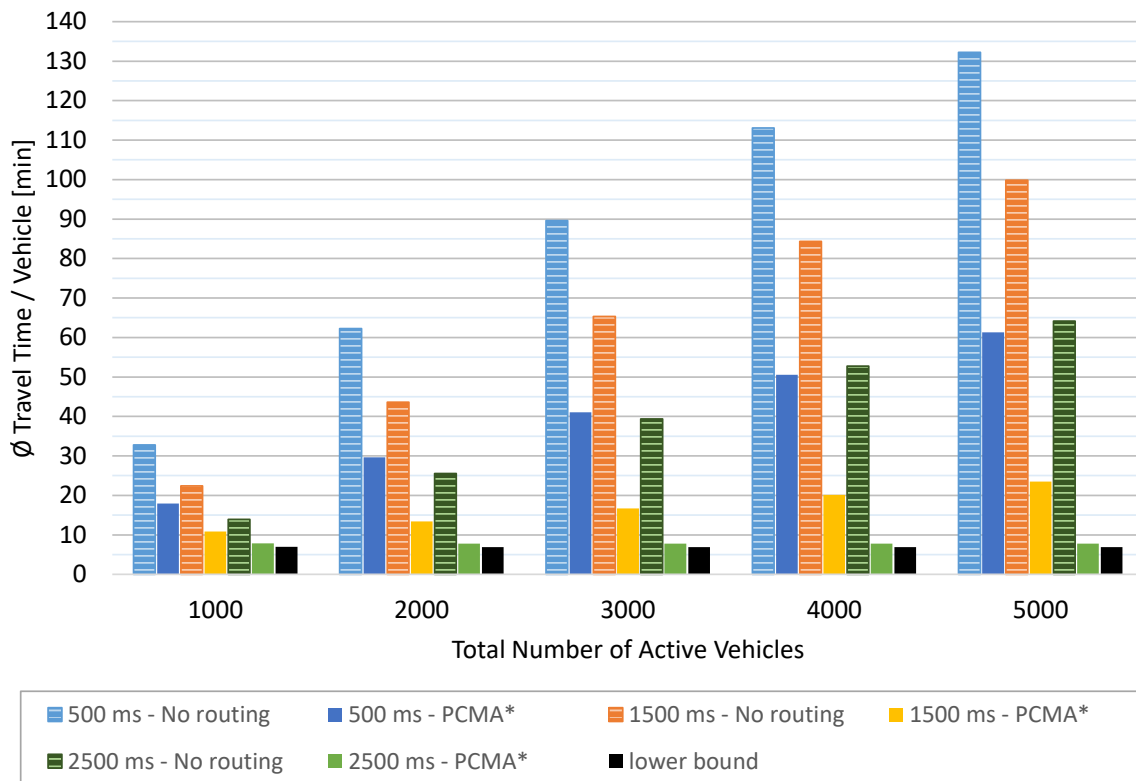


Figure 6.2: Evaluation with different vehicle amount and density for scenario 2

between configurations with no routing (represented by the horizontal line pattern) and routed configurations (solid bars) are of interest. For example, similar travel times can be observed when looking at the bar group of 3000 active vehicles and comparing the solid blue and dark green, patterned bars which are of similar heights. This means an induced travel up to a density increase represented by decreasing inter-arrival times from 2500 to 500 ms is acceptable when applying PCMA*, if the goal is not to worsen the performance. Furthermore, another pair of equal heights can be identified. The configuration with disabled routing, an IAI of 500 ms and 2000 active vehicles (patterned blue bar) achieves similar average travel times to the same configuration with 5000 vehicles, represented by solid blue bar in the rightmost bar group. It can be summarized that figure 6.2 reveals the acceptable amount of induced traffic in terms of higher density or more vehicles which is still acceptable after applying PCMA*, if aiming to improve traffic flow.

Finally, the question rises what can be done to decrease negative impacts of the inevitable induced travel, and as a consequence also road congestion. Explanations from literature propose a solution which is called congestion pricing [22, 185]. A majority of roads has a great deal of underused capacity. During rush hours, severe congestion occurs while the roads are nearly free at other times of the day. This is where action is needed,

by means of increasing the cost of driving depending on the current traffic conditions. The extra cost of driving apart from the increased travel time makes alternative options like public transport, cycling, walking or traveling at another time more attractive. This system has been applied successfully in Stockholm [186], London [187] and Singapore [188]. Despite the positive effect of congestion pricing, it is still a political challenge to establish it, since no voter likes to pay for something which was free before. This was one of the reasons for New York's government to fail introducing it in 2008 [189].

A similar approach aims at regulating of car parking. In urban areas, a considerable amount of VMT is generated by vehicles just for drivers to find a parking lot. This number is estimated to be between 10 and 30 % [190]. Thus, similar to congestion pricing, intelligent park meters which adapt hourly parking rates based on demand can improve the situation in terms of both cruising time and probability of finding a nearby parking space [191]. The example of San Francisco shows very positive effects by applying such a parking management strategy and a reduction of cruising time by 50 % [192].

6.4 Future Directions

As directions for future research in the field of traffic optimization we suggest to further perform investigations regarding automatic adaptation of the parameters of the routing algorithm, but also others relevant for communication. Therefor a classification of the road network, which somehow describes the characteristic features of the network, could help to select the best possible optimization strategy, also depending on current traffic volume.

Obviously, the spatial area of operation needs somehow to be limited, for both reasons performance issues and also meaningfulness of the size in terms of optimization potential. It makes no sense to extend the area of application to such a huge size so that the single hotspot areas and vehicles passing them do not have any influence to each other. For optimization of very large areas within the scale of multiple cities and also rural areas in-between or hundreds or even thousands of kilometers, clustering of particular areas to which optimization should be applied exclusively in each case is necessary. In addition, the interconnection of such clusters is suggestive and can provide advantages for long distance trips between clusters, which is another area for further investigations. A completely different approach for scalability would be the usage of distributed calculation algorithms instead of a centralized system.

Furthermore, situations could be considered where certain drivers ignore the proposed guidance, but still are able to provide information or vice versa. The reasons could be subject to the driver's current feelings, or subjectively perceived better knowledge. Also, cities must agree to alternative routes in order not to move traffic to lower level roads

within urban housing complexes. This could require a further weighting of roads, like a prioritization of potential alternative routes. This enables road operators to steer the respective drivers to better suited roads.

Besides that, future work could contain investigations with local deviations of communication network parameters due to poor signal reception or environments with different characterizations, such as urban or rural areas. In other words, detailed simulations for particular areas with specific fading characteristics can be used to determine the applicability there.

Probably the most exciting experiment in my opinion would be the validation of the proposed system in a real environment rather than simulations. As mentioned in section 3.3, this could be done either via built-in navigation systems in cars or by an external device that provides route data. Although the effort for such an experiment is definitely high, the demonstration of PCMA* in real-life makes the system more tangible, and probably gains a lot more attention in the end.

Overall, apart from the mentioned future work, there are still a great number of research questions open in the interesting field of traffic optimization connected with real-time applicability as well as utilization in non-ideal environments.

List of Acronyms

2G 2nd Generation

3G 3rd Generation

3GPP 3rd Generation Partnership Project

4G 4th Generation

ACC Adaptive Cruise Control

ADT Average Daily Traffic

ARQ Automatic Repeat Request

ATM Advanced Traffic Management

BER Bit Error Rate

BS Base Station

CAH Constant-Acceleration Heuristic

CAM Cooperative Awareness Message

C-ITS Cooperative Intelligent Transport Systems

CLLxt Cooperative Lane Change and Longitudinal Behavior Model Extension

CSMA Carrier Sense Multiple Access

DENM Decentralized Environmental Notification Message

DMRS Demodulation Reference Signal

DSRC Dedicated Short Range Communication

- DTA** Dynamic Traffic Assignment
- EDGE** Enhanced Data Rates for GSM Evolution
- EIDM** Extended Intelligent Driver Model
- ETSI** European Telecommunications Standards Institute
- FBkSP** Flow Balanced k-Shortest Paths
- FCD** Floating Car Data
- FDD** Frequency Division Duplex
- FEC** Forward Error Correction
- FER** Frame Error Rate
- GE** Gilbert-Elliot
- GS** Greenshield's Model
- GSM** Global System for Mobile Communications
- HSPA** High Speed Packet Access
- IAI** Inter-Arrival Interval
- ICT** Information and Communication Technology
- IDM** Intelligent Driver Model
- IEEE** Institute of Electrical and Electronics Engineers
- ITS** Intelligent Transportation System
- KSP** k-Shortest Paths
- LTE** Long Term Evolution
- LTE-A** LTE Advanced
- LTE-U** LTE in unlicensed spectrum
- MAC** Medium Access Control
- MBMS** Multimedia Broadcast Multicast Service
- MCS** Modulation and Coding Scheme
- MIMO** Multiple-Input-Multiple-Output

MOBIL	Minimizing Overall Braking Induced by Lane Changes
MS	Mobile Station
nemo	Networks and Mobility
ODMsg	On-Demand Message
OFDMA	Orthogonal Frequency-division Multiple Access
OSM	OpenStreetMap
PCMA*	Predictive Congestion Minimization in combination with an A*-based Router
PDF	Probability Density Function
PHY	Physical Layer
PMF	Probability Mass Function
PMsg	Periodic Message
QGis	Quantum Geographic Information System
RS	Road Segment
RTT	Roundtrip Time
SA	Speed Average Model
SC-FDMA	Single-carrier Frequency-division Multiple Access
TDD	Time Division Duplex
TTI	Transmission Time Interval
UAS	University of Applied Sciences
UMTS	Universal Mobile Telecommunications System
V2I	Vehicle-to-Infrastructure
V2V	Vehicle-to-Vehicle
V2X	Vehicle-to-Everything
VANET	Vehicular Ad-hoc Network
VHT	Vehicle Hours Traveled
VMT	Vehicle Miles Traveled

WAVE Wireless Access for Vehicular Environments

WLAN Wireless LAN

List of Symbols

K_{RS}	$[m^{-1}]$	current vehicle density per RS	40
K_{jam}	$[m^{-1}]$	maximum possible vehicle density	40
NV		number of vehicles per road segment	39–41
$P_i^{(S)}$		summarized node footprint for node i	41, 43, 45
R_{eval}	$[s]$	range of future evaluation	41, 42
Δt	$[s]$	discretization time interval for footprint	41–46, 64–66, 72, 75, 77
η_s		route distance threshold	47, 75–77, 90
η_t		route time threshold	47, 75–77, 90
λ		parameter for geometric distribution of message delay	65, 66, 96–102
$\overline{len_V}$		average vehicle length	40
$\theta^{(P)}$	$[veh./s]$	congestion threshold for the prediction algorithm	45, 48, 77
$\theta_{GS}^{(R)}$		reactive congestion detection threshold with GS method	40, 75, 76
$\theta_{SA}^{(R)}$		reactive congestion detection threshold with SA method	40, 75, 76
gap_{min}	$[m]$	minimum gap between vehicles	40
len_{RS}	$[m]$	length of a road segment	37, 40, 42
$t_{p,RS}$	$[s]$	passage time for a road segment	42
t_{travel}	$[s]$	overall travel time for a vehicle	42
$v_{RS,GS}$	$[m/s]$	road segment speed, estimated with GS method	40
$v_{RS,SA}$	$[m/s]$	road segment speed, estimated with SA method	39
v_{RS}	$[m/s]$	estimated average road segment speed	40, 42

v_{max}	[m/s]	speed limit	37, 39, 40
$w_{RS,GS}$		weight of a road segment with GS averaging	40
$w_{RS,SA}$		weight of a road segment with SA averaging	39, 40
w_{RS}		weight of a road segment	37, 39

Bibliography

- [1] W. H. Frey. A Big City Growth Revival? [Online]. Available: [Link ↗](#) (visited on 2015-03-26). 2
- [2] United Nations, “World Population 2015,” *Department of Economic and Social Affairs, Population Division*, no. ST/ESA/SER.A/378, 2015. [Online]. Available: [Link ↗](#) 2
- [3] United Nations, “World Urbanization Prospects, the 2014 Revision,” *Department of Economic and Social Affairs*, 2014. 2
- [4] D. Schrank, B. Eisele, T. Lomax, and J. Bak, “2015 Urban Mobility Scorecard,” *Texas A&M Transportation Institute*, Aug. 2015. [Online]. Available: [Link ↗](#) (visited on 2017-04-14). 2
- [5] G. Cookson and B. Pishue, “INRIX Global Traffic Scorecard,” *INRIX*, Feb. 2017. [Online]. Available: [Link ↗](#) (visited on 2017-04-14). 2
- [6] OÖN. Das steckt hinter dem Zahlenspiel mit den Tempolimits auf der Westautobahn. [Online]. Available: [Link ↗](#) (visited on 2017-04-14). 2
- [7] G. Laporte, P. Toth, and D. Vigo, “Vehicle routing: historical perspective and recent contributions,” *EURO Journal on Transportation and Logistics*, vol. 2, no. 1, pp. 1–4, 2013. [Online]. Available: [Link ↗](#) 3
- [8] J. Calvo-Gallego and F. Perez-Martinez, “Simple traffic surveillance system based on range-doppler radar images,” *Progress In Electromagnetics Research*, vol. 125, pp. 343–364, 2012. 3
- [9] X. Yan, H. Zhang, and C. Wu, “Research and Development of Intelligent Transportation Systems,” in *2012 11th International Symposium on Distributed Computing and Applications to Business, Engineering Science (DCABES)*, Oct. 2012, pp. 321–327. 3
- [10] “The bright side of sitting in traffic: Crowdsourcing road congestion data.” [Online]. Available: [Link ↗](#) (visited on 2015-05-06). 3
- [11] “How Google Tracks Traffic.” [Online]. Available: [Link ↗](#) (visited on 2015-05-06). 3
- [12] “TomTom Traffic.” [Online]. Available: [Link ↗](#) (visited on 2015-04-14). 3
- [13] J. Markoff, “Microsoft Introduces Tool for Avoiding Traffic Jams,” *The New York Times*, Apr. 2008. [Online]. Available: [Link ↗](#) (visited on 2015-07-01). 3
- [14] “Bing Maps provides more accurate trip times worldwide | Maps Blog.” [Online]. Available: [Link ↗](#) (visited on 2015-07-01). 3

- [15] V. Goel, "Google Expands Its Boundaries, Buying Waze for \$1 Billion." [Online]. Available: [Link ↗](#) (visited on 2017-04-27). 3
- [16] J. Heidenwag, P. Niethammer, and T. Sanwald, "Übersicht und Evaluation am Markt erhältlicher Routenplaner auf Web- bzw. Android-Plattform," *Online Publikationen der Universität Stuttgart*, 2013. [Online]. Available: [Link ↗](#) (visited on 2017-05-04). 3
- [17] C. Backfrieder, G. Ostermayer, and C. F. Mecklenbräuker, "Increased Traffic Flow Through Node-Based Bottleneck Prediction and V2x Communication," *IEEE Transactions on Intelligent Transportation Systems*, vol. 18, no. 2, pp. 349–363, Feb. 2017. 3, 4, 10, 36
- [18] (2017, 01) Connected cars by the numbers. [Online]. Available: [Link ↗](#) 4
- [19] Z. Hameed Mir and F. Filali, "LTE and IEEE 802.11p for vehicular networking: a performance evaluation," *EURASIP Journal on Wireless Communications and Networking*, vol. 2014, no. 1, p. 89, 2014. [Online]. Available: [Link ↗](#) (visited on 2016-04-26). 4, 58
- [20] A. Aw and M. Rascle, "Resurrection of" second order" models of traffic flow," *SIAM journal on applied mathematics*, vol. 60, no. 3, pp. 916–938, 2000. [Online]. Available: [Link ↗](#) (visited on 2017-05-04). 5
- [21] D. Helbing and M. Treiber, "Gas-kinetic-based traffic model explaining observed hysteretic phase transition," *Physical Review Letters*, vol. 81, no. 14, p. 3042, 1998. [Online]. Available: [Link ↗](#) (visited on 2017-05-04). 5
- [22] G. Duranton and M. A. Turner, "The fundamental law of highway congestion: Evidence from the US," *Processed, University of Toronto*, 2008. [Online]. Available: [Link ↗](#) (visited on 2017-05-04). 5, 110
- [23] M. Hansen and Y. Huang, "Road supply and traffic in california urban areas," *Transportation Research Part A: Policy and Practice*, vol. 31, no. 3, pp. 205–218, 1997. [Online]. Available: [Link ↗](#) 5, 6, 7, 8
- [24] D. Levinson and A. Kumar, "Activity, travel, and the allocation of time," *Journal of the American Planning Association*, vol. 61, no. 4, pp. 458–470, 1995. [Online]. Available: [Link ↗](#) (visited on 2017-05-04). 5
- [25] T. Litman, "Generated traffic and induced travel," *Victoria Transport Policy Institute*, vol. 22, 2001. [Online]. Available: [Link ↗](#) (visited on 2017-04-21). 5, 6
- [26] S. Handy and M. G. Boarnet, "Impact of Highway Capacity and Induced Travel on Passenger Vehicle Use and Greenhouse Gas Emissions," *California Environmental Protection Agency, Air Resources Board, Retrieved August*, vol. 28, p. 2015, 2014. [Online]. Available: [Link ↗](#) (visited on 2017-05-04). 5, 7
- [27] A. Downs, "The law of peak-hour expressway congestion," *Traffic Quarterly*, vol. 16, no. 3, 1962. [Online]. Available: [Link ↗](#) 5
- [28] K. M. Hymel, K. A. Small, and K. Van Dender, "Induced demand and rebound effects in road transport," *Transportation Research Part B: Methodological*, vol. 44, no. 10, pp. 1220–1241, 2010. [Online]. Available: [Link ↗](#) 6, 7
- [29] L. M. Fulton, R. B. Noland, D. J. Meszler, and J. V. Thomas, "A statistical analysis of induced travel effects in the US mid-atlantic region," *Journal of Transportation and Statistics*, vol. 3, no. 1, pp. 1–14, 2000. 6, 7

- [30] R. B. Noland, "Relationships between highway capacity and induced vehicle travel," *Transportation Research Part A: Policy and Practice*, vol. 35, no. 1, pp. 47–72, 2001. [Online]. Available: [Link ↗](#) (visited on 2017-05-04). 6, 7
- [31] R. B. Noland and W. A. Cowart, "Analysis of metropolitan highway capacity and the growth in vehicle miles of travel," *Transportation*, vol. 27, no. 4, pp. 363–390, 2000. [Online]. Available: [Link ↗](#) 6, 7
- [32] C. J. Rodier, J. E. Abraham, R. A. Johnston, and J. D. Hunt, "Anatomy of induced travel using an integrated land use and transportation model in the sacramento region," in *80th Annual Meeting of the Transportation Research Board, Washington, DC*, 2001. 6, 7
- [33] R. Cervero, "Road expansion, urban growth, and induced travel: A path analysis," *Journal of the American Planning Association*, vol. 69, no. 2, pp. 145–163, 2003. [Online]. Available: [Link ↗](#) 7
- [34] R. G. Schiffer, M. W. Steinvorth, and R. T. Milam, "Comparative evaluations on the elasticity of travel demand," in *TRB 2005 Annual Meeting, Washington, DC*, 2005. 7, 8
- [35] European Commission, "TRACE-elasticity handbook: Elasticities for prototypical contexts (deliverable 5), costs of private road travel and their effects on demand, including short and long term elasticities, prepared for the european commission, directorate-general for transport," *Contract No: RO-97-SC*, vol. 2035, 1999. [Online]. Available: [Link ↗](#) 7
- [36] T. Litman, "Understanding transport demands and elasticities," *How prices and other factors affect travel behavior. (Victoria Transport Policy Institute: Litman) Available at http://www.vtpi.org/elasticities.pdf [Verified 22 November 2013]*, 2013. 7
- [37] D. Lee Jr, L. Klein, and G. Camus, "Induced traffic and induced demand," *Transportation Research Record: Journal of the Transportation Research Board*, no. 1659, pp. 68–75, 1999. 7
- [38] M. Hansen, D. Gillen, A. Dobbins, Y. Huang, and M. Puvathingal, "The air quality impacts of urban highway capacity expansion: Traffic generation and land use change," *University of California Transportation Center*, 1993. [Online]. Available: [Link ↗](#) (visited on 2017-05-04). 7, 9
- [39] N. L. Marshall, "Evidence of induced demand in the texas transportation institute's urban roadway congestion study data set," in *Transportation Research Board 79th Annual Meeting Preprint CD-ROM, Transportation Research Board, National Research Council, Washington DC*, 2000. 7
- [40] R. Cervero and M. Hansen, *Road Supply-Demand Relationships: Sorting Out Casual Linkages*. University of California Transportation Center, 2000. 7
- [41] J. G. Strathman, K. Dueker, T. W. Sanchez, J. Zhang, and A.-E. Riis, "Analysis of induced travel in the 1995 NPTS," in *Center for Urban Studies Publications and Reports*, 2000. [Online]. Available: [Link ↗](#) 7
- [42] P. L. Mokhtarian, F. J. Samaniego, R. H. Shumway, and N. H. Willits, "Revisiting the notion of induced traffic through a matched-pairs study," *Transportation*, vol. 29, no. 2, pp. 193–220, 2002. [Online]. Available: [Link ↗](#) (visited on 2017-05-05). 7, 9
- [43] R. Cervero, "Induced travel demand: Research design, empirical evidence, and normative policies," *CPL bibliography*, vol. 17, no. 1, pp. 3–20, 2002. 7

- [44] R. B. Noland and L. L. Lem, “A review of the evidence for induced travel and changes in transportation and environmental policy in the US and the UK,” *Transportation Research Part D: Transport and Environment*, vol. 7, no. 1, pp. 1–26, 2002. 7
- [45] M. Hansen, “Do new highways generate traffic?” *ACCESS Magazine*, vol. 1, no. 7, 1995. [Online]. Available: [Link ↗](#) (visited on 2017-05-05). 8
- [46] C. Backfrieder, C. F. Mecklenbrauker, and G. Ostermayer, “TraffSim – A Traffic Simulator for Investigating Benefits Ensuing from Intelligent Traffic Management,” in *Modelling Symposium (EMS), 2013 European*. IEEE, 2013, pp. 451–456. [Online]. Available: [Link ↗](#) (visited on 2017-05-04). 10
- [47] C. Backfrieder, G. Ostermayer, and C. Mecklenbräuker, “Extended from EMS2013: TraffSim – a traffic simulator for investigations of congestion minimization through dynamic vehicle rerouting,” *International Journal of Simulation Systems, Science and Technology*, vol. 15, no. 15, pp. 8–13, 2015. 10, 34, 105
- [48] M. Lindorfer, C. Backfrieder, C. Kieslich, J. Krösche, and G. Ostermayer, “Environmental-Sensitive Generation of Street Networks for Traffic Simulations,” in *2013 European Modelling Symposium*, Nov. 2013, pp. 457–462. 10, 70
- [49] A. Lindenmayer, “Mathematical models for cellular interactions in development i. filaments with one-sided inputs,” *Journal of theoretical biology*, vol. 18, no. 3, pp. 280–299, 1968. 10
- [50] C. Backfrieder and G. Ostermayer, “Modeling a Continuous and Accident-Free Intersection Control for Vehicular Traffic in TraffSim,” in *2014 European Modelling Symposium*, Oct. 2014, pp. 332–337. 10, 26, 28
- [51] M. Lindorfer, C. Backfrieder, C. F. Mecklenbräuker, G. Ostermayer, and U. U. Austria, “Modeling isolated traffic control strategies in TraffSim,” in *19th International Conference on Computer Modelling and Simulation (UKSim)*. UKSim, 2017. 10
- [52] C. Backfrieder, G. Ostermayer, M. Lindorfer, and C. F. Mecklenbräuker, “Cooperative Lane-Change and Longitudinal Behaviour Model Extension for TraffSim,” in *Smart Cities*, ser. Lecture Notes in Computer Science, E. Alba, F. Chicano, and G. Luque, Eds. Springer International Publishing, Jun. 2016, pp. 52–62, doi: 10.1007/978-3-319-39595-1_6. [Online]. Available: [Link ↗](#) (visited on 2017-02-16). 10, 19, 21
- [53] C. Backfrieder, M. Lindorfer, C. F. Mecklenbräuker, and G. Ostermayer, “Effects of cooperative lane-change behavior on vehicular traffic flow,” in *International Conference on Computer Aided Systems Theory (EUROCAST)*. Springer, 2017, p. Accepted for Publication. 10
- [54] C. Backfrieder, M. Lindorfer, C. F. Mecklenbräuker, and G. Ostermayer, “Impact of varying penetration rate of intelligent routing capabilities on vehicular traffic flow,” in *Vehicular Technology Conference (VTC-Fall), 2017 IEEE 86th*. IEEE, 2017, p. Accepted for Publication. 10
- [55] C. Backfrieder, M. Lindorfer, C. F. Mecklenbräuker, and G. Ostermayer, “Robustness of intelligent vehicular rerouting towards non-ideal communication delay,” in *Future of Information and Communication Conference (FICC)*. SAI Conferences, 2018, p. Accepted for Publication. 10
- [56] C. Backfrieder and G. Ostermayer, “Analysis of an Adaptive Switching Point for LTE TDD by Dynamic System-Level Simulations,” *International Journal of Electronics and Telecommunications*, vol. 61, no. 2, pp. 171–178, 2015. [Online]. Available: [Link ↗](#) (visited on 2017-05-04). 10

- [57] T. Blazek, C. Backfrieder, C. Mecklenbräuker, and G. Ostermayer, “Improving communication reliability in intelligent transport systems through cooperative driving,” in *10th IFIP Wireless and Mobile Networking Conference (WMNC)*, IEEE, Ed., 2017, talk: 10th IFIP Wireless and Mobile Networking Conference (WMNC), Valencia; 2017-09-25 – 2017-09-27. 11
- [58] B. Werth, E. Pitzer, M. Affenzeller, and C. Backfrieder, “Parameter selection for PCMA* using surrogate-assisted black-box optimization and microscopic traffic simulation,” *Proceedings of EMSS 2017*, pp. 117–124, 2017. [Online]. Available: [Link ↗](#) (visited on 2017-11-24). 11
- [59] T. Blazek, G. Ghiaasi, C. Backfrieder, G. Ostermayer, and C. Mecklenbräuker, “Ieee 802.11p performance for vehicle-to-anything connectivity in urban interference channels,” in *European Conference on Antennas and Propagation (EuCAP)*. SAI Conferences, 2018, p. Submitted. 11
- [60] M. Lindorfer, C. Backfrieder, C. Mecklenbräuker, and G. Ostermayer, “Driver behavior injection in microscopic traffic simulations,” in *Asian Simulation Conference*. Springer, 2017, pp. 237–248. 11
- [61] N. T. Ratrout and S. M. Rahman, “A comparative analysis of currently used microscopic and macroscopic traffic simulation software,” *The Arabian Journal for Science and Engineering*, vol. 34, no. 1B, pp. 121–133, 2009. [Online]. Available: [Link ↗](#) (visited on 2017-05-05). 14, 25
- [62] D. Helbing, “From microscopic to macroscopic traffic models,” *A perspective look at nonlinear media*, pp. 122–139, 1998. [Online]. Available: [Link ↗](#) (visited on 2017-05-05). 14
- [63] J. Hueper, G. Dervisoglu, A. Muralidharan, G. Gomes, R. Horowitz, and P. Varaiya, “Macroscopic modeling and simulation of freeway traffic flow,” *IFAC Proceedings Volumes*, vol. 42, no. 15, pp. 112–116, 2009. [Online]. Available: [Link ↗](#) (visited on 2017-05-10). 14
- [64] D. Helbing, “Derivation and empirical validation of a refined traffic flow model,” *Physica A: Statistical mechanics and its applications*, vol. 233, no. 1-2, pp. 253–282, 1996. [Online]. Available: [Link ↗](#) (visited on 2017-05-10). 14
- [65] D. Helbing, A. Hennecke, V. Shvetsov, and M. Treiber, “Micro-and macro-simulation of freeway traffic,” *Mathematical and computer modelling*, vol. 35, no. 5-6, pp. 517–547, 2002. [Online]. Available: [Link ↗](#) (visited on 2017-05-05). 14
- [66] M. Bando, K. Hasebe, K. Nakanishi, A. Nakayama, A. Shibata, and Y. Sugiyama, “Phenomenological study of dynamical model of traffic flow,” *Journal de Physique I*, vol. 5, no. 11, pp. 1389–1399, 1995. [Online]. Available: [Link ↗](#) (visited on 2017-05-10). 14
- [67] C. F. Daganzo, “Requiem for second-order fluid approximations of traffic flow,” *Transportation Research Part B: Methodological*, vol. 29, no. 4, pp. 277–286, 1995. [Online]. Available: [Link ↗](#) (visited on 2017-05-10). 14
- [68] K. Erlemann, “Objektorientierte mikroskopische Verkehrsflusssimulation,” Ph.D. dissertation, Ruhr-Universität Bochum, 2007. [Online]. Available: [Link ↗](#) (visited on 2017-05-11). 15
- [69] Staffan Algers, Eric Bernauer, Marco Boero, Laurent Breheret, Carlo Di Taranto, Mark Dougherty, Ken Fox, and Jean-François Gabard, “SMARTTEST Project - Review of Micro-Simulation Models,” European Commission, Project Deliverable D3, Aug. 1997. [Online]. Available: [Link ↗](#) (visited on 2017-05-11). 15

- [70] M. Treiber and A. Kesting, *Traffic Flow Dynamics*. Berlin, Heidelberg: Springer Berlin Heidelberg, 2013. [Online]. Available: [Link ↗](#) (visited on 2015-04-27). 15, 16, 18, 21, 22, 23, 24, 25
- [71] A. Kesting, M. Treiber, and D. Helbing, “Enhanced intelligent driver model to access the impact of driving strategies on traffic capacity,” *Philosophical Transactions of the Royal Society A: Mathematical, Physical and Engineering Sciences*, vol. 368, no. 1928, pp. 4585–4605, Oct. 2010. [Online]. Available: [Link ↗](#) (visited on 2013-06-05). 15, 17
- [72] D. Helbing, M. Treiber, A. Kesting, and M. Schönhof, “Theoretical vs. empirical classification and prediction of congested traffic states,” *The European Physical Journal B-Condensed Matter and Complex Systems*, vol. 69, no. 4, pp. 583–598, 2009. [Online]. Available: [Link ↗](#) (visited on 2017-05-11). 16
- [73] A. K. Martin Treiber, “Modeling lane-changing decisions with MOBIL,” *Traffic and Granular Flow 2007*, pp. 211–221, 2009. 17, 18
- [74] M. Rahman, M. Chowdhury, Y. Xie, and Y. He, “Review of Microscopic Lane-Changing Models and Future Research Opportunities,” *IEEE Transactions on Intelligent Transportation Systems*, vol. 14, no. 4, pp. 1942–1956, Dec. 2013. 19
- [75] C. C. Caprani, E. J. O’Brien, and A. Lipari, “Extension of a lane-changing model to a micro-simulation tool,” *Proceedings of the Irish Transport Research Network 2011, Cork, 31 August-1 September 2011*, 2011. 19
- [76] B. Heißing and M. Ersoy, *Chassis Handbook: Fundamentals, Driving Dynamics, Components, Mechatronics, Perspectives*. Springer Science & Business Media, Nov. 2010. 22
- [77] M. T. Oliver-Hoyo and G. Pinto, “Using the relationship between vehicle fuel consumption and CO₂ emissions to illustrate chemical principles,” *Journal of Chemical Education*, vol. 85, no. 2, pp. 218–220, 2008. 23
- [78] J. J. Klemeš, *Assessing and measuring environmental impact and sustainability*. Butterworth-Heinemann, 2015. 23
- [79] E. Brockfeld, R. Kühne, and P. Wagner, “Calibration and validation of microscopic traffic flow models,” *Transportation Research Record: Journal of the Transportation Research Board*, no. 1876, pp. 62–70, 2004. 24
- [80] A. Kesting and M. Treiber, “Calibrating car-following models by using trajectory data: Methodological study,” *Transportation Research Record: Journal of the Transportation Research Board*, no. 2088, pp. 148–156, 2008. 24
- [81] M. Treiber and A. Kesting, “Microscopic calibration and validation of car-following models—a systematic approach,” *Procedia-Social and Behavioral Sciences*, vol. 80, pp. 922–939, 2013. 24
- [82] A. Kesting, M. Treiber, and D. Helbing, “General lane-changing model MOBIL for car-following models,” *Transportation Research Record: Journal of the Transportation Research Board*, no. 1999, pp. 86–94, 2007. 24
- [83] W. Schakel, V. Knoop, and B. van Arem, “Integrated lane change model with relaxation and synchronization,” *Transportation Research Record: Journal of the Transportation Research Board*, no. 2316, pp. 47–57, 2012. 24
- [84] M. Pursula, “Simulation of traffic systems—an overview,” *Journal of Geographic Information and Decision Analysis*, vol. 3, no. 1, pp. 1–8, 1999. [Online]. Available: [Link ↗](#) (visited on 2017-05-29). 25

-
- [85] “MATLAB MAT-file Format.” [Online]. Available: [Link ↗](#) (visited on 2017-05-24). 26
- [86] “MATLAB - MathWorks.” [Online]. Available: [Link ↗](#) (visited on 2017-05-24). 26
- [87] “JOSM - an extensible editor for OpenStreetMap.” [Online]. Available: [Link ↗](#) (visited on 2017-05-24). 29, 70
- [88] “OSM Wiki - Tags.” [Online]. Available: [Link ↗](#) (visited on 2017-05-30). 29
- [89] E. W. Dijkstra, “A note on two problems in connexion with graphs,” *Numerische mathematik*, vol. 1, no. 1, pp. 269–271, 1959. [Online]. Available: [Link ↗](#) 32
- [90] P. E. Hart, N. J. Nilsson, and B. Raphael, “A formal basis for the heuristic determination of minimum cost paths,” *IEEE transactions on Systems Science and Cybernetics*, vol. 4, no. 2, pp. 100–107, 1968. [Online]. Available: [Link ↗](#) 32
- [91] W. Jianjun, Q. Liping, H. Qianqian, and Y. Fashun, “Quasi-dynamic Traffic Assignment Method Based on Traffic Control Strategy under Freeway Net,” in *2010 International Conference on Intelligent Computation Technology and Automation (ICICTA)*, vol. 2, May 2010, pp. 959–962. 32, 73
- [92] M. Carey, “Nonconvexity of the dynamic traffic assignment problem,” *Transportation Research Part B: Methodological*, vol. 26, no. 2, pp. 127–133, Apr. 1992. 32, 73
- [93] B. N. Janson, “Dynamic traffic assignment for urban road networks,” *Transportation Research Part B: Methodological*, vol. 25, no. 2, pp. 143–161, Apr. 1991. 32
- [94] A. Haurie and P. Marcotte, “On the relationship between nash-cournot and wardrop equilibria,” *Networks*, vol. 15, no. 3, pp. 295–308, 1985. [Online]. Available: [Link ↗](#) 32
- [95] I. Skog and P. Handel, “In-Car Positioning and Navigation Technologies #x2014;A Survey,” *IEEE Transactions on Intelligent Transportation Systems*, vol. 10, no. 1, pp. 4–21, Mar. 2009. 33
- [96] W. Chen, L. Chen, Z. Chen, and S. Tu, “WITS: A Wireless Sensor Network for Intelligent Transportation System,” in *First International Multi-Symposiums on Computer and Computational Sciences, 2006. IMSCCS '06*, vol. 2, Jun. 2006, pp. 635–641. 33, 91
- [97] M. Yamaguchi, T. Kitamura, S. Jinno, and T. Tajima, “The interactive CDRG using infrared beacons,” in *1999 IEEE/IEEJ/JSAI International Conference on Intelligent Transportation Systems, 1999. Proceedings, 1999*, pp. 278–283. 33
- [98] D. Hung, K.-Y. Lam, E. Chan, and K. Ramamritham, “Processing of location-dependent continuous queries on real-time spatial data: the view from RETINA,” in *14th International Workshop on Database and Expert Systems Applications, 2003. Proceedings, Sep. 2003*, pp. 961–965. 33
- [99] J. Rice and E. van Zwet, “A simple and effective method for predicting travel times on freeways,” *IEEE Transactions on Intelligent Transportation Systems*, vol. 5, no. 3, pp. 200–207, Sep. 2004. 33
- [100] D. F. Sangsoo Lee, “Application of Subset Autoregressive Integrated Moving Average Model for Short-Term Freeway Traffic Volume Forecasting,” *Transportation Research Record*, vol. 1678, no. 1, pp. 179–188, 1999. 33

- [101] A. Stathopoulos and M. G. Karlaftis, "A multivariate state space approach for urban traffic flow modeling and prediction," *Transportation Research Part C: Emerging Technologies*, vol. 11, no. 2, pp. 121–135, Apr. 2003, (visited on 2014-11-11). 33
- [102] B. Ghosh, B. Basu, and M. O'Mahony, "Multivariate Short-Term Traffic Flow Forecasting Using Time-Series Analysis," *IEEE Transactions on Intelligent Transportation Systems*, vol. 10, no. 2, pp. 246–254, Jun. 2009. 33
- [103] Y.-A. Daraghmi, C.-W. Yi, and T.-C. Chiang, "Negative Binomial Additive Models for Short-Term Traffic Flow Forecasting in Urban Areas," *IEEE Transactions on Intelligent Transportation Systems*, vol. 15, no. 2, pp. 784–793, Apr. 2014. 33, 58
- [104] Y. Kamarianakis and P. Prastacos, "Forecasting Traffic Flow Conditions in an Urban Network: Comparison of Multivariate and Univariate Approaches," *Transportation Research Record*, vol. 1857, no. 1, pp. 74–84, Jan. 2003, (visited on 2014-11-11). 33
- [105] S. Sun, C. Zhang, and G. Yu, "A bayesian network approach to traffic flow forecasting," *IEEE Transactions on Intelligent Transportation Systems*, vol. 7, no. 1, pp. 124–132, Mar. 2006. 33
- [106] B. Zhang, K. Xing, X. Cheng, L. Huang, and R. Bie, "Traffic clustering and online traffic prediction in vehicle networks: A social influence perspective," in *2012 Proceedings IEEE INFOCOM*, Mar. 2012, pp. 495–503. 33
- [107] M. Gramaglia, M. Calderon, and C. Bernardos, "ABEONA Monitored Traffic: VANET-Assisted Cooperative Traffic Congestion Forecasting," *IEEE Vehicular Technology Magazine*, vol. 9, no. 2, pp. 50–57, Jun. 2014. 33, 58
- [108] J. Pan, I. Popa, K. Zeitouni, and C. Borcea, "Proactive Vehicular Traffic Rerouting for Lower Travel Time," *IEEE Transactions on Vehicular Technology*, vol. 62, no. 8, pp. 3551–3568, Oct. 2013. 34, 37, 40, 73, 74, 91, 106
- [109] T. Atomode, "Assessment of Traffic Delay Problems and Characteristics at Urban Road Intersections: A Case Study of Ilorin, Nigeria." *IOSR Journal Of Humanities And Social Science*, vol. 12, no. 4, pp. 06–16, 2013. 36, 44
- [110] J. Y. Yen, "Finding the K shortest loopless paths in a network," *Management Science*, vol. 17, pp. 712–716, 1971. 37
- [111] V. Akgün, E. Erkut, and R. Batta, "On finding dissimilar paths," *European Journal of Operational Research*, vol. 121, no. 2, pp. 232 – 246, 2000. 37
- [112] Y. Lim and H. Kim, "A shortest path algorithm for real road network based on path overlap," *Journal of the Eastern Asia Society for Transportation Studies*, vol. 6, pp. 1426–1438, 2005. 37
- [113] L. Yun and Z. Shengrui, "Analysis on Actual Capacity of Long Tunnel by Using Greenshields Model," in *2012 International Conference on Connected Vehicles and Expo (ICCVE)*, Dec. 2012, pp. 252–255. 40
- [114] D. Chen, J. Zhang, S. Tang, and J. Wang, "Freeway traffic stream modeling based on principal curves and its analysis," *IEEE Transactions on Intelligent Transportation Systems*, vol. 5, no. 4, pp. 246–258, Dec. 2004. 40
- [115] B. D. Greenshields, "A study of traffic capacity," in *Proceedings of the highway research board*, vol. 14, 1935, pp. 448–477. 40, 73, 75

-
- [116] P. Papadimitratos, A. D. L. Fortelle, K. Evenssen, R. Brignolo, and S. Cosenza, "Vehicular communication systems: Enabling technologies, applications, and future outlook on intelligent transportation," *IEEE Communications Magazine*, vol. 47, no. 11, pp. 84–95, Nov. 2009. 52
- [117] K. Dar, M. Bakhouya, J. Gaber, M. Wack, and P. Lorenz, "Wireless communication technologies for ITS applications [Topics in Automotive Networking]," *IEEE Communications Magazine*, vol. 48, no. 5, pp. 156–162, May 2010. 52
- [118] C. F. Mecklenbrauker, A. F. Molisch, J. Karedal, F. Tufvesson, A. Paier, L. Bernadó, T. Zemen, O. Klemp, and N. Czink, "Vehicular channel characterization and its implications for wireless system design and performance," *Proceedings of the IEEE*, vol. 99, no. 7, pp. 1189–1212, 2011. [Online]. Available: [Link ↗](#) 53, 59, 60
- [119] V. D. Khairnar and K. Kotecha, "Performance of vehicle-to-vehicle communication using IEEE 802.11 p in vehicular ad-hoc network environment," *arXiv preprint arXiv:1304.3357*, 2013. [Online]. Available: [Link ↗](#) 53, 56
- [120] K. Bilstrup, *A survey regarding wireless communication standards intended for a high-speed vehicle environment*. Halmstad University, 2007. [Online]. Available: [Link ↗](#) 53, 58
- [121] D. Jiang and L. Delgrossi, "IEEE 802.11 p: Towards an international standard for wireless access in vehicular environments," in *Vehicular Technology Conference, 2008. VTC Spring 2008. IEEE*. IEEE, 2008, pp. 2036–2040. [Online]. Available: [Link ↗](#) 54
- [122] J. B. Kenney, "Dedicated short-range communications (DSRC) standards in the United States," *Proceedings of the IEEE*, vol. 99, no. 7, pp. 1162–1182, 2011. [Online]. Available: [Link ↗](#) 54
- [123] J. Kunisch and J. Pamp, "Wideband car-to-car radio channel measurements and model at 5.9 GHz," in *Vehicular Technology Conference, 2008. VTC 2008-Fall. IEEE 68th*. IEEE, 2008, pp. 1–5. [Online]. Available: [Link ↗](#) 54
- [124] A. Paier, R. Tresch, A. Alonso, D. Smely, P. Meckel, Y. Zhou, and N. Czink, "Average downstream performance of measured IEEE 802.11 p infrastructure-to-vehicle links," in *Communications Workshops (ICC), 2010 IEEE International Conference on*. IEEE, 2010, pp. 1–5. [Online]. Available: [Link ↗](#) 54
- [125] M. A. Ingram, "Six time-and frequency-selective empirical channel models for vehicular wireless LANs," *IEEE Vehicular Technology Magazine*, vol. 2, no. 4, pp. 4–11, 2007. [Online]. Available: [Link ↗](#) 54
- [126] A. Paier, J. Karedal, N. Czink, H. Hofstetter, C. Dumard, T. Zemen, F. Tufvesson, A. F. Molisch, and C. F. Mecklenbrauker, "Car-to-car radio channel measurements at 5 GHz: Pathloss, power-delay profile, and delay-Doppler spectrum," in *Wireless Communication Systems, 2007. ISWCS 2007. 4th International Symposium on*. IEEE, 2007, pp. 224–228. [Online]. Available: [Link ↗](#) 54
- [127] project - DRIVE C2x. [Online]. Available: [Link ↗](#) (visited on 2017-06-22). 54
- [128] simTD - Sichere Intelligente Mobilität Testfeld Deutschland. [Online]. Available: [Link ↗](#) (visited on 2017-06-22). 54
- [129] Intelligent Transportation Systems - Connected Vehicle Safety Pilot. [Online]. Available: [Link ↗](#) (visited on 2017-06-22). 54
- [130] 3GPP, "Release 12." [Online]. Available: [Link ↗](#) (visited on 2017-06-23). 54

-
- [131] 3GPP, “Release 14.” [Online]. Available: [Link ↗](#) (visited on 2017-06-23). 54, 58
- [132] Dino Flore, “Initial Cellular V2x standard completed.” [Online]. Available: [Link ↗](#) (visited on 2017-06-23). 54
- [133] H. Holma and A. Toskala, *LTE for UMTS: Evolution to LTE-Advanced*. John Wiley & Sons, May 2011. 55
- [134] 3GPP, “LTE Overview.” [Online]. Available: [Link ↗](#) (visited on 2017-06-23). 55
- [135] Jeanette Wannstrom, “LTE-Advanced,” Jun. 2013. [Online]. Available: [Link ↗](#) (visited on 2017-06-23). 55
- [136] G. Araniti, C. Campolo, M. Condoluci, A. Iera, and A. Molinaro, “LTE for vehicular networking: a survey,” *IEEE Communications Magazine*, vol. 51, no. 5, pp. 148–157, 2013. [Online]. Available: [Link ↗](#) 56
- [137] E. ETSI, “302 665 v1. 1.1: Intelligent transport systems (ITS),” *Communications architecture*, 2010. 56
- [138] L. C. Tung and M. Gerla, “LTE resource scheduling for vehicular safety applications,” in *2013 10th Annual Conference on Wireless On-demand Network Systems and Services (WONS)*, Mar. 2013, pp. 116–118. 57
- [139] W. Chen, *Vehicular Communications and Networks: Architectures, Protocols, Operation and Deployment*. Elsevier, Mar. 2015. 57
- [140] B. S. Kerner, C. Demir, R. G. Herrtwich, S. L. Klenov, H. Rehborn, M. Aleksic, and A. Haug, “Traffic state detection with floating car data in road networks,” in *Intelligent Transportation Systems, 2005. Proceedings. 2005 IEEE*. IEEE, 2005, pp. 44–49. [Online]. Available: [Link ↗](#) 57
- [141] Alessio Filippi, Kees Moerman, Gerardo Daalderop, Paul D. Alexander, Franz Schober, and Werner Pfliegl, “Why 802.11p beats LTE and 5g for V2x,” Apr. 2016. [Online]. Available: [Link ↗](#) (visited on 2017-06-22). 57
- [142] P. Cerwall, *Ericsson mobility report, mobile world congress edition*. Ericsson, June 2016. 57
- [143] Z. Liang and Y. Wakahara, “Real-time urban traffic amount prediction models for dynamic route guidance systems,” *EURASIP Journal on Wireless Communications and Networking*, vol. 2014, no. 1, p. 85, May 2014, (visited on 2014-11-06). 58
- [144] Y. Li, W. Ren, D. Jin, P. Hui, L. Zeng, and D. Wu, “Potential Predictability of Vehicular Staying Time for Large-Scale Urban Environment,” *IEEE Transactions on Vehicular Technology*, vol. 63, no. 1, pp. 322–333, Jan. 2014. 58
- [145] K. Y. Chan, T. Dillon, and E. Chang, “An Intelligent Particle Swarm Optimization for Short-Term Traffic Flow Forecasting Using on-Road Sensor Systems,” *IEEE Transactions on Industrial Electronics*, vol. 60, no. 10, pp. 4714–4725, Oct. 2013. 58
- [146] N. Nafi, R. Khan, J. Khan, and M. Gregory, “A predictive road traffic management system based on vehicular ad-hoc network,” in *Telecommunication Networks and Applications Conference (ATNAC), 2014 Australasian*, Nov. 2014, pp. 135–140. 58
- [147] Z. Cao, S. Jiang, J. Zhang, and H. Guo, “A Unified Framework for Vehicle Rerouting and Traffic Light Control to Reduce Traffic Congestion,” *IEEE Transactions on Intelligent Transportation Systems*, vol. PP, no. 99, pp. 1–16, 2016. 58

- [148] K. Kim, M. Kwon, J. Park, and Y. Eun, "Dynamic Vehicular Route Guidance Using Traffic Prediction Information," *Mobile Information Systems*, vol. 2016, p. e3727865, Jul. 2016, (visited on 2017-05-04). 58
- [149] B. Zhang, M. Ma, C. Liu, and Y. Shu, "Delay guaranteed MDP scheduling scheme for HCCA based on 802.11p protocol in V2r environments," *International Journal of Communication Systems*, pp. n/a–n/a, Jan. 2017. 58
- [150] B. A. Zafar, S. Ouni, N. Boulila, and L. Saidane, "Communication delay guarantee for IEEE 802.11 p/wave Vehicle networks with RSU control," in *Networking, Sensing, and Control (ICNSC), 2016 IEEE 13th International Conference on*. IEEE, 2016, pp. 1–7. 58
- [151] G. C. Madueño, N. K. Pratas, C. Stefanovic, and P. Popovski, "Massive M2M access with reliability guarantees in LTE systems," in *Communications (ICC), 2015 IEEE International Conference on*. IEEE, 2015, pp. 2997–3002. [Online]. Available: [Link](#) ↗ 58
- [152] X. Chen, Z. Zhang, and C. Yuen, "Resource Allocation for Cost Minimization in Limited Feedback MU-MIMO Systems With Delay Guarantee," *IEEE Systems Journal*, vol. 9, no. 4, pp. 1229–1236, 2015. 58
- [153] D. W. Matolak, "Modeling the vehicle-to-vehicle propagation channel: A review," *Radio Science*, vol. 49, no. 9, pp. 721–736, 2014. [Online]. Available: [Link](#) ↗ 59, 60
- [154] A. Paier, J. Karedal, N. Czink, C. Dumard, T. Zemen, F. Tufvesson, A. F. Molisch, and C. F. Mecklenbräuker, "Characterization of vehicle-to-vehicle radio channels from measurements at 5.2 GHz," *Wireless personal communications*, vol. 50, no. 1, pp. 19–32, 2009. [Online]. Available: [Link](#) ↗ 59
- [155] L. Reichardt, T. Fugen, and T. Zwick, "Influence of antennas placement on car to car communications channel," in *2009 3rd European Conference on Antennas and Propagation*, Mar. 2009, pp. 630–634. 60
- [156] M. Hassan, M. M. Krunz, and I. Matta, "Markov-based channel characterization for tractable performance analysis in wireless packet networks," *IEEE Transactions on Wireless Communications*, vol. 3, no. 3, pp. 821–831, 2004. [Online]. Available: [Link](#) ↗ 60
- [157] R. B. Ertel, P. Cardieri, K. W. Sowerby, T. S. Rappaport, and J. H. Reed, "Overview of spatial channel models for antenna array communication systems," *IEEE personal communications*, vol. 5, no. 1, pp. 10–22, 1998. [Online]. Available: [Link](#) ↗ 60
- [158] S. Schwarz, J. C. Ikuno, M. Šimko, M. Tarantetz, Q. Wang, and M. Rupp, "Pushing the Limits of LTE: A Survey on Research Enhancing the Standard," *IEEE Access*, vol. 1, pp. 51–62, 2013. 60
- [159] S. Parkvall, M. Karlsson, M. Samuelsson, L. Hedlund, and B. Goransson, "Transmit diversity in WCDMA: link and system level results," in *Vehicular Technology Conference Proceedings, 2000. VTC 2000-Spring Tokyo. 2000 IEEE 51st*, vol. 2. IEEE, 2000, pp. 864–868. [Online]. Available: [Link](#) ↗ 60
- [160] W. Nie and H. Yang, "A new link level to system level simulation interface method," in *2010 International Conference on Audio, Language and Image Processing*, Nov. 2010, pp. 1311–1314. 60
- [161] A. M. Mourad, A. Guéguen, and R. Pyndiah, "Quantifying the Impact of the MC-CDMA Physical Layer Algorithms on the Downlink Capacity in a Multi-cellular Environment," in *Multi-Carrier Spread-Spectrum*. Springer, Dordrecht, 2006, pp. 109–118, doi: 10.1007/1-4020-4437-2_11. [Online]. Available: [Link](#) ↗ (visited on 2017-06-29). 60

- [162] K. Chan, *Future Communication Technology and Engineering: Proceedings of the 2014 International Conference on Future Communication Technology and Engineering (FCTE 2014), Shenzhen, China, 16-17 November 2014*. CRC Press, Mar. 2015, google-Books-ID: Oo7YCQAAQBAJ. 61
- [163] T. ETSI, “102 637-2 (V1. 2.1):” Intelligent Transport Systems (ITS),” *Vehicular Communications*, 2011. 62
- [164] E. N. Gilbert, “Capacity of a burst-noise channel,” *Bell Labs Technical Journal*, vol. 39, no. 5, pp. 1253–1265, 1960. 67
- [165] E. O. Elliott, “Estimates of error rates for codes on burst-noise channels,” *The Bell System Technical Journal*, vol. 42, no. 5, pp. 1977–1997, 1963. 67
- [166] H. S. Wang and N. Moayeri, “Finite-state markov channel-a useful model for radio communication channels,” *IEEE transactions on vehicular technology*, vol. 44, no. 1, pp. 163–171, 1995. 67, 68
- [167] J.-P. Ebert and A. Willig, “A gilbert-elliott bit error model and the efficient use in packet level simulation,” *TKN-99-002 of Technical Reports Series, TU Berlin*, 1999. 68
- [168] P. Sadeghi, R. A. Kennedy, P. B. Rapajic, and R. Shams, “Finite-state markov modeling of fading channels-a survey of principles and applications,” *IEEE Signal Processing Magazine*, vol. 25, no. 5, 2008. 68
- [169] G. Haßlinger and O. Hohlfeld, “The gilbert-elliott model for packet loss in real time services on the internet,” in *Measuring, Modelling and Evaluation of Computer and Communication Systems (MMB), 2008 14th GI/ITG Conference-*. VDE, 2008, pp. 1–15. 68
- [170] S. Frohn, S. Gübner, and C. Lindemann, “Analyzing the effective throughput in multi-hop IEEE 802.11 n networks,” *Computer Communications*, vol. 34, no. 16, pp. 1912–1921, 2011. 68
- [171] A. Lindenmayer, “Mathematical models for cellular interactions in development I. Filaments with one-sided inputs,” *Journal of Theoretical Biology*, vol. 18, no. 3, pp. 280–299, Mar. 1968, (visited on 2015-08-04). 70
- [172] OSM file formats - OpenStreetMap Wiki. [Online]. Available: [Link ↗](#) (visited on 2015-04-27). 70
- [173] Merkaartor - small OSM editor. [Online]. Available: [Link ↗](#) (visited on 2015-04-28). 70
- [174] Quantumgis - A Free and Open Source Geographic Information System. [Online]. Available: [Link ↗](#) (visited on 2015-04-28). 70
- [175] J. A. Bondy, U. S. R. Murty, and others, *Graph theory with applications*. Citeseer, 1976, vol. 290. [Online]. Available: [Link ↗](#) 71
- [176] osm2po Java Routing Library. [Online]. Available: [Link ↗](#) (visited on 2015-04-28). 71
- [177] C. Silva, T. Farias, H. C. Frey, and N. M. Roupail, “Evaluation of numerical models for simulation of real-world hot-stabilized fuel consumption and emissions of gasoline light-duty vehicles,” *Transportation Research Part D: Transport and Environment*, vol. 11, no. 5, pp. 377 – 385, 2006. 78
- [178] A. V. Aho and J. E. Hopcroft, *The Design and Analysis of Computer Algorithms*, 1st ed. Boston, MA, USA: Addison-Wesley Longman Publishing Co., Inc., 1974. 89

-
- [179] D. Schultes, "Route Planning in Road Networks," Ph.D. dissertation, Universität Fridericiana zu Karlsruhe, 2008. 89
- [180] J. Eriksson, L. Girod, B. Hull, R. Newton, S. Madden, and H. Balakrishnan, "The Pothole Patrol: Using a Mobile Sensor Network for Road Surface Monitoring," in *The Sixth Annual International conference on Mobile Systems, Applications and Services (MobiSys 2008)*, Breckenridge, U.S.A., June 2008. 91
- [181] M. Haklay and P. Weber, "OpenStreetMap: User-Generated Street Maps," *IEEE Pervasive Computing*, vol. 7, no. 4, pp. 12–18, Oct. 2008. 91
- [182] I. Skog and P. Handel, "In-Car Positioning and Navigation Technologies #x2014;A Survey," *IEEE Transactions on Intelligent Transportation Systems*, vol. 10, no. 1, pp. 4–21, Mar. 2009. 91
- [183] P. Mogensen, W. Na, I. Z. Kovács, F. Frederiksen, A. Pokhariyal, K. I. Pedersen, T. Kolding, K. Hugl, and M. Kuusela, "LTE capacity compared to the shannon bound," in *Vehicular Technology Conference, 2007. VTC2007-Spring. IEEE 65th.* IEEE, 2007, pp. 1234–1238. 102
- [184] E. Dahlman, S. Parkvall, and J. Skold, *4G: LTE/LTE-Advanced for Mobile Broadband*, 1st ed. Academic Press, 2011. 102
- [185] A. W. Evans, "Road congestion pricing: when is it a good policy?" *Journal of transport economics and policy*, pp. 213–243, 1992. 110
- [186] J. Eliasson, L. Hultkrantz, L. Nerhagen, and L. S. Rosqvist, "The stockholm congestion-charging trial 2006: Overview of effects," *Transportation Research Part A: Policy and Practice*, vol. 43, no. 3, pp. 240–250, 2009. 111
- [187] T. Litman, "London congestion pricing-implications for other cities," *CESifo DICE Report*, vol. 3, no. 3, pp. 17–21, 2005. 111
- [188] S.-Y. Phang and R. S. Toh, "Road congestion pricing in singapore: 1975 to 2003," *Transportation Journal*, pp. 16–25, 2004. 111
- [189] B. Schaller, "New york city's congestion pricing experience and implications for road pricing acceptance in the united states," *Transport Policy*, vol. 17, no. 4, pp. 266–273, 2010. 111
- [190] D. C. Shoup, "Cruising for parking," *Transport Policy*, vol. 13, no. 6, pp. 479–486, 2006. 111
- [191] N. Zheng and N. Geroliminis, "Modeling and optimization of multimodal urban networks with limited parking and dynamic pricing," *Transportation Research Part B: Methodological*, vol. 83, pp. 36–58, 2016. 111
- [192] A. Millard-Ball, R. R. Weinberger, and R. C. Hampshire, "Is the curb 80% full or 20% empty? assessing the impacts of san francisco's parking pricing experiment," *Transportation Research Part A: Policy and Practice*, vol. 63, pp. 76–92, 2014. 111